

Manometric determination of supercritical gas sorption in coal

Manometric determination of supercritical gas sorption in coal

Proefschrift

ter verkrijging van de graad van doctor
aan de Technische Universiteit Delft,
op gezag van de Rector Magnificus prof.dr.ir. J.T. Fokkema,
voorzitter van het College voor Promoties,
in het openbaar te verdedigen op dinsdag 1 september 2009 om
10:00 uur

door

Patrick VAN HEMERT

doctorandus in de Geochemie

geboren te 's-Hertogenbosch

Dit proefschrift is goedgekeurd door de promotor:
Prof.dr. J. Bruining

Copromotor:
Dr. K-H.A.A. Wolf

Samenstelling promotiecommissie:

Rector Magnificus	voorzitter
Prof.dr. J. Bruining	Technische Universiteit Delft, promotor
Dr. K-H.A.A. Wolf	Technische Universiteit Delft, copromotor
Prof.dr. J.J.C. Geerlings	Technische Universiteit Delft
Prof.dr. J. Palarski	Politechnika Śląska
Prof.dr. C.J. Spiers	Universiteit Utrecht
Dr. E.S.J. Rudolph	Technische Universiteit Delft
Dr. J.G. Maas	Shell International Exploration & Production
Prof.dr.ir. P.L.J. Zitha	Technische Universiteit Delft, reservelid

The research described in this thesis is performed at the Department of Geotechnology, Faculty of Civil Engineering and Geosciences, Delft University of Technology, The Netherlands as part of the Dutch CATO program for the capture, transport and storage of carbon dioxide.

Copyright © 2009 by P. van Hemert
ISBN 978-90-9024537-9
Printed by Ipskamp Drukkers
Cover design by www.hollandsgras.nl

Aan iedereen van wie ik geleerd heb.

Abstract

A topic of current interest is the reduction or stabilization of the atmospheric carbon dioxide concentration. On the other hand, carbon dioxide emitting fossil fuels will be required to meet the growing demand for energy for at least the next 100 years. Sequestration of carbon dioxide in underground coal can prevent the emission of carbon dioxide, while increasing the production of methane from underground coal can help meeting the local or global demand for energy. It has been hypothesized that the production of coalbed methane can be enhanced by the injection of carbon dioxide containing gas.

The global resources of coalbed methane are approximately as large as the global proven reserves of natural gas, while the storage potential for carbon dioxide of underground coal is estimated at 300-964 Gigatonne, which is 10 to 30 times the annual global emission of carbon dioxide. In addition, the omnipresence of coal implies that such technology is of interest to many countries, including the Netherlands.

Computer simulations of reservoirs are used to determine whether the production of coalbed methane and the sequestration of carbon dioxide in a particular underground coal is economically viable. The predictive ability of such models will improve with better understanding of the occurring physical and chemical processes. In addition, the relationship between these processes and the properties of the coal can be important for the production and sequestration. These physical and chemical processes and their relationship with the properties of the coal are not yet fully understood. Experimental research is a powerful tool for the investigation of these processes and their relationship with the properties of the coal.

The sorption of gas in coal is expected to be one of the important processes in the production of methane from and sequestration of carbon dioxide in underground coal. Several hypotheses have been formulated for the sorption of supercritical gas in coal. However, none of these hypotheses have been va-

validated for a wide range of conditions. It is expected that a large database is required to identify the correct hypothesis because of the heterogeneity of coal and the dependence of the hypotheses on empirical parameters. Moreover, the differences between the sorption behavior of the various hypotheses can be quite small. Therefore, accurate data of the sorption of gas in coal is required.

The manometric method is an often-used method in the Earth Sciences and the Chemical Engineering for the determination of sorption. However, it has been suggested that its accuracy is insufficient for experiments at conditions relevant to underground coal. Therefore, the first and second aim of this thesis are to optimize the manometric method for such conditions and to investigate the accuracy of the optimized method. The third aim of this thesis is to use the apparatus to obtain experimental data of the sorption of various gases in coal for various pressure and temperature conditions. The following topics have been addressed in this thesis:

- the production of methane from coal when injecting carbon dioxide, nitrogen, a mixture of nitrogen and carbon dioxide or a mixture of hydrogen and carbon dioxide;
- development of a state-of-the-art manometric apparatus with *a priori*¹ error analysis;
- verification of the equation of state for carbon dioxide at the conditions of interest;
- an independent assessment of the accuracy of the developed manometric apparatus with an inter-laboratory comparison;
- experimental data of the sorption of carbon dioxide, methane and nitrogen in Selar Cornish coal for pressures between 1.0 and 16.0 MPa at a temperature of 318 and 338 K.

All these aspects contribute to either improving the manometric method for the determination of sorption or provide observations on the sorption processes in coal.

The main achievement is the development of a state-of-the-art manometric apparatus with an *a priori* error estimate ranging between 0.02 and 0.08

¹*A priori* errors are estimated from the limitations of the measurements, assumptions and equations used in the determination.

mole/kg, a maximum *a posteriori*² error of 0.2 mole/kg and a maximum deviation of 13% in the fitted parameters when compared to the weighted average of the inter-laboratory comparison. The following interesting observations regarding the sorption of supercritical gas in coal have been made

- the sorption of gas at equilibrium in Selar Cornish coal depends on pressure, temperature and the properties of the gas;
- the sorption and desorption isotherms of methane and nitrogen in Selar Cornish coal at 318 and 338 K show no hysteresis;
- more time than previously assumed is required to attain sorption equilibrium;
- the time required to attain sorption equilibrium in Selar Cornish coal depends on the temperature and the properties of the gas.

In conclusion, the manometric method has been improved to provide accurate data of sorption of supercritical gas in coal. Using the improved apparatus, the construction of a large database of sorption determinations has been initiated. This database will allow the development of a theory that describes the sorption process. This theory provides better understanding of some of the physical and chemical processes occurring in underground coal when producing coalbed methane from or storing carbon dioxide in underground coal. This theory will improve the predictive ability of reservoir models used to identify economically viable projects for the production of methane or the sequestration of carbon dioxide. Moreover, the production of methane or the sequestration of carbon dioxide of such projects can be optimized using these models. Implementation of these projects will contribute to meeting the local or global demand for energy by increasing the production of methane or to reducing the emission of carbon dioxide by sequestration of carbon dioxide in underground coal.

²A *a posteriori* errors are the observed discrepancies between duplicate measurements.

Samenvatting

De vermindering of stabilisatie van de hoeveelheid koolstofdioxide in de atmosfeer staat tegenwoordig in de maatschappelijke belangstelling vanwege een mogelijk sterk verband met het globale klimaat. Tegelijkertijd stijgt de wereldwijde vraag naar energie, waardoor het gebruik van koolstofdioxide producerende fossiele brandstoffen nog zeker 100 jaar nodig zal zijn. Uitstoot van deze koolstofdioxide naar de atmosfeer kan worden voorkomen door het op te slaan in ondergrondse steenkool. Het is mogelijk om methaan te produceren uit dezelfde ondergrondse steenkool. Er wordt bovendien verwacht dat de opslag van koolstofdioxide leidt tot een verhoging van de methaan productie. Deze methaan kan natuurlijk voorzien in een deel van de toekomstige lokale en globale vraag naar energie.

De productie van methaan uit en de opslag van koolstofdioxide in ondergrondse steenkool is interessant voor veel landen, inclusief Nederland, door de wereldwijde verspreidheid van steenkool. De wereldwijde hoeveelheid van methaan aanwezig in ondergrondse steenkool is van dezelfde orde van grootte als de bewezen wereldwijde winbare voorraad van aardgas. De hoeveelheid koolstofdioxide die opgeslagen kan worden in ondergrondse steenkool wordt geschat op 300-964 Gigatonne. Dit komt overeen met tien tot dertig jaar wereldwijde uitstoot van koolstofdioxide. Deze hoeveelheden maakt het interessant om het potentieel van deze technologie te onderzoeken.

Computer simulaties worden gebruikt om te bepalen of de productie van methaan, of de opslag van koolstofdioxide, op een specifieke locatie economisch rendabel is. Deze simulaties zijn gebaseerd op vergelijkingen die de fysische en chemische processen in de ondergrond weergeven. De fysische en chemische processen gerelateerd aan de productie van methaan uit of de opslag van koolstofdioxide in steenkool worden nog niet goed begrepen. Tegelijkertijd is de relatie tussen de eigenschappen van de steenkool en deze processen niet

helemaal uitgezocht. Het voorspellende vermogen en de bruikbaarheid van de computer simulaties zullen verbeteren als deze processen en deze relatie beter begrepen worden. Wetenschappelijk laboratorium onderzoek is hiervoor essentieel.

Het proces waardoor steenkool gas opneemt dan wel uitstoot is waarschijnlijk zeer belangrijk in de productie van methaan uit dan wel opslag van koolstofdioxide in een ondergrondse steenkool. Er is nog geen theorie ontwikkeld die dit proces, genaamd sorptie, goed kan beschrijven. De ontwikkeling van deze theorie is ingewikkeld doordat er waarschijnlijk verschillende processen tegelijkertijd optreden en doordat steenkool zeer heterogeen is. Deze heterogeniteit bemoeilijkt onderzoek doordat mogelijk belangrijke parameters moeilijk te scheiden zijn in laboratorium proeven. Een grote en nauwkeurige database van sorptie van gassen in verschillende steenkolen onder verschillende condities zal de ontwikkeling van een theorie bevorderen.

De manometrische methode wordt gebruikt in de Aardwetenschappen en de Chemische Technologie om het sorptie proces te onderzoeken. Echter, de betrouwbaarheid van deze methode voor bepalingen bij *in situ* condities van ondergrondse steenkool staat ter discussie. Daarom is een doel van dit onderzoek, de optimalisatie van de manometrische methode en het in kaart brengen van zijn beperkingen. Een ander doel van dit onderzoek is de constructie van een database met de sorptie van verschillende gassen in steenkool onder verschillende condities. Om dit te bewerkstelligen worden de volgende onderwerpen behandeld in dit proefschrift:

- productie van methaan uit een steenkool door de injectie van stikstof, koolstofdioxide, een mengsel van stikstof en koolstofdioxide en een mengsel van waterstof en koolstofdioxide;
- ontwikkeling van een geavanceerd manometrisch apparaat met een *a priori*¹ fouten analyse;
- verificatie van de toestandsvergelijking waarmee de dichtheid van koolstofdioxide wordt berekend;
- een onafhankelijke evaluatie van de nauwkeurigheid van het manometrisch apparaat door een vergelijking met andere laboratoria;
- bepaling van sorptie van koolstofdioxide, methaan en stikstof in Selar Cornish steenkool bij een temperatuur van 318 K en 338 K bij drukken tussen 1.0 en 16.0 MPa.

Deze aspecten dragen bij aan de verificatie van de manometrische methode of aan de kennis over de opname en emissie van gas in steenkool.

Dit proefschrift presenteert een geavanceerd manometrisch apparaat met een *a priori*¹ fout van tussen de 0.02 en 0.08 mole/kg, een discrepantie in herhaalde metingen van maximaal 0.2 mole/kg en een afwijking van maximaal 13 % in de sorptie parameters, wanneer vergeleken met het gewogen gemiddelde van verschillende laboratoria. Er zijn verschillende interessante observaties gedaan aangaande de sorptie van gas in steenkool:

- het evenwicht tussen de gas en de sorptie fase is afhankelijk van de druk, de temperatuur en het soort gas voor Selar Cornish steenkool;
- het evenwicht tussen methaan in de gas fase en de sorptie fase is alleen afhankelijk van de druk bij een constante temperatuur voor Selar Cornish steenkool, dus de manier waarop deze druk tot stand is gekomen is niet van belang; hetzelfde kan gezegd worden voor stikstof;
- het sorptie proces verloopt langzamer dan eerder werd aangenomen;
- de tijd nodig voor het bereiken van evenwicht tussen de gas fase en de sorptie fase in Selar Cornish steenkool is afhankelijk van de temperatuur en het soort gas.

Wat met dit proefschrift is bereikt, is de ontwikkeling van een verbeterde versie van de manometrische methode, bruikbaar voor experimenteel onderzoek naar de opname en uitstoot van gassen in steenkool. Met deze methode kan onderzocht worden in welke mate het sorptie proces afhangt van temperatuur, druk, eigenschappen van de steenkool en eigenschappen van het gas. Een grote en nauwkeurige database met deze informatie, waarvoor een eerste set metingen is gedaan in dit proefschrift, is essentieel voor de ontwikkeling dan wel verificatie van een theorie die de sorptie van gas in steenkool beschrijft. Het voorspellende vermogen van computer simulaties voor de productie van methaan uit en de opslag van koolstofdioxide in ondergrondse steenkool zal verbeteren door aanwending van deze theorie. Een groter voorspellend vermogen van deze simulaties vergemakkelijkt de identificatie van economische rendabele methaan productie en koolstofdioxide opslag projecten. Tegelijkertijd zal het voorspellend vermogen van die simulaties aangewend worden voor

¹A *priori* fouten worden afgeschat m.b.v. de beperkingen van de gebruikte sensoren, aandames en vergelijkingen.

de optimalisatie van deze projecten ten opzichte van tijd, geld of energie. Uitvoering van deze projecten zal bijdragen aan de vermindering van de uitstoot van koolstofdioxide en de verhoging van de wereldwijde methaan productie.

Contents

1	Introduction	1
1.1	General introduction	1
1.2	Potential for Enhanced Coalbed methane and CO ₂ storage in coal beds	2
1.3	Current state of knowledge on fundamental aspects of gas sorption in coal particles	3
1.4	Research objective	5
1.5	Scope of thesis	6
1.6	Outline of thesis	8
2	Output gas stream composition from CH₄ saturated coal during N₂, CO₂, N₂/CO₂ and H₂/CO₂ injection	11
2.1	Introduction	12
2.2	Material and methods	14
2.3	Results and discussion	19
2.4	Conclusions	26
3	Improved manometric apparatus for the determination of sorption	27
3.1	Introduction	28
3.2	Experimental methods	30
3.3	Results and discussion	35
3.4	Summary	39
4	Estimating the uncertainty in the equations of state of He and CO₂	41
4.1	Introduction	42
4.2	Material and methods	45
4.3	Results and discussion	49

CONTENTS

4.4	Conclusions	55
5	Inter-laboratory comparison	57
5.1	Introduction	58
5.2	Materials and methods	60
5.3	Results and discussion	65
5.4	Conclusions	71
6	Sorption of N₂, CH₄ and CO₂ in coal	73
6.1	Introduction	74
6.2	Materials and methods	75
6.3	Results and discussion	80
6.4	Summary	84
7	Conclusions	87
A	Publications	91
B	Derivation of data interpretation equation	93
C	Influence of contamination on the determination of CO₂ sorption	95
D	Leak-rate model	97
E	Negligibility of the influence of sorption on the leakage correction	99
F	<i>A priori</i> uncertainty analysis	103
G	Interpretation of helium sorption experiment	107
H	Determination of micropore volume and sorbed phase density	109
I	Pressure development due to sorption in coal	111
J	Excess sorption data of CO₂ on Chemviron Filtrasorb 400	113
	Bibliography	115
	Acknowledgments	125
	About the author	129

List of Figures

2.1	Iso-surface of the CT-scan of the cylindrical Tupton coal sample.	15
2.2	Combined view of the CT-scan of the fractures, minerals and matrix of the cylindrical Tupton coal sample.	16
2.3	Separate views of the CT-scan of the fractures, minerals and matrix of the Tupton coal sample.	17
2.4	Technical drawing of the apparatus used for the flooding experiments.	20
2.5	Composition of the output gas when injecting pure CO ₂	22
2.6	Composition of the output when injecting pure N ₂	23
2.7	Composition of the output when injecting a mixture of 20 vol-% CO ₂ in N ₂	24
2.8	Composition of the output when injecting a mixture of 20 vol-% CO ₂ in H ₂	25
3.1	Technical drawing of the improved manometric apparatus.	31
3.2	Excess sorption of CO ₂ on Filtrasorb 400 at 318 K.	36
3.3	Excess sorption of CO ₂ on Filtrasorb 400 at 318 K normalized by the regressed specific micropore volume.	38
4.1	Density of carbon dioxide as a function of pressure and temperature.	44
4.2	Technical drawing of the improved manometric apparatus.	45
4.3	Deviations in CO ₂ density for different equations of state.	49
4.4	Discrepancies between the actual volume of the sample cell and the volume determined using He.	50
4.5	Error estimate of the helium equations of state.	51

LIST OF FIGURES

4.6	Discrepancies between the actual volume of the sample cell and the volume determined using CO ₂	52
4.7	Error estimate of the carbon dioxide equations of state.	54
5.1	CO ₂ sorption in Filtrasorb F400 vs. pressure.	67
5.2	CO ₂ sorption in Filtrasorb 400 vs. gas density.	69
6.1	Technical drawing of the standard accuracy manometric apparatus.	77
6.2	N ₂ sorption in Selar Cornish coal.	81
6.3	CH ₄ sorption in Selar Cornish coal.	82
6.4	CO ₂ sorption in Selar Cornish coal.	84
E.1	Ratios of the leaked gas amount as calculated by the simple and more complicated leak model vs. time for a large leak.	101
E.2	Ratios of the leaked gas amount as calculated by the simple and more complicated leak model vs. time for a small leak.	102
F.1	Relative error in the density of CO ₂ at 318.1 K for 1 kPa, 20 mK and 0.02% in the EoS uncertainty.	105
F.2	Uncertainty in sorption for the uncertainties in V^s , leakage and ρ 's.	106
G.1	Helium sorption in Filtrasorb 400 at 318.11 K.	108
I.1	Pressure increase for desorption in Brzeszcze and Velenje coal of CO ₂	111
I.2	Pressure decrease during sorption in Selar Cornish coal of N ₂ , CH ₄ and CO ₂ at 318 and 338 K.	112

List of Tables

1.1	Comparison of CBM resources, conventional (conv.) natural gas and CO ₂ emissions.	3
2.1	Properties of the Tupton coal.	14
2.2	Experimental conditions of the flooding experiments.	18
2.3	Amount of injected and produced gas for the flooding experiments.	20
3.1	Specification of components of the improved manometric apparatus.	32
3.2	Specification of the experimental parameters used in the determination of the sorption of CO ₂ on Filtrasorb 400.	35
3.3	Regressed micropore volumes and extrapolated density of sorbed CO ₂ on Filtrasorb 400.	37
3.4	Nomenclature of chapter 3.	40
4.1	Overview of the tested equations of state.	43
5.1	Proximate analysis of the Filtrasorb 400.	61
5.2	Ultimate analysis of the Filtrasorb 400.	61
5.3	Details of the experiments.	62
5.4	Specifics of the apparatus of the different laboratories.	62
5.5	Experimental parameters.	66
5.6	Fitted parameters of a Langmuir-type equation for the sorption of CO ₂ on Filtrasorb 400	68
5.7	Fitted parameters of a DubininRadushkevich-type equation for the sorption of CO ₂ on Filtrasorb 400	70
5.8	Nomenclature of chapter 5	72

LIST OF TABLES

6.1	Properties of the U.K. Selar Cornish coal.	75
6.2	Critical properties and purity of the gases used in chapter 6	76
6.3	Experimental conditions and parameters of chapter 6.	78
E.1	Input parameters for the comparison of the forward and leak-rate models.	101
H.1	Accuracy of the linear regressions to estimate specific micropore volume and sorbed phase density.	110
J.1	Excess sorption data of CO ₂ on Chemviron Filtrasorb 400 at 318.11 K.	114

Chapter 1

Introduction

1.1 General introduction

The availability of affordable energy has contributed to the current level of global prosperity. Fossil fuels have always been the main source of abundant energy, but recently many governments and institutions have declared that other low cost energy sources must be developed. The reasons for this switch are the desire for energy independence, securing the energy supply, environmental damage associated with fossil fuels and the long-term prospect of diminishing fossil fuel production.

In spite of the increasing importance of alternative energy sources, supported by major research efforts, fossil fuels will be required to meet energy demands for at least the next 100 years (Zupanc et al., 2007). Fortunately, estimates of reserves and resources ¹ indicate that sufficient fossil fuels are available for this period. However, local or temporary shortages caused by political and economical developments or armed conflicts are still possible ².

An additional topic of current societal interest is the reduction or stabilization of the atmospheric CO₂ concentration. This interest has been brought about by the scientific consensus that atmospheric CO₂ concentration plays a role in determining the global climate (Solomon et al., 2007; Whorf and Keeling, 1998) and a more than 30% increase in the atmospheric CO₂ concentration due to anthropogenic emissions in the last 60 years. CO₂ absorbs infrared

¹<http://www.bp.com/statisticalreview>

²<http://www.peakoil.nl/2007/01/28/video-peakoil-conferentieprof-dr-stefan-luthi-tu-delft/>

light that would otherwise radiate outward into space, thus decreasing the loss of heat from the earth. Many interacting processes determine the global climate and the exact influence of rising atmospheric CO₂ concentration is outside the scope of this thesis.

It is expected that future use of fossil fuels will require steps to compensate for the associated CO₂ emissions. One feasible option is the storage of CO₂ in geological formations, such as saline aquifers, depleted oil reservoirs, depleted conventional gas reservoirs, depleted (solution) salt mines, hydrates and coal layers (Bachu, 2008).

It is obvious that fossil fuel production enhancement with concomitant CO₂ storage (CS) is of great industrial and societal interest. Injection of CO₂ is already being used to enhance oil and conventional gas production. Coal bed methane (CBM) is a fossil fuel of which production may be enhanced by CO₂ injection. Enhancing CBM production by injection of CO₂ is referred to as CO₂ Enhanced Coal bed Methane (CO₂-ECBM). CBM is CH₄ present in coal layers. Many aspects of the physical mechanisms of (E)CBM and CO₂ storage in coal beds are not understood. This lack of knowledge limits both the application of ECBM and the assessment of potential reservoirs. Current estimates on (E)CBM and CO₂ storage in coal beds potential are discussed in the next section. This thesis confines its interest to clarifying the physics of CO₂, CH₄ and N₂ sorption in coal particles.

1.2 Potential for Enhanced Coalbed methane and CO₂ storage in coal beds

The U.S. is the world's greatest producer of coal bed methane (CBM): 7.9 percent of the U.S. dry gas production in 2001 was CBM. CBM production has been spectacularly successful in the United States in general and in the San Juan basin in particular. The success of CBM production in the San Juan basin has been attributed to its exceptionally favorable permeability characteristics. The San Juan coal is relatively young higher grade coal, explaining its high permeability and high methane content. Other CBM producing countries are Canada, China and Australia. Many countries have access to coal bed methane resources, although production is not always feasible due to the low permeabilities of the coal layers. The technical and economical feasibility for production of coal bed methane resources in the Netherlands and other countries is still under investigation (Ham; van Bergen et al., 2007).

1.3 Current state of knowledge on fundamental aspects of gas sorption in coal particles

Table 1.1: Comparison of CBM resources, conventional (conv.) natural gas and CO₂ emissions.

	Worldwide	Netherlands	
Coalbed Methane resources	⁴ 84.38-262.21	³ 0.0072-0.5407	Tm ³
proven reserves of natural gas	⁷ 177.36	⁷ 1.25	Tm ³
annual production of natural gas	⁷ 2.940	⁷ 0.0645	Tm ³
annual consumption of natural gas	⁷ 2.9219	⁷ 0.0372	Tm ³
CBM CO ₂ storage potential	⁴ 300-964	³ 0.0388-2.8522	Gt
Annual CO ₂ emissions	⁶ 29.0	⁵ 0.1727	Gt

Table 1.1 demonstrates that (E)CBM and the subsequent CO₂ storage (CS) potential is considerable. The global CBM resources as estimated by White (White et al., 2005) is 48 % to 148 % of the current global CH₄ reserves. Furthermore, the estimated CO₂ storage potential of global CBM reservoirs as estimated by White (White et al., 2005) is sufficient to store 10 to 33 years of global CO₂ emissions. The Dutch CBM resources as estimated by (van Bergen et al., 2007) is 0.6 % to 43 % of the current Dutch CH₄ reserves. Furthermore, the accompanying CO₂ storage potential of Dutch CBM reservoirs is sufficient to store 0.2 to 17 years of annual (2007) Dutch CO₂ emissions.

1.3 Current state of knowledge on fundamental aspects of gas sorption in coal particles

The technical feasibility and economical viability of ECBM production depend on many factors, such as permeability behavior, transport processes in the cleat system, sorption behavior and the initial amount and composition of the fluid in place (Katyal et al., 2007; White et al., 2005). Important parameters for the application of (E)CBM and CO₂ storage in coalbeds (CSC) are the amount of recoverable CH₄, amount of sequestrable CO₂ and the rates associated with

³P90 value for depth <1500 m and P10 value for depth >1500 m from van Bergen et al. (2007)

⁴White et al. (2005)

⁵2007 value, Centraal Bureau voor de Statistiek (<http://www.cbs.nl>)

⁶2006 value, Energy Information administration (<http://eia.doe.gov/iea>)

⁷2007 value, British Petroleum (<http://www.bp.com/statisticalreview>)

production and storage. The main focus of this thesis is the sorption behavior of the different gases on coal. This sorption behavior is expected to be an important physical process for the recovery of CH₄ from and sequestration of CO₂ in underground coals. The main investigative tool for optimization of the strategy for (E)CBM production and CSC is a predictive reservoir-scale model. This model must be based on sound physical and chemical principles with parameters related to the physical properties of the coal to be of practical use. Numerous journal articles have been published reporting experimental data on the sorption of gas on coal. A few theories on the physics of gas sorption on coal have been hypothesized. These theories differ considerably as to the parameters that determine sorption behavior.

Four contemporary theories on the physics of equilibrium sorption of gas on coal demonstrate the current disparity:

- Simplified local-density theory (SLD)

The simplified local-density (SLD) theory states that sorption of gas on coal is related to the product of the density increase of the sorbate, the gas, and the microporosity of the coal (Fitzgerald et al., 2003, 2006), the sorbent. The density increase of the sorbate is caused by the additional interactions of the solid on the fluid in the micropores. The sorbent, is thus described as a collection of micro-pores. The density behavior of the sorbate is described with a Equation of State (EoS) modified for the description of the sorbate. The parameters of this modified EoS are determined by fitting the model to experimental sorption data.

- Lattice density functional theory (LDF)

The lattice density functional theory (LDF) states that sorption of gas on coal is the product of the number of lattice sites, the size of these sites, the fraction of filled sites and the constant density increase of the sorbate (Ottiger et al., 2008). The sorbent is described as a collection of lattice sites. The number of occupied lattice sites increases with increasing pressure.

- Multiple sorption theory (MS)

The multiple sorption theory (MS) (Jodlowski et al., 2007; Milewska-Duda and Duda, 1993; Milewska-Duda et al., 2000) considers the sorption of gas on coal as a combination of three processes; absorption of sorbate molecules in the molecular structure, placement of sorbate molecules in

1.4 Research objective

submicropores, which is assumed to enlarge the submicroporosity volume and placement of molecules in micropores without affecting the volume of the microporosity. Coal is considered as a submicroporous, heterogeneous polymer with a significant fraction of elastic polymer-like chains and some fraction of crystal-like aromatic hydrocarbons.

- Pore filling combined with linear dissolution of gas in the coal (ST)
Sakurov postulated (Day et al., 2008a,b; Sakurovs et al., 2007, 2008) that sorption of gas on coal is a combination of pore filling and absorption. The pore filling is described by a Dubinin-Radushkevich equation modified for supercritical gas and absorption is described by a linear relationship with gas density.

1.4 Research objective

The first research objective of this thesis is the development of an accurate manometric apparatus for the determination of sorption of gas in coal. The second objective is to use the developed apparatus to obtain a starting data set of equilibrium sorption of gas in coal. A database describing the relationship of sorption of gas in coal with temperature, pressure, properties of the coal and properties of the gas is required for the development of a theory that describes sorption. Some examples of the potential of experimental sorption data to validate⁸ hypotheses are provided below.

- Validation of a sorption hypothesis using the relationship between pressure and sorption.
For example, the SLD model states that the density of the gas sorbed in the microporosity increases with the bulk phase pressure following a modified Equation of State. The pressure-sorption relationship as a function of gas type should follow the same trend as pressure-density relationship as a function of gas type. This trend can be tested by measuring the sorption at different pressures for different gases.
- Validation of a sorption hypothesis using the relationship between temperature and sorption.

⁸It can be argued that experimental data can only be used to falsify theories.

For example, the LDF states that with increasing temperature the number of filled lattice sites decreases while the size distribution of filled lattice sites remains unaltered. This implies that there is no correlation between the temperature-sorption relationship and microporosity of the sorbent. This lack of correlation can be examined by comparing the temperature-sorption relationship of similar sorbents with different micropore size distributions.

- Validation of a sorption hypothesis using the relationship between sorption and the chemical and maceral composition of the coal sorbent.

Every theory contains fitted parameters related to the composition of the coal sorbent. These fitted parameters must thus be correlated with the coal composition. This correlation can be tested by measuring the sorption of gas for different coal types.

- Validation of a sorption hypothesis using the relationship between sorption and the microporosity of the coal.

The theories differ considerably in the influence the size distribution of the microporosity on the sorption. e.g., the sorption capacity in the ST theory is not related to the size distribution of the microporosity. Comparing the sorption of gases with the microporosity for a large number of coals can test the validity of the different theories.

- Validation of a hypothesis using the relationship between sorption and the properties of the sorbing gas.

Sorption theories postulate a relationship between the properties of the sorbing gas and its sorption behavior. These postulates can be tested using sorption data for different gases. e.g., the MS theory has gas dependent parameters for absorption in a coal or a polymer. The trend in gas dependent parameters for these two types of sorbents should be consistent. This can be tested by comparing the sorption of different gases.

1.5 Scope of thesis

This thesis presents experimental research on the sorption of supercritical gases in coal particles.

1.5 Scope of thesis

An understanding of the physical mechanisms of gas sorption in coal is lacking in the literature. Experimental sorption data can provide insight in these mechanisms or validate current sorption theories. Central to this thesis is the construction of an apparatus for measuring sorption on coal and the verification of the accuracy of the measurements. The manometric method is a common tool for sorption determination in Earth Sciences and Chemical Engineering. Previously published experimental sorption data show deviating and inconsistent behavior, especially for CO₂ above its critical point. These deviations reflect the complicated nature of supercritical gas sorption in a heterogeneous sorbate. An alternative hypothesis is that the deviations are experimental errors. This concern about the reliability motivated the construction of a high accuracy manometric set-up. Furthermore, the accuracy of this set-up has been investigated with a comprehensive error analysis and verified with an inter-laboratory comparison. In addition, a normal accuracy manometric apparatus is constructed for sorption measurements with CH₄ and N₂. Comparison of experimental results to current sorption models is outside the scope of this thesis. The focus of this thesis is to improve the understanding of the sorption process. Therefore, experiments are performed using dry samples to exclude additional effects, e.g., dissolution, chemical reactions and electro-chemical aspects.

Sorption isotherms have been determined for CO₂, CH₄ and N₂. The relevance of CH₄ and CO₂ in ECBM and CSC is obvious. N₂ is of interest, because it can be a major impurity in the CO₂ to be stored. Furthermore, N₂ injection can also be used to enhance CBM production (Jessen et al., 2008).

The temperature dependency of equilibrium sorption in coal is investigated for CO₂, CH₄ and N₂ on one type of coal, Selar Cornish, at 318.0 and 338.0 K. The temperature of 318.0 K is typical for deep coalbeds in Europe. The temperature of 338.0 K is above the in-situ conditions of deep coalbeds suitable for ECBM, but is included to elucidate the temperature dependency of equilibrium sorption.

All sorption data were obtained in the pressure range between 0 to 17 MPa, with emphasis on data between 8 and 14 MPa. Experimental data in the literature generally lie below 10 MPa. Indeed, most experimental data for CO₂ are limited to subcritical conditions. The pressure of coalbeds suitable for (E)CBM and CO₂ sequestration can extend to 15 MPa. Hence the need for sorption measurements at higher pressures. In addition, extension of the pressure range provides insight in the pressure behavior of sorption processes.

In addition to the manometric pure gas experiments, the potential for enhancing CBM production by gas injection under in-situ conditions has been

investigated by means of core flooding experiments. CH₄ production from a cylindrical coal sample for different gas injectants has been investigated at conditions typical for a deep coalbed (8 MPa and 318 K). The use of a cylindrical coal sample is unique and allows the investigation of the processes in a matrix coupled to a cleat system. The investigated injectants are pure CO₂, pure N₂, a 20% CO₂ in N₂ mixture and a 20% CO₂ in H₂ mixture. The CO₂ in H₂ mixture is added to examine the influence of the sorbing strength on the composition of the production stream.

1.6 Outline of thesis

The main text of the thesis is organized in five articles, featured in chapters 2 to 6. Three of these articles are published in peer-reviewed journals and one is submitted to a peer-reviewed journal. Chapter 2 presents experimental research on the influence of injected gas composition on enhancing CBM production under in-situ conditions. Chapter 3 explains the high accuracy manometric apparatus in detail. Chapter 4 discusses experiments with CO₂ in an empty high accuracy manometric apparatus to verify the accuracy of the CO₂ Equation of State used in the experiments. Chapter 5 presents an international inter-laboratory comparison of CO₂ sorption data on activated carbon F400 to validate the accuracy of the apparatus. Chapter 6 presents CO₂, CH₄ and N₂ sorption isotherms on Selar Cornish coal at 318 and 338 K. Subjects not directly related to the main topic of the thesis are delegated to the appendices. Below we discuss each chapter in more detail.

Chapter 2 investigates (1) the effectiveness of methane production by injection of a gas mixture in a methane-saturated coal sample and (2) how the composition of the production stream varies when weak sorbing component (N₂) is replaced by an even weaker sorbing component (H₂).

Chapter 3 gives a detailed description of the high accuracy manometric apparatus. Duplicate measurements of sorption and desorption of CO₂ at 318.0 K up to 17 MPa on Filtrasorb 400 are presented and compared to literature data. Furthermore, the accuracy of the measurements has been estimated by a comprehensive a priori error analysis. This paper has been published in *Review of Scientific Instruments*.

Chapter 4 presents determinations of the volumes of the cells in the high accuracy manometric apparatus by means of pressurization with He and CO₂. The differences between the He and CO₂ determinations have been identified

1.6 Outline of thesis

and described. In this way, the use of the equation of state in the sorption determinations could be verified. This paper has been published in *SPE Journal*.

Chapter 5 presents the sorption of CO₂ at 318 K up to 17 MPa on Filtrasorb 400 as determined by the Delft University of Technology, RWTH Aachen, Polytechnique Mons and University of Toulouse. Sorption data are compared to literature data. Furthermore, the accuracy of the equipment of all laboratories is compared. A modified version of this paper has been accepted for publication in *Carbon*.

Chapter 6 presents results of the study of equilibrium sorption of CO₂, CH₄ and N₂ on Selar Cornish coal at 318.0 K and 338.0 K up to 16.0 MPa. This paper is submitted for publication in *International Journal of Coal Geology*.

Chapter 2

Output gas stream composition from CH₄ saturated coal during N₂, CO₂, N₂/CO₂ and H₂/CO₂ injection

Abstract

Proven global methane reserves can be increased from 177 Tm³ to 210-308 Tm³ (+19 to 74%) if 50% of global coalbed methane resources are deemed producible. As primary recovery methods for CBM produce at most 50% of the methane present, there is considerable interest in enhancing recovery by gas injection. It is not clear which composition of the injection gas is most efficient for enhancing methane recovery as the physical and chemical processes associated with gas injection are not fully understood. A previous experimental study has shown that the time for breakthrough increases with increasing sorption capacity of the injected gas when injecting a mixture of gases in a methane saturated coal.

The aim of this study is to investigate how the properties of a weakly sor-

bing gas influence the composition of the produced gas stream when injecting a binary mixture in a CH₄ saturated coal. Therefore, the composition of the produced gas is compared for the injection of a mixture of 20 vol.-% CO₂ in N₂ and of 20 vol.-% CO₂ in H₂ in an intact dry CH₄ saturated cylindrical coal sample at a pore pressure of 8.0±0.1 MPa and a temperature of 318±1 K. i.e., the weakly sorbing gas N₂ is replaced by the even more weakly sorbing gas H₂. In this study, CO₂ is the strongly sorbing component, CH₄ is the intermediately sorbing component, N₂ is the weakly sorbing component and H₂ the most weakly sorbing component.

The production of H₂ when injecting a mixture of CO₂ and H₂ is earlier than the production of N₂ when injecting a mixture of CO₂ and N₂. This agrees with the observed trend that the breakthrough time of an injected component increases with the components sorption capacity. The production of CO₂ does not change if a mixture of CO₂ and H₂ is injected instead of a mixture of CO₂ and N₂ mixture. i.e., the properties of the weakly sorbing component has minimal influence on the retention of the strongly sorbing component.

2.1 Introduction

The production of coalbed methane (CBM) accounts for nearly 10% of the natural gas production in the United States of America. This success and the global coalbed methane resources of 67.4 to 262 Tm³ (White et al., 2005), 38-150% compared to the current global proven methane reserves, has led to worldwide increased interest in CBM production. The foremost focus of CBM related research is the development of CBM production methods with high recovery factors as primary recovery produce less than 50% of the CH₄ present (Stevens et al., 1998a). The decrease of the pressure-dependent cleat permeability during CH₄ production is the main limitation for CBM production. The recovery method known as Enhanced Coalbed Methane (ECBM) in which gas is injected into the coalbed is considered a viable secondary recovery method. This increases pore pressure and, in this way, counteracts the decrease of permeability due to decreased pore pressure (Reeves, 2003; Yu et al., 2007).

Stevens et al. (1998a,b) demonstrated the large-scale technical feasibility of ECBM by injection of CO₂ in a producing CBM field. Following this success, several smaller ECBM pilots have been conducted (e.g. van Wageningen et al. (2009)). The effect using ECBM can not be predicted as many of the relevant physical and chemical processes, such as multi-component sorption, coal swelling and the permeability changes in a coalbed, are only partly understood. In

2.1 Introduction

addition, the interaction between these simultaneously occurring processes is difficult to model. Therefore, scientific research on the fundamental processes is of direct interest for the production of coalbed methane.

Natural choices of injection gases in ECBM are N_2 and CO_2 . The advantages of N_2 are that it is abundant, non-corrosive and non-hazardous. CO_2 is not always available, corrosive and hazardous, but it has a late breakthrough because of its strongly sorption on coal. In addition, as the injected CO_2 is effectively stored in coalbeds, it is synergetic with CO_2 storage projects (White et al., 2005). However, Mazumder and Wolf (Mazumder et al., 2008) have shown that injection of CO_2 leads to swelling and hence may impair the permeability of the coalbed. Injection of a mixture of CO_2 and N_2 may be an economically interesting secondary recovery method, if the physical response is favourable. Unfortunately, relevant published information is limited. Specifically, only a few publications (Jessen et al., 2008; Mazumder et al., 2008) on methane displacement from a coal by continuous injection of a gas mixture are available.

Experiments by Mazumder et al. (Mazumder et al., 2008) have shown that water in coal complicates CH_4 production by means of gas injection. Therefore, the experiments in this study are performed on dry coal. In addition, these experiments demonstrate that the breakthrough of CO_2 is later than the breakthrough of N_2 when injecting a multi-component gas mixture. Jessen et al. (Jessen et al., 2008) published experiments demonstrating that mixtures of CO_2 and N_2 in varying ratios produce CH_4 effectively and that the breakthrough time of CO_2 decreases with increasing CO_2 concentration.

The aim of this study is to investigate the production stream change when replacing the weakly sorbing component in a continuously injected binary mixture. Therefore, the composition of the production stream is measured while injecting a 20/80 vol.-% mixture of CO_2 and N_2 and while injecting a 20/80 vol.-% mixture of CO_2 and H_2 in an dry CH_4 saturated cylindrical coal sample. The coal sample is cut from a single coal block to keep the core as close to in-situ conditions as possible. The experiments are performed at a pore pressure of 8.0 MPa and a temperature of 318 K: conditions typical for European coalbeds at a depth of 0.8 km. The coal sample originates from the Nottinghamshire coal field in the United Kingdom. Experiments with injection of pure N_2 and pure CO_2 are included as a reference. It should be noted that this study focuses on the underlying physical and chemical processes of CBM production by gas injection. Therefore, a single coal sample is used, which allows comparison of the data. This study is not intended to give an overview of the efficiency of the method to enhance CBM production by injecting gas mixtures

into various kinds of coal.

2.2 Material and methods

The experiments are performed on a single cylindrical (D=75 mm , L=183 mm) coal core of 899 g taken from a coal block originating from the Nottinghamshire coal field, Westphalian A strata. The maturity of the coal is high volatile bituminous A. The sample is drilled parallel to the bedding of the coal in order to retain its in-situ permeability characteristics. The total volume accessible to gas is 150±5 cm³: this encompasses cleat porosity, micropore porosity and tubing. The overall, cleat and minerals CT-scans of the coal core, performed after the flooding experiments, are shown in Fig. 2.1, 2.2 and 2.3. Table 2.1 reports the ultimate, proximate and microscopic analysis of the coal block.

Table 2.1: Properties of the Tupton coal (Siemons, 2007).

Proximate analysis				
Moisture mass-%	Vol. matter mass-% (w.f.)	Ash mass-% (w.f.)	Fix. Carbon mass-% (d.a.f.)	Cal. value MJ/m ³
10.09-15.7	29.2-36.15	2.05-6.2	63.24	26.2
Ultimate analysis				
Carbon mass-%	Hydrogen mass-%	Nitrogen mass-%	Sulfur mass-%	Oxygen mass-%
73.01	5.26	1.95	0.57	5.53
Microscope analysis				
R _{max} %	Vitrinite vol-%	Liptinite vol-%	Inertinite vol-%	Minerals vol-%
0.53±0.01	59.4	14	25.8	0.8

2.2.1 Sample preparation

The coal core is air-dried in an oven at 378 K for two weeks to remove volatile components before it is built into the set-up. The sample is wrapped in lead foil to minimize gas transport and a rubber sachet to distribute the annular pressure evenly. The rubber sleeve is wired to the inlet and outlet Sieperm plates. For more information on sample preparation procedures see Mazumder (2007). At the start of each experiment, the coal core in the reactor cell is evacuated

2.2 Material and methods

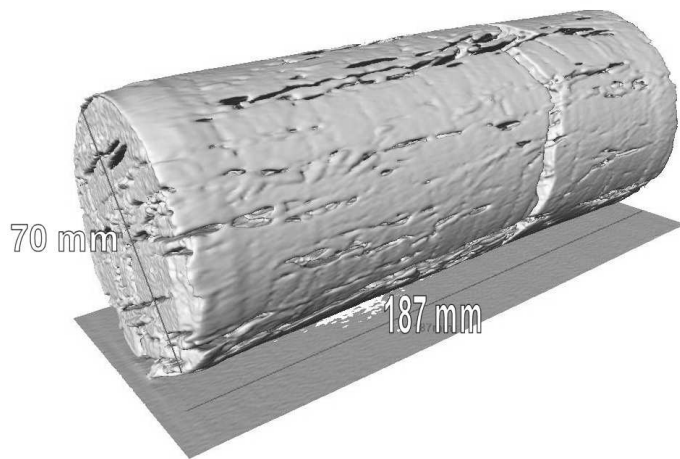


Figure 2.1: Iso-surface of the CT-scan of the cylindrical Tufton coal sample.



Figure 2.2: Combined view of the CT-scan of the fractures, minerals and matrix of the cylindrical Tupton coal sample.

2.2 Material and methods

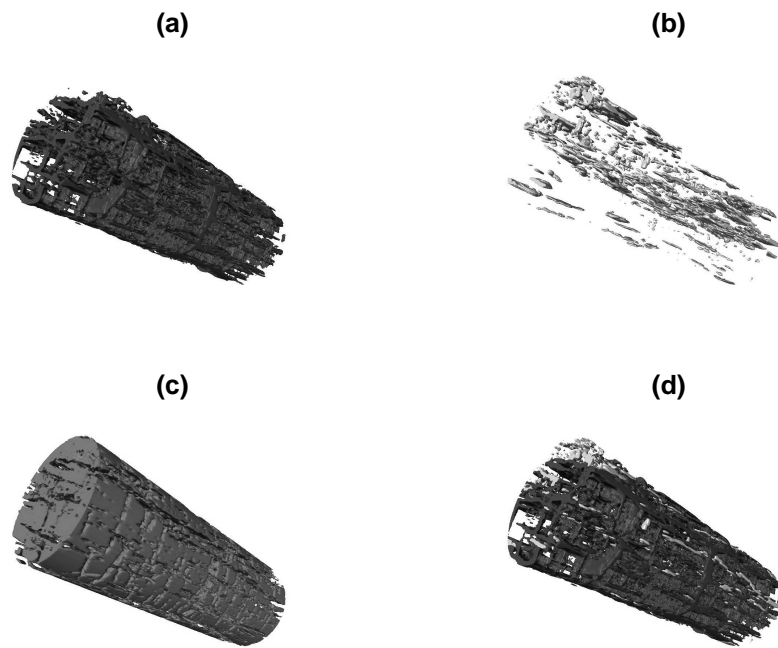


Figure 2.3: CT-scan of the cylindrical Tupton coal sample in separate view for the different phases; (a) the fractures, (b) the minerals, (c) the matrix (d) combined view of the minerals and fractures.

Output gas stream composition from CH₄ saturated coal during N₂, CO₂, N₂/CO₂ and H₂/CO₂ injection

with a rotating vacuum pump at 318 ± 1 K for 24 to 72 hours. Experiments are performed at a pore pressure of approximately 8.0 MPa and a temperature of 318 K (see table 2.2). After evacuation, the isolated reactor cell is filled with CH₄ to a pressure between 7.8 and 8.9 MPa. Approximately one week is necessary for adequate saturation of the coal with CH₄. Pressure over 8.0 MPa is blown off at the start of the experiment. The annular oil confining the coal core is held at constant pressure, which is 2.0 to 2.5 MPa higher than the pore pressure.

Table 2.2: Experimental conditions of the flooding experiments.

exp	gas	T _{reactor} [K]	P _{reactor} [MPa]	T _{ISCO} [K]	P _{init} [MPa]
1	N ₂	317.8-320.5	7.91-8.25	292.3-301.3	8.16
2	N ₂	318.4-319.0	8.01-8.25	291.2-300.7	8.47
3	CO ₂ -N ₂	317.4-318.3	7.96-8.29	289.4-297.4	8.91
4	CO ₂ -N ₂	317.4-318.7	7.97-8.23	289.2-294.5	8.28
5	CO ₂ -H ₂	317.5-318.7	7.92-8.28	288.6-294.2	8.43
6	CO ₂ -H ₂	317.6-318.5	7.94-8.39	290.1-297.8	8.54
7	CO ₂	317.3-318.5	7.76-8.47	293.6-297.6	8.69
8	CO ₂	317.3-318.7	7.91-8.29	293.0-296.1	7.83
9	N ₂	317.5-318.4	8.00-8.34	291.7-295.9	8.86

Preparation of the coal sample for flooding experiments is labor intensive and prone to all kinds of difficulties (e.g. maintaining sample integrity during drilling and drying). Therefore, all experiments have been performed on a single coal sample. The final experiment is a duplicate of the first experiment to examine whether performing multiple experiments on one sample changes the composition of the production stream. The repeatability is acceptable, and it is concluded that the multiple uses of a single sample is legitimate.

Experiments are performed using pure N₂, pure CO₂, a mixture of 20 vol-% CO₂ in N₂ and a mixture of 20 vol-% CO₂ in H₂. All gases have been purchased from Linde Gas. The contaminations are specified by the manufacturer as 0.3 vol-% in the pure CO₂, 0.005 vol-% in the pure N₂; the composition of the trace amounts in the mixtures are unknown.

2.2.2 Apparatus

Fig. 2.4 is a technical drawing of the laboratory set-up. A full description of the apparatus and sample preparations are given by Mazumder (Mazumder, 2007).

2.3 Results and discussion

The gas inflow is controlled by an ISCO Syringe pump 620D set at a constant rate of 1.00 cm³/h at room temperature and 8.0 MPa. Refilling the ISCO pump takes less than one hour and is not considered in the data processing. The coal core is pressurized using an oil to a pressure of 10.0 MPa. The outflow of gas is controlled by a back pressure valve set at 8.0 MPa. The composition of the produced gas is analyzed every 30 minutes using a Agilent 3000A micro gas chromatograph with a Molsieve 5Å and U columns. An Actaris laboratory wet gas meter determines the cumulative volume at ambient conditions of the gas produced. Pressures are determined at the in- and outlet of the reactor cell using GE sensing pressure transmitters of type PTX611. Temperatures are determined at the top and bottom of the cell using K-type thermocouples. The data acquisition system records the pressure, temperature and cumulative amount of gas produced in one minute intervals. The duration of the experiments varies from 10 to 35 days.

2.3 Results and discussion

The amounts of produced and injected gas are given in Table 2.3. Cumulative injected and produced gases agree within 10 mole-%, except for the experiments with injection of pure CO₂. The 10% discrepancy is within the accuracy of these measurements. However, this uncertainty makes it unrealistic to expect reliable mass-balance calculations on the composition of the sorbed amount. Gas injection is an effective method to produce CH₄ as 88% to 99% of the original present CH₄ has been produced. Unfortunately, the accuracy of the experiments is insufficient to determine how methane recovery varies with the different compositions of the injected gases. The gas initially in place (GIIP) of experiment 9 is considered to be erroneous as this value is 30% higher than the other values with a similar amount of cumulative produced CH₄.

For the experiments where pure CO₂ is injected, the mass of the cumulative amount of produced gas is a factor of two lower than the mass of the cumulative amount of injected gas. This discrepancy is much larger than the difference that can be explained by the maximum possible sorption and gas density of CO₂. It is interesting to note that only experiments with injection of pure CO₂ have been affected and that the cumulative amount of produced CH₄ in the same experiment is in good agreement with the amount of originally present CH₄. The diffusion and dissolution of the CO₂ in the annular oil is suggested as a possible cause for the mass balance discrepancy.

Preliminary calculations have shown that the experimental results in Figs.

Output gas stream composition from CH₄ saturated coal during N₂, CO₂, N₂/CO₂ and H₂/CO₂ injection

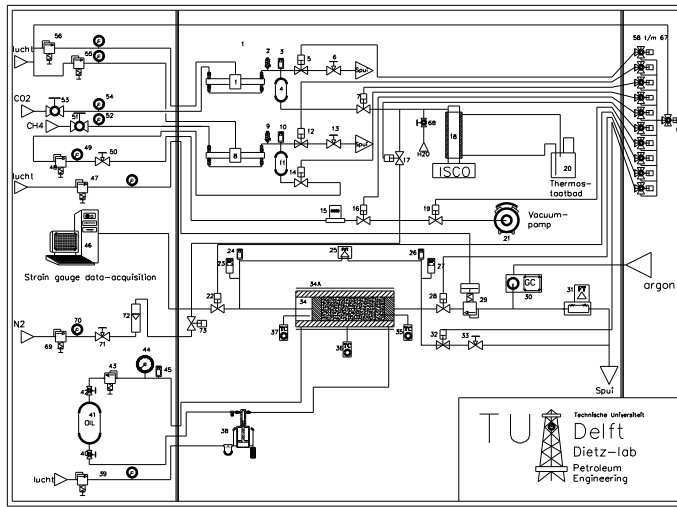


Figure 2.4: Detailed technical drawing of the laboratory flooding equipment. The essential components are gas boosters (1, 8), ball taps (6, 13 33, 50 51, 53, 71), air-actuated valves (5, 14, 16, 17, 19, 22, 28, 32), thermostatic bath (20), safety valves (23, 27) pressure difference transducer (25, but not used in these experiments), pressure transducers (24, 26), digital flow meter (31), gas chromatograph (30), ISCO pump (18), vacuum pump (21), data acquisition system (strain gages not used in these experiments), thermocouple (35, 36 37) and a pressure vessel (34A).

Table 2.3: Amount of injected and produced gas for the flooding experiments.

Exp.	inj. gas	GIIP ¹ [mole]	produced CH ₄ [mole]	injected gas [mole]	produced gas ² [mole]
1	N ₂	0.793	0.70	2.22	2.07
2	N ₂	-	0.67	2.21	2.22
3	N ₂ /CO ₂	0.799	0.79	2.83	2.62
4	N ₂ /CO ₂	0.806	0.76	2.53	2.42
5	H ₂ /CO ₂	0.848	0.76	2.76	2.48
6	H ₂ /CO ₂	0.897	0.80	2.62	2.64
7	CO ₂	0.875	0.81	4.27	1.9
8	CO ₂	1.055	0.98	4.43	1.7
9	N ₂	1.316	0.81	2.85	3.17

2.3 Results and discussion

2.5, 2.6, 2.7 and 2.8 can be adequately fitted by either a model based solely on the diffusive mixing of gas or by a model solely based on exchange of gases through competitive sorption. Both processes definitely influence the composition of the production stream. Typically, gas diffusion through the coal sample at conditions of the experiment will take approximately 20 days. This is significant compared to the duration of the experiments (10 to 35 days). In addition, sorption effects occur as they occur in binary and multi-component systems determine the retention of the gas by the coal. The coupling between the diffusion and sorption is not yet clear and can not be deduced from the experiments in this study. Therefore, only a description and a tentative qualitative interpretation of the experiments is given.

Fig. 2.5 shows the composition of the produced gas for the experiments with pure CO₂ injection. The production gas shows a relatively sharp front in the composition of the produced gas for pure CO₂ injection in a CH₄ saturated coal core. Furthermore, the fraction of CH₄ in the produced gas stream at the end of the experiment is zero. Breakthrough of 0.1 mole fraction of CO₂ occurs after injection of the cumulative amount of CO₂ of 0.66 mole and 0.82 mole. Both limited diffusive mixing and non-linear sorption behavior are likely mechanisms to explain the resulting composition profile of the production stream.

In contrast, Fig. 2.6 shows a wide front in the composition of the produced gas when injecting pure N₂. Furthermore, a CH₄ fraction of 0.03 is present in the produced gas stream after injection of 6.3 PVI (2.85 mole). Breakthrough of 0.1 mole fraction of N₂ occurs after the cumulative injection of 0.21 and 0.18 mole. Considerable diffusive mixing and limited replacement of sorbed CH₄ by N₂ are likely mechanisms to explain the wide front and the remaining presence of CH₄.

The composition of the produced gas stream when injecting a mixture of 20 vol.-% CO₂ in N₂ in a CH₄ saturated coal core is shown in Fig. 2.7. The N₂ fraction shows similar behavior as the experiment with injecting pure N₂, except that the N₂ fraction increases to 0.85-0.87 and not to 0.97 as observed in Fig. 2.6. The 5-7% difference between the injected and produced N₂ fractions is within the experimental accuracy of the experiment and therefore no further conclusions are drawn. The strongly sorbing CO₂ is produced later than the weakly sorbing N₂. The time required for breakthrough increases with the sorption capacity of the gas. The retention of the gas by the coal increases with the sorption capacity of the gas. This agrees with findings by Mazumder et al. (2008) and Jessen et al. (2008).

The composition of the produced gas stream, when injecting a mixture of 20 vol.-% CO₂ in H₂ in a CH₄ saturated coal core, is shown in Fig. 2.8. The

Output gas stream composition from CH₄ saturated coal during N₂, CO₂, N₂/CO₂ and H₂/CO₂ injection

composition of the produced gas stream is similar to that of 20 vol.-% CO₂ in N₂ injection. The main difference is the faster breakthrough of H₂ and its concurrent change in CH₄ fraction. The H₂ fraction at the end of the experiment is 0.82-0.83, which agrees with the injected fraction of 0.80 within the experimental accuracy. The sorption capacity of H₂ is low causing minimal retention by the coal leading to a fast breakthrough. In addition, the faster breakthrough may be also caused by faster diffusion of H₂ in CH₄. The CO₂ content in the produced gas stream is the same when injecting either of the two mixtures. Thus, the retention of CO₂ by the coal does not change when a weakly sorbing concomitantly injected component is replaced.

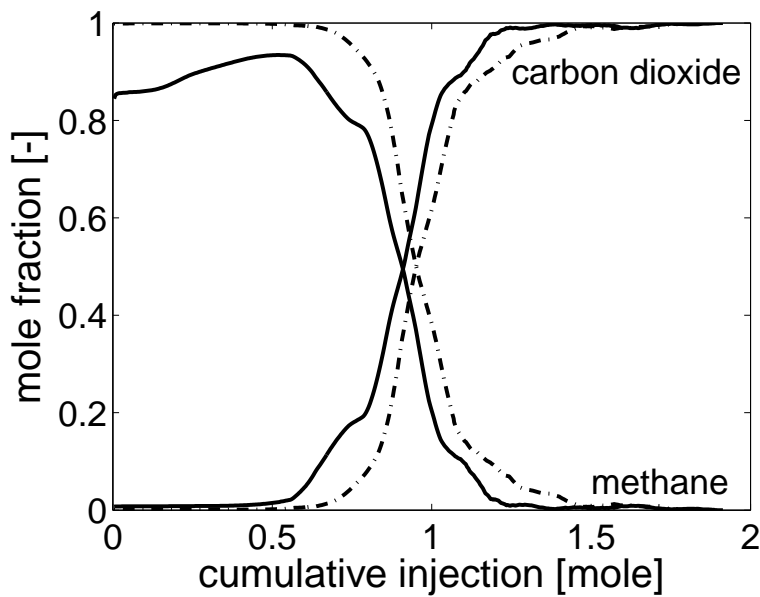


Figure 2.5: Composition of the produced gas vs. cumulative produced amount for the injection of pure CO₂. Duplicate experiments (7 and 8 in Table 2.3) are in fair agreement and depicted in solid and dotted lines, respectively. The difference in breakthrough is caused by the inaccuracy of the determination of the injected amount of CO₂. The H₂ fraction and concurrent low CH₄ fraction in experiment 7 are an experimental artifact due to insufficient evacuation after experiment 6.

2.3 Results and discussion

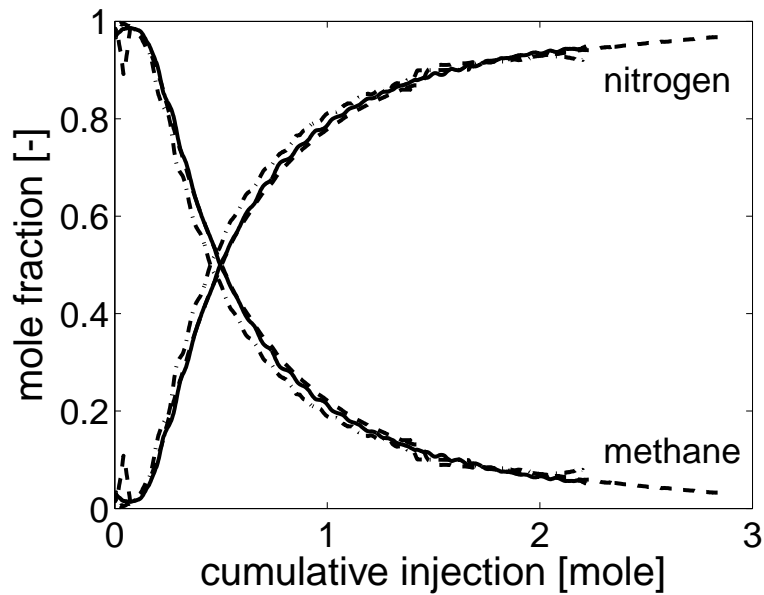


Figure 2.6: Composition of the produced gas vs. cumulative injected amount for the injection of pure N_2 . The three experiments (1, 2 and 9 in Table 2.3 are in good agreement and depicted in blue, black and red, respectively. The initial unexpected deviation in the composition of the production stream is an experimental artifact caused by remnant CO_2 due to insufficient evacuation. The N_2 production starts after injection of a cumulative amount of 0.1 mole. N_2 mole fraction increases with decreasing rate up to 0.97 during the experiment.

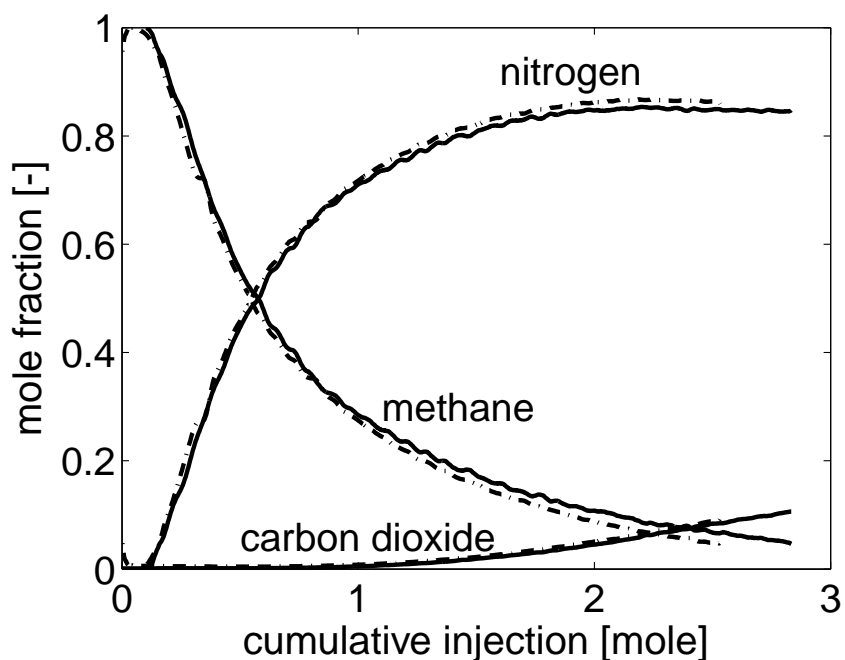


Figure 2.7: Composition of the produced gas vs. cumulative injected gas for the injection of a mixture of 20 vol-% CO₂ in N₂. Duplo experiment (3 and 4 in Table 2.3) are in good agreement and depicted in black and red, respectively. The initial presence of CO₂ in both experiments and the concurrent low CH₄ fraction are artifacts due to insufficient evacuation. N₂ production occurs after injection of 0.1 mole and rises with decreasing rate up to 0.85-0.87 after injection of 2.0 mole of gas mixture. CO₂ production starts when 0.7 mole is injected and rises linearly up to 0.11 during the experiment. The CH₄ fraction is 0.05 at the end of the experiment. Compositional equilibrium in the produced gas stream has not been attained after injection of 2.8 moles.

2.3 Results and discussion

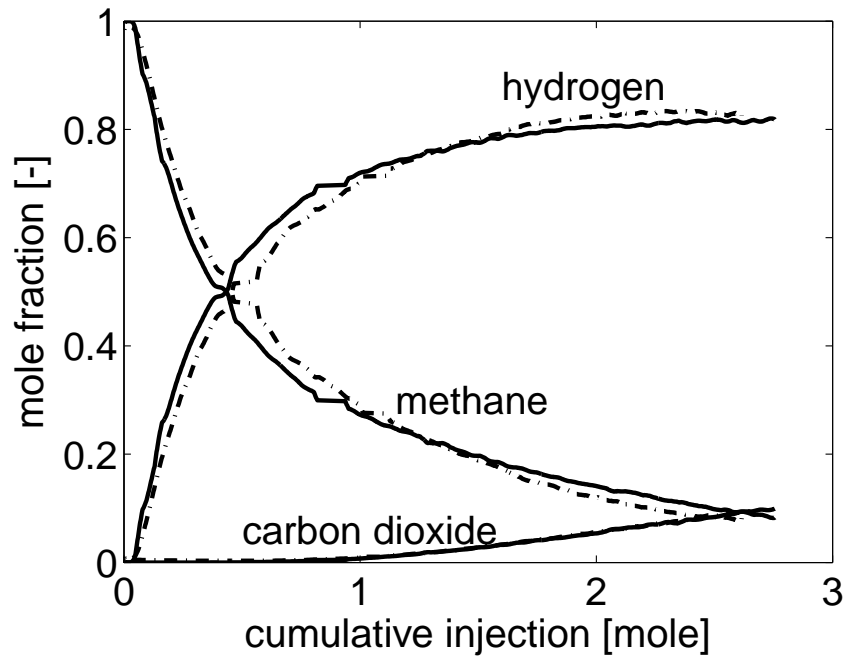


Figure 2.8: Composition of the produced gas vs. cumulative injected gas for the injection of a gas mixture of 20 vol-% CO₂ in H₂. Duplo experiment (5 and 6 in table 2.3) are in good agreement and depicted in red and black, respectively. H₂ production is almost instantaneous and rises with decreasing rate up to 0.82-0.83 after injecting 2 moles of gas mixture. The production of CO₂ is identical to results of the experiment with injecting a mixture of 20 vol-% CO₂ in N₂. The CH₄ fraction is 0.1 at the end of the experiment (2.7 moles injected).

2.4 Conclusions

Laboratory experiments on the production of CH₄ from an intact Nottinghamshire coal sample by injection of pure N₂, pure CO₂, a mixture of 20 vol-% CO₂ in N₂ and a mixture of 20 vol-% CO₂ in H₂ at a pore pressure of 8.0 MPa, a confining of pressure of 10 MPa and a temperature of 318 K have been performed. These experiments show production of at least 88% of the gas (CH₄) initially in place: one condition for the economical feasibility of production of coalbed methane by injection of pure N₂, pure CO₂ or a mixture of 20 vol-% CO₂ in N₂ is satisfied.

The experiment for which a mixture of 20 vol-% CO₂ in N₂ is injected shows that the breakthrough of CO₂ occurs later than that of N₂. This verifies earlier findings by Mazumder et al. (2008) and Jessen et al. (2008) that the time necessary for production of simultaneously injected components increases with increasing sorption capacity of the gas.

The experiment for which a mixture of 20 vol-% CO₂ in H₂ is injected differs minimally from the experiments for which a mixture of 20 vol-% CO₂ in N₂ is injected. H₂ is produced faster than N₂, which agrees with the expectation that the lower sorption capacity of coal for H₂ results in an earlier breakthrough. The CO₂ composition in the production stream is nearly identical for the experiments with both mixtures suggesting that the sorbing properties of the weakly sorbing gas do not influence the retention of the strongly sorbing component. It should be noted that this study focuses on the underlying physical and chemical processes of CBM production by gas injection. Therefore, a single coal sample is used, which allows comparison of the data. This study is not intended to give an overview of the efficiency of the method to enhance CBM production by injecting gas mixtures into various kinds of coal.

Chapter 3

Improved manometric apparatus for the determination of sorption

Abstract

An improved version of the manometric apparatus and its procedures for measuring excess sorption of supercritical carbon dioxide are presented in detail with a comprehensive error analysis. An improved manometric apparatus is necessary for accurate excess sorption measurements with supercritical carbon dioxide due to the difficulties associated with the high sensitivity of the density with pressure and temperature changes. The accuracy of the apparatus is validated by a duplicate measurement and comparison with literature data. Excess sorption and desorption data of CO₂ on Filtrasorb 400 at 318.11 K up to a CO₂ density of 1.7×10^4 mole/m³ (15.5 MPa) is reported for the validation of the apparatus.

The measured excess sorption maxima are 7.79 ± 0.04 mole CO₂ per kg of Filtrasorb 400 at a CO₂ density of 2253 mole/m³ for the first sorption isotherm and 7.91 ± 0.05 mole/kg at 2670 mole/m³ for its subsequent desorption isotherm. The sorption and desorption peaks of the duplicate experiments are 7.92 ± 0.04 mole/kg at 2303 mole/m³ and 8.10 ± 0.05 mole/kg at 2879 mole/m³, respectively. Both data sets show desorption data being higher than the sorp-

tion data of the same data set. The maximum discrepancy between the desorption and sorption isotherm of one data set is 0.15 mole/kg. The discrepancy between the two excess sorption isotherms is 0.12 mole/kg or less. The a priori error of the excess sorption measurements is between 0.02 and 0.06 mole/kg. The error due to He contamination is between 0.01 and 0.05 mole/kg. The difference between the a priori uncertainty and the observed maximum discrepancies is considered to be acceptable.

The sorption isotherms show the same qualitative behavior as data in literature. However, the peak height and the linear decrease of the excess sorption at high gas densities are 10% higher. A plot of the excess sorption versus the density is used to obtain the sorbed phase density and the specific micropore volume. These sorbed phase densities are in excellent agreement with data in literature. Furthermore, scaling of the excess sorption data with the specific micropore volumes results in a single curve representing data from this study and from literature.

3.1 Introduction

The amount of carbon dioxide (CO₂) that can be sorbed in coal plays an important role in CO₂ storage in underground coalbeds. Accurate sorption experiments of near critical CO₂ on coal are required for the following applications: (1) acquisition of fundamental understanding of CO₂ sorption on coal; (2) determination of the economic feasibility of enhanced coalbed methane (ECBM) projects; (3) determination of optimal operating conditions for CO₂ storage and methane (CH₄) production enhancement. A comprehensive overview on CO₂ storage in underground coal combined with the production of CH₄ is given by White (White et al., 2005).

Experimental data of near supercritical CO₂ sorption on any type of material are scarce; a limited number of gravimetric (Bae and Bhatia, 2006; Gao et al., 2004; Goodman et al., 2007; Hocker et al., 2003; Hoshino et al., 1993; Humayun and Tomasko, 2000; Jones et al., 1959; Ottiger et al., 2006; Pini et al., 2006, 2008; Sakurovs et al., 2007; Staudt et al., 2005), manometric (Busch et al., 2006, 2007; Chen et al., 1997; Goodman et al., 2007; Krooss et al., 2002; Siemons and Busch, 2007; Zhou et al., 2003) and volumetric (Fitzgerald et al., 2005; Sudibandriyo et al., 2003) studies have been published. Additional measurements are thus important. Several researchers (e.g. Humayun (Humayun and Tomasko, 2000) and Pini (Pini et al., 2006)) have expressed their concern with respect to the accuracy of supercritical CO₂ sorption determinations. The

3.1 Introduction

accuracy of the gravimetric method for supercritical CO₂ sorption has recently been discussed by Pini (Pini et al., 2006). The focus of the present article is the accuracy of the manometric method.

The accuracy of the manometric method far below (Borghard et al., 1991; Hersee and Ballingall, 1990; Kim et al., 2005; Pendleton and Badalyan, 2005; Robens et al., 1999; Rouquerol et al., 1999) and far above (Blackman et al., 2006; Broom, 2007; Mavor et al., 2004; Poirier et al., 2005) the critical point has been discussed in the literature. However, no literature regarding the quantification of the accuracy of near critical manometric sorption measurements could be found. All the same, a number of references report experimental manometric sorption data of CO₂ on coal (Busch et al., 2006, 2007; Goodman et al., 2007; Krooss et al., 2002; Siemons and Busch, 2007) and other materials (Chen et al., 1997; Zhou et al., 2003) in the near critical region. Recent gravimetric sorption measurements of CO₂ on coal (Bae and Bhatia, 2006; Ottiger et al., 2006; Sakurovs et al., 2007) show similar behavior, while results from recent manometric measurements differ considerably (see e.g. Goodman et al., 2007)). It is the opinion of the author that these variations in the manometric experiments are artifacts. These artifacts are caused by small uncertainties in the pressure and temperature measurements and by impurities. The proximity to the critical point magnifies these errors considerably.

In spite of the fact that the requirement of highly pure CO₂ has been recognized, no article mentions the possible effects of contamination due to poor flushing and evacuation of the set-up and its tubing. Using the Peng-Robinson EoS (Reid et al., 1987) it can be shown that an impurity of 0.3 mole% of N₂ changes the density by 2% at 10.0 MPa and 318 K. Other causes for artifacts are insufficient spatial and temporal temperature stability and inaccurate pressure and temperature measurements. e.g., at 10.0 MPa and 318 K a 10 kPa and 0.10 K fluctuation changes the CO₂ density by 0.6% and 2.0%, respectively. The sensitivity of an excess sorption isotherm on density errors varies considerably. e.g., an error of 2.0% in the density leads to an excess sorption error ranging from 2% to 70% for CO₂ excess sorption on F400 at 318.11 K, depending on which data point is influenced.

The accuracy of previous manometric experiments is impaired by the aforementioned errors. Therefore, we have developed a high accuracy manometric apparatus which reduces these errors by an order of magnitude. The main improvement of this apparatus is the higher accuracy of the pressure and temperature sensors. Furthermore, the accuracy is estimated with a comprehensive a priori error analysis (see Appendix F). The apparatus, the sample treatment and the experimental procedures are discussed in section 3.2. Duplicate

sorption measurements of CO₂ on Filtrasorb 400 at 318.11 K are compared to each other and to literature data in section 3.3. Findings are summarized in section 3.4. The appendices contain (B) the derivation of the data interpretation equation, (C) demonstration of the small influence of He contamination on the excess sorption measurements, (D) the leak-rate model, (E) demonstration of the negligibility of the influence of sorption on the leak-rate model, (F) an a priori uncertainty analysis, (G) the data processing procedure for the determination of the volume accessible to gas with a He experiment and (H) a concise explanation on regression of sorbed phase density, ρ_{sorbed} , and the specific micropore volume, $\bar{V}_{\text{micropore}}$, from excess sorption measurements.

3.2 Experimental methods

Manometric measurement of sorption is based on the principle of mass conservation. The excess sorption is defined as the difference between the total and the apparent amount of gas in the set-up. The total amount is the sum of gas added minus gas extracted and leaked. The apparent amount of gas is determined by multiplication of the gas density with the volume accessible to gas. This volume is determined by He sorption experiments before and after the actual CO₂ experiment (see appendix G).

3.2.1 Manometric apparatus

The manometric apparatus (Fig. 3.1 and table 3.1) consists of a sample cell (A) and a reference cell consisting only of tubing (B). The reference cell B consists of tubing with a total volume of $3524 \pm 4 \times 10^{-9} \text{ m}^3$. The volume of the reference cell can be enlarged to $12152 \pm 9 \times 10^{-9} \text{ m}^3$ by opening valve 1 to include vessel C. The option of an extendable reference cell is new for this type of set-up. It allows better control of the amount of added and extracted gas. Two similar sample cells are used to minimize the down time during sample exchange. The volumes of these two sample cells are $7833 \pm 6 \times 10^{-8}$ and $7590 \pm 10 \times 10^{-8} \text{ m}^3$. The uncertainty in the empty sample cell volume does not affect the accuracy of the sorption data.

The stainless steel sample cell (A) was designed at Delft University of Technology. It holds a maximum of $6 \times 10^{-5} \text{ m}^3$ of sorbent sample. The sample cell is sealed with Swagelok gaskets (SS-16-VCR-2GR) to minimize leakage. It contains filters of high porous sintered metal to minimize sample loss during

3.2 Experimental methods

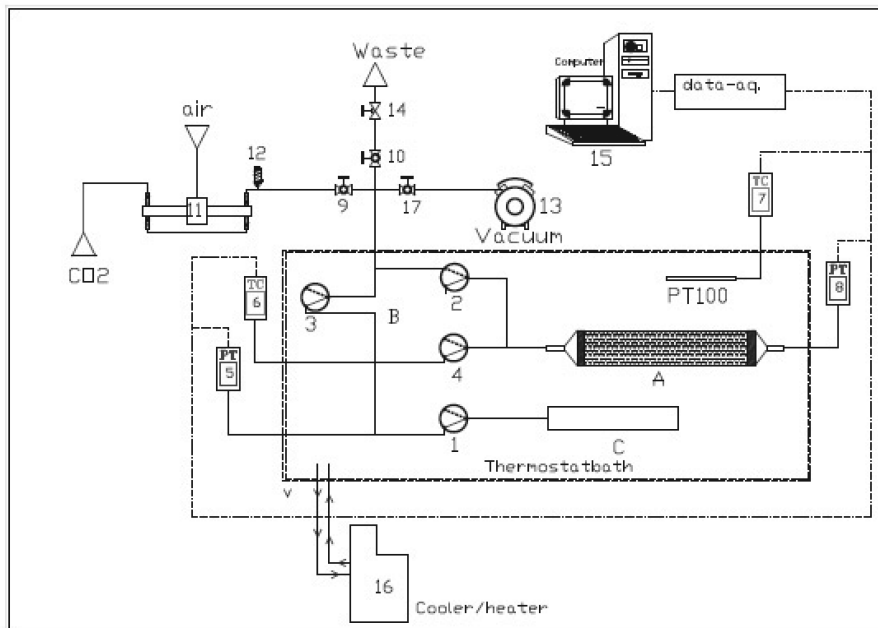


Figure 3.1: Technical drawing of the improved manometric apparatus. Details are given in the text.

Improved manometric apparatus for the determination of sorption

the desorption run.

A Paroscientific pressure sensor (8) monitors the pressure continuously. Its precision and accuracy¹ are reported by the manufacturer as 1 and 0.1 kPa in the temperature range of interest. The PT100 temperature sensor (7) monitors the temperature continuously. Its precision and accuracy¹ are reported by the manufacturer as 1 and 20 mK. Less accurate pressure (5) and temperature sensors (6) are used to monitor pressure in the sample cell and temperature in the reference cell. However, these lower accuracy measurements are not used in the determination of the excess sorption. Valves (1, 2, 3 and 4) have been selected based on their low leakage characteristics. However, they limit the experimental temperature to a maximum of 340 K. Furthermore, their internal diameter limits the evacuation of the set-up to a minimum pressure between 15 and 25 kPa. The thermostatically controlled bath has a volume of about $40 \times 10^{-3} \text{ m}^3$. A temperature control device (16) keeps the temperature constant within 20 mK. The gas added to the set-up is pressurized with a booster (11). The gas is extracted from the set-up with an evacuation pump (13). All tubing is 1/8" Swagelok 316SS and only metal connections are used.

Table 3.1: Specification of components of the improved manometric apparatus.

#	Name, type	Manufacturer
1,2,3,4	4 port 2-pos. Valve, air actuated, N60/H	VICI ag int.
5	Pressure transmitter, PTX600 0-250 bar	Druck NI. bv.
6	Thermocouple, K-type	Thermocoax
7	Thermoelement PT100 + F200 reader	Automated System Laboratories
8	Pressure transmitter, 9000 series	Paroscientific
9,10,17	Ball-valve, SS-43S4	Swagelok NS&S
11	Gas booster air actuated, two stage	Haskel
12	Relief valve Spring act., SS-RL3M4-S4	Swagelok NS&S
13	Vacuum pump, N820.3FT.40.18	KNF
14	Metering valve, SS-31-RS4	Swagelok NS&S
15	Data acquisition unit	Delft Uni. Tech.
16	Thermostat bath, Proline RP485	Lauda

The PTX611 and the K-type thermocouple are connected to a Keithley KPCI-3108 data-acquisition and control card, which is connected to a personal

¹Precision is defined in this thesis as the fluctuation in the measurement, while accuracy is defined as the expected maximum deviation from the true value.

3.2 Experimental methods

computer with a 16 channel 16 bits single ended analog input. The Paroscientific pressure sensor and PT100 are connected to the computer through RS232 interfaces. The valves are computer controlled via the data-acquisition and control card. Control of the valves is on a time interval basis. The acquisition software is written in Testpoint V3.4. The acquisition software scans the measurements every second and records them every 10 seconds.

The Helium (He) has a purity of 99.996 vol-%, and its critical properties are 5.1953 K, 227.46 kPa and 17399 mole/m³. The CO₂ has a purity of 99.990 vol-% and its critical properties are 304.1282 K, 7.3773 MPa and 10624.9 mole/m³. Gases are supplied by Linde Gas.

3.2.2 Sample selection and treatment

The experiments in this work are performed on Chemviron Filtrasorb 400, charge reference FE 05707A. This material, referred to as F400, is selected because it is a well-defined synthetic material with high sorption characteristics and its molecular structure and its micropore size distribution are considered to be similar to coal. Furthermore, three other publications report the excess sorption of CO₂ at 318 K on other Filtrasorb 400's. This makes it the best represented sorbent in the literature for supercritical CO₂ sorption measurements. The sorption data in this work is compared to the literature data in Sec. 3.3. Characterization of the sample is presented in 5.2.1.

Prior to the sorption experiments the sample cell, already filled with F400, is evacuated for 24 hours in an oven at a constant temperature of 473 K. To avoid air contamination the sample cell is filled with He above atmospheric pressure before its transfer from the oven to the set-up. Sample weight is measured within 0.02 g when transferring the cell from the oven to the set-up.

3.2.3 Experimental procedure

One experiment consists of four consecutive procedures: (1) He leak rate determination, (2) determination of the volume accessible to gas by a He sorption experiment, (3) actual sorption experiment with CO₂, (4) control measurement of He sorption. The second He sorption experiment is performed to ensure that the volume accessible to gas has not changed during the experiment.

The He leak rate is determined at approximately 20 MPa and the experimental temperature for more than 24 hours. The set-up is evacuated at the

experimental temperature for 24 hours before the start of the sorption experiment. A sorption experiment consists of the determination of the sorption isotherm followed by the determination of the desorption isotherm. For the sorption isotherm, gas is added step-wise to the evacuated sample cell until a pressure between 16 and 18 MPa is reached. For the desorption isotherm, gas is extracted sequentially from the sample cell until a pressure of 2 to 5 MPa is reached. Gas is added or removed after pressure and temperature are stable. Pressure stability is attained after 10^3 s for both CO₂ and He experiments. However, time intervals longer than 10^3 s, i.e., 10^4 s and 10^5 s are used to ensure stability.

3.2.4 Data analysis

Measured properties are pressure and temperature; these are converted to density values, ρ in mole/m³, using a highly accurate reference EoS (Span and Wagner, 1996). The volume accessible to gas in the sample, $V^{s,He}$ in m³, is determined from He sorption experiments (see appendix G). The sample mass, M in kg, is determined before the sample cell is built into the set-up. The parameters of the two CO₂ sorption experiments are shown in Table 3.2.

The excess amount of CO₂ sorbed is computed with Eq. (3.1) (derivation in Appendix B):

$$m_N^{\text{excess,CO}_2,\text{F400}} = \sum_{i=1}^N \frac{V_i^r}{M} \left(\rho_i^{\text{f,CO}_2} - \rho_i^{\text{e,CO}_2} \right) - \frac{\rho_N^{\text{e,CO}_2} V^{s,He} + n_N^{\text{l,CO}_2}}{M} \quad (3.1)$$

with

$$n_N^{\text{l,CO}_2} = \sum_{i=1}^N \rho_i^{\text{e,CO}_2} \left(V^{s,He} + V_i^r \right) \left[e^{t_i^e k^{\text{CO}_2} / (V^{s,He} + V_i^r)} - 1 \right] + V^{s,He} \sum_{i=1}^{N-1} \rho_i^{\text{e,CO}_2} \left[1 - e^{-t_i^f k^{\text{CO}_2} / V^{s,He}} \right]. \quad (3.2)$$

Here m_N^{excess} in mole/kg is the N^{th} determined excess sorption point. ρ_i^{e} is the gas density after stabilization of the reference and sample cell in step i . ρ_i^{f} is the stable gas density after gas addition to the reference cell for step i . n_N^{l} in mole is the cumulative gas leaked out of the sample cell at the N^{th} sorption determination (Derivation in Appendix D). V_i^r is the volume of the reference

3.3 Results and discussion

cell used in step i . k in m^3/s is the leak-rate coefficient. t_i^e and t_i^f are the times noted after equilibration and after filling, respectively.

The first term in Eq. 3.1 describes the summed difference between the number of moles in the reference cell for the filling and equilibrium phases. The second term describes the number of moles in the free phase in the sample cell. The first and second term in Eq. (3.2) are the cumulative number of moles leaked during the equilibrium phases and filling phases, respectively.

Table 3.2: Specification of the experimental parameters used in the determination of the sorption of CO_2 on Filtrasorb 400.

Exp.	M [$10^{-5} \times \text{kg}$]	T [K]	$V^{s,\text{He}}$ [cm^3]	$\rho^{s,\text{F400,He}}$ ¹ [kg/m^3]	k^{CO_2} ⁴ [mm^3/s]	duration [$10^5 \times \text{s}$]
1	3495 ± 3	318.12 ²	59.2 ³	2080 ± 40	3.1×10^{-4}	74.3
2	3557 ± 1	318.11 ²	61.1 ³	2060 ± 40	2.1×10^{-4}	4.3

¹ Mass density for He is calculated with $M \times (V_{empty}^s - V^{s,\text{He}})^{-1}$.

² Experimental accuracy of the temperature is 0.02 K.

³ Experimental accuracy of the volume accessible to gas is 0.1 cm^3 .

⁴ $k^{\text{CO}_2} \approx k^{\text{He}}/3$

3.3 Results and discussion

The determined mass density of F400 for the two experiments agree within the experimental uncertainty. Fig. 3.2 shows the two determined CO_2 excess sorption isotherms on F400 of this work and the literature data near 318 K on other F400's (Fitzgerald et al., 2005; Humayun and Tomasko, 2000; Pini et al., 2006). Experimental data of this work is shown in in Table J.1 (Appendix J). Table 3.2 shows the parameters for the two CO_2 sorption experiments.

The maxima of the excess sorption isotherms are 7.79 mole of CO_2 per kg of Filtrasorb 400 at 2253 mole/ m^3 and 7.92 mole/kg at a CO_2 density of 2303 mole/ m^3 . The maxima of the excess desorption isotherms are 7.91 mole/kg at 2670 mole/ m^3 and 8.10 mole/kg at 2879 mole/ m^3 . The desorption isotherms of both experiments are higher than the corresponding sorption data. The maximum observed discrepancy between desorption and sorption data is 0.15 mole/kg. The discrepancy of the sorption data sets is generally less than 0.12 mole/kg. The a priori error estimate of the excess sorption measurements is

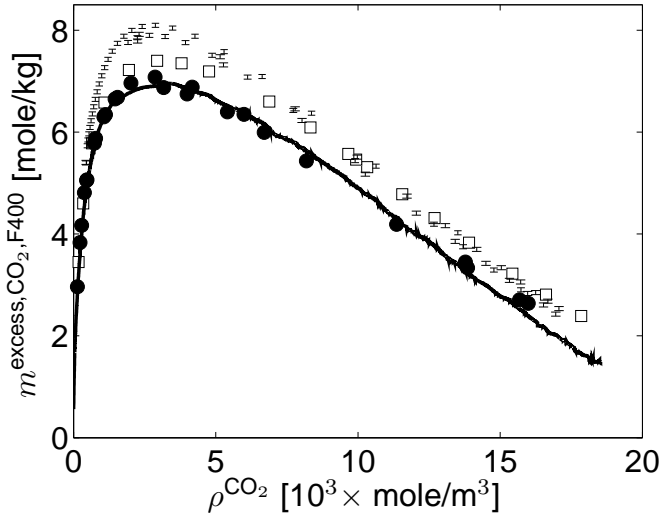


Figure 3.2: CO₂ excess sorption data of this work (error bars) and literature data on F400 at 318 K. The data show typical excess sorption behavior. Excess sorption data increases sharply with gas density to a peak value of 7 to 8 mole/kg near 3.0×10^3 mole/m³. The data decreases after the peak with a linear decrease for gas densities above 6×10^3 to 7×10^3 mole/m³. The data from Humayun and Tomasko (2000) (line) and Fitzgerald et al. (2005) (filled circles) are lowest and in excellent agreement. The data of this work (Table J.1) is in good internal agreement, but 10% higher than the data of Tomasko and Gasem. the data from Pini (Pini et al., 2006) (open squares) is in between the data of this work and that of Tomasko and Gasem.

0.02 to 0.06 mole/kg. The largest source of error varies throughout the experiment, as discussed in detail in Appendix F with the main source of error in the determination of V^s at high gas density. The difference between the *a priori* uncertainty and the observed maximum discrepancies is acceptable. However, it must be noted that possible causes for the discrepancies are (1) underestimation of the *a priori* error due to possibly underestimating the leakage and (2) the existence of an additional, slow, sorption process. The sorption isotherms of this work show the same qualitative behavior as literature. The quantitative match is also good, but the height of the sorption data and the linear decrease at high gas densities are 10% higher in this work than in literature.

3.3 Results and discussion

The high density part of the excess sorption isotherm can be interpreted with $m^{\text{excess}} = \bar{V}_{\text{micropore}} (\rho_{\text{sorbed}} - \rho)$, where $\bar{V}_{\text{micropore}}$ is the specific micropore volume of F400 and ρ_{sorbed} is the sorbed phase density. Humayun (Humayun and Tomasko, 2000) discusses how $\bar{V}_{\text{micropore}}$ and ρ_{sorbed} are determined from excess sorption measurements. This concept is concisely repeated in Appendix H. Table 3.3 shows the estimated sorbed phase densities and specific micropore volumes for all excess sorption isotherms.

The specific micropore volume of this work is the highest in comparison to literature data (Table 3.3). This is consistent with the excess sorption isotherm of this work (Fig. 3.2) being the highest. The differences in the specific micropore volumes of the F400 samples are expected to depend on the raw material and procedures used for F400 production. A 10% higher micropore volume is an acceptable variation of the properties of F400. The extrapolated sorbed phase density data of this work lies between the values reported by Tomasko and Gasem. All sorbed phase densities are in good agreement; with the value of Pini deviating the most. The cause of this deviation may be the limited accuracy of the regression (see Appendix H) due to the limited number of data points. The sorbed phase density is expected to vary minimally due to differences of the chemical composition and distributions of the micro-porosity of various Filtrasorb 400's. The data (Table 3.3) is in agreement with this hypothesis.

Table 3.3: Regressed micropore volumes and extrapolated density of sorbed CO₂ on Filtrasorb 400.

	T [K]	$\bar{V}_{\text{micropore}}^{\text{F400,CO}_2}$ [10 ⁻⁶ × m ³ /kg]	$\rho_{\text{sorbed}}^{\text{CO}_2,\text{F400}}$ [kmole/m ³]
Humayun and Tomasko (2000)	318.1(5)	364	22.9(3)
Fitzgerald et al. (2005)	318.1(5)	376	22.6(30)
Pini et al. (2006) ³	318.4	393±4	23.8±0.1
This work ³	318.11	429±4	22.7±0.2

Fig. 3.2 suggests that the excess isotherms determined by various authors agree within a constant proportionality factor. In agreement with this, we have found that the extrapolated sorbed phase density of CO₂ is more or less the same; the peak of the excess sorption is found at the same density value of

²Nomenclature in Table 3.4.

³Appendix H for details on regression.

2300 mole/m³. This leads to the postulate that the excess sorption is proportional to the specific micropore volume that can be accessed by CO₂. Hence, the ratio between the various excess sorption isotherms is equal to the ratio of these specific micropore volumes. This point of view is corroborated in Fig. 3.3, which shows the CO₂ isotherms on F400 at 318 K normalized to their estimated specific micropore volumes, $m^{\text{excess}}/\bar{V}^{\text{micropore}}$. The correlation between $\bar{V}^{\text{micropore}}$ and the BET surface area or the Dubinin-Radushkevich micropore volume is limited (see Chapter 5) as also noted by Humayun and Tomasko (2000).

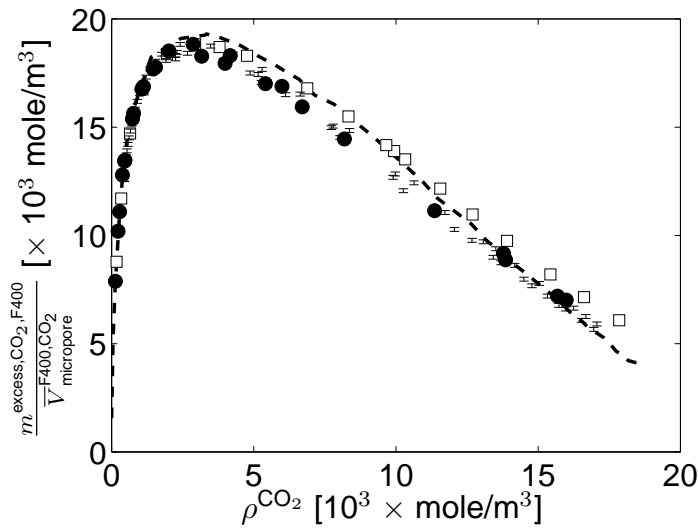


Figure 3.3: CO₂ excess sorption data on F400 at 318 K normalized by the specific micropore volumes. Plotted are the data of this article (error bars), Fitzgerald et al. (2006) (filled circles), Humayun and Tomasko (2000) (dashed line, smoothed, every 100th point plotted) and Pini et al. (2008) (open squares). All isotherms lie on a single curve (not shown); with most values agreeing within 1 mole/m³ ($\approx 5\%$ of the maximum excess sorption).

3.4 Summary

The details of an improved manometric apparatus and its accompanying procedures for accurate determinations of the sorption of supercritical CO₂ have been discussed. Two separate sets of experimental data of the excess sorption of CO₂ on Filtrasorb 400 at 318.11 K up to 1.7×10^4 mole/m³ have been presented. The variation between the two sets is 0.15 mole/kg at most, seeing that the *a priori* error is 0.06 mole/kg. This means that the observed discrepancy is a factor 2.5 larger, which is acceptable. The main source of uncertainty at high gas densities lies in the determination of V^s by means of He sorption experiments.

The isotherms of CO₂ on Filtrasorb 400 at 318 K from this work and from literature show qualitative similar behavior. The data in this work are 10% higher than literature. It was shown that the ratio between excess sorption isotherms was constant. This is consistent with an interpretation in terms of different specific micropore volumes. The good repeatability and excellent agreement with literature data confirms the accuracy of the improved manometric apparatus. The nomenclature used in this chapter is shown in Table 3.4.

Improved manometric apparatus for the determination of sorption

Table 3.4: Nomenclature

<i>Symbol</i>	<i>Unit</i>	<i>Physical quantity</i>
m^{excess}	mole/kg	(Gibbs) Excess sorption
m^{absolute}	mole/kg	Absolute sorption of gas
n^l	mole	Amount of leaked gas
n^{start}	mole	Amount of gas in sample cell before experiment
V_i^r	m^3	Reference cell volume used at step i
V^s	m^3	Volume accessible to gas in the sample cell
$\bar{V}_{\text{micropore}}$	m^3/kg	Specific micropore volume of sorbent
k	m^3/s	Leak-rate coefficient
t	s	time
ρ	mole/m^3	Molar density of free gas
ρ_{sorbed}	mole/m^3	Molar density of sorbed gas
ρ^*	kg/m^3	Mass density
T	K	Temperature
 <i>Superscripts</i>		
e		parameter related to equilibrium
f		parameter related to filling
vacuum		parameter related to vacuum
CO ₂		parameter determined with or specific for CO ₂
He		parameter determined with or specific for He
F400		parameter determined for F400
 <i>Subscripts</i>		
i		Parameter at step i
N		Parameter at step N

Chapter 4

Estimating the uncertainty in the equations of state of He and CO₂

Abstract

The sorption of gases on coal is of great importance for the use of gas injection to enhance coalbed methane production. Furthermore, when injecting carbon dioxide (CO₂) the project is eligible for carbon credits as the CO₂ is sequestered.

Accurate measurements of sorption at in-situ conditions have proven to be a complicated matter. Especially, the sorption of CO₂, pure or in a mixture, is particularly sensitive to experimental errors, because common in-situ conditions of deep coalbeds are near the critical point of CO₂. One source of uncertainty in sorption measurements is the accuracy with which gas densities have been determined. Accurate determinations of gas densities at in-situ conditions are complex and require the inclusion of specialized equipment. Therefore, gas densities are usually calculated from pressure and temperature measurements using an Equation of State (EoS). The accuracy of this EoS then influences the uncertainty in the sorption measurement. Therefore, it is essential that an EoS is used that is most accurate at the experimental conditions. However, there is generally little information available on the accuracy of an EoS for the

conditions of interest. This is particularly true for the calculation of densities of mixtures with an EoS.

The paper at hand describes an experimental method to estimate the accuracy of an EoS using a manometric sorption apparatus. This is demonstrated using He and CO₂ at 318.11 K and pressures between 0.1 and 17 MPa, which covers the range of interest for deep coalbeds.

The accuracies of the following EoS's have been estimated; Peng Robinson with Stryjek-Vera modification for CO₂; Peng Robinson with an alpha parameter proposed by Twu in 1995 for He; multi-parameter crossover equation of state by Sun et al. (2005) for CO₂; modified Benedict-Webb-Rubin EoS by McCarty and Arp (1990) for He; the reference EoS for CO₂ by Span and Wagner (1996).

It is found that the experimental method provides a lower limit estimate of the accuracy for an EoS. This estimate can be used as a first approximation of the EoS accuracy in the *a priori* error analysis of manometric sorption experiments.

4.1 Introduction

The production of coalbed methane reservoirs can be enhanced by carbon dioxide (CO₂) injection, as has been demonstrated for the San Juan basin (Scott et al., 1994). The production of coalbed methane with CO₂ injection is synergetic with CO₂ sequestration, as the injected CO₂ is stored in the underground coalbed (Gentzis, 1998). Because of the world's growing energy consumption (see Zupanc et al., 2007) and concerns on global warming (Metz et al., 2005), CO₂ enhanced coalbed methane production and the concurrent CO₂ sequestration receive much interest (Hackley et al., 2005; Katyal et al., 2007; Yu et al., 2007). The global coalbed methane reserves have been estimated to range from 84 to 262 Tm³ (White et al., 2005). Based on this the global storage capacity estimate is between 300 and 964 Gt of carbon dioxide by White et al.. However, it has not yet been proven that simultaneous methane production and CO₂ storage in coalbeds is energetically favorable. In order to investigate this, an exergy analysis is necessary (see de Swaan Arons et al., 2004; Graveland and Gisolf, 1998; Hinderink et al., 1996). Such an analysis requires a clear definition of the involved processes and a better understanding of the physics.

Experiments determining the sorption of gas on coal are done for two reasons: (1) To quantify the sequestrable amount of CO₂ in underground coal layers. This is an important factor in the exergy and cost-benefit analyses of

4.1 Introduction

enhanced coalbed methane (ECBM) projects; (2) To study the prevailing mechanism of sorption of gases and their mixtures in coal. This is crucial in order to improve the understanding of the physics of gas in coal for ECBM and/or sequestration of CO₂ in underground coal.

The sorption of gas on coal currently receives much experimental interest (see e.g. Busch et al., 2007; Day et al., 2008b; Fitzgerald et al., 2005; Goodman et al., 2004, 2007; Ottiger et al., 2008; Siemons and Busch, 2007). Several research groups have commented on the necessity of an accurate EoS in sorption experiments. However, no suggestions on how to test the quality of the EoS in combination with manometric sorption equipment have been made. Accurate density determinations are no trivial matter as demonstrated by Klimeck et al. (2001); Nowak et al. (1997).

The paper at hand presents a method to estimate EoS accuracy using a manometric sorption apparatus. This method is demonstrated using He and CO₂ at 318.11 K and for pressures ranging between 0.1 and 17 MPa. Typical conditions for deep coals are temperatures between 300 and 340 K and pressures between 7 and 12 MPa. Accurate EoS's are available for pure He and CO₂ at these conditions. This allows a comparison of the actual and estimated EoS accuracy. Additionally, the choice of He and CO₂ as gases is based on the difference in the proximity of the critical point at the experimental conditions: viz. the critical point of CO₂ is at 304.182 K and 7.3773 MPa, while the critical point of He is at 5.1953 K and 227.46 kPa. Consequently, the method is tested for nearly 'ideal' behavior (He) and for strongly 'non-ideal' behavior (CO₂; see Fig. 4.1). In addition, He is commonly used for empty volume and sample density determinations (see e.g. Suzuki, 1983), while the sorption of CO₂ is an interesting topic in itself (van Hemert et al., 2009).

Table 4.1: The equations of state (EoS's) tested in this study. The EoS's of the two gases are tabulated in order of increasing accuracy, i.e. the reference EoS's are the most accurate.

	cubic EoS	high accuracy EoS	reference ¹ EoS
He	Peng-Robinson with Twu's 1995 α (Poling et al., 2001)	n.a.	McCarty and Arp (1990)
CO ₂	Stryjek and Vera (1986)	Sun et al. (2005)	Span and Wagner (1996)

¹A reference EoS is an equation that represents all available experimental data within its experimental error.

Estimating the uncertainty in the equations of state of He and CO₂

Table 4.1 shows the EoS's of which the accuracy has been tested. The accuracy of an EoS is tested by measuring the volume of an empty cell using gas expansion. Commonly, He is used as gas because of its inert behavior (Suzuki, 1983). CO₂ is not inert and therefore not used for volume determinations. The method is based on the principle of mass conservation. The accuracy of the EoS is estimated by adding a constant relative random error to the densities determined by the EoS (see also subsection: data processing and error analysis). The magnitude of the EoS error is estimated by comparing the observed and calculated deviation of the volumes.

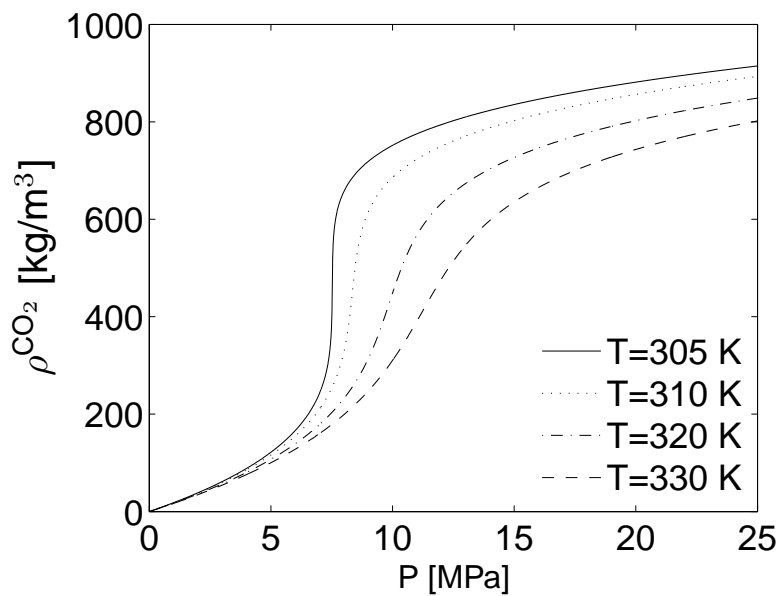


Figure 4.1: Density of CO₂ vs. pressure, above the critical temperature of 304.1285 K as calculated with the EoS by Span and Wagner (1996). At temperatures below the critical temperature, there is a discontinuous increase in the density from gas to liquid. This discontinuity disappears above the critical temperature. At 310 K the density varies continuously, but increases steeply from 300 kg/m³, characteristic for gaseous CO₂, to 700 kg/m³, characteristic for a liquid. The figure clearly demonstrates the sensitivity of the CO₂ density to pressure and temperature.

4.2 Material and methods

4.2 Material and methods

4.2.1 Apparatus

A technical drawing of the manometric apparatus is shown in Fig. 4.2. A detailed description of the apparatus is given in chapter 3.2.1. The volume of the sample cell, V_s , and the reference cell, V_r , are $78.33 \pm 0.06 \text{ cm}^3$ and $12.152 \pm 0.009 \text{ cm}^3$, respectively. Both cells are completely immersed into a thermostatically controlled bath, which is kept at a constant temperature of $318.11 \pm 0.02 \text{ K}$. Temporal and spatial temperature variations are within 0.02 K . Temperature is measured with an Automated System Laboratories Thermo-element PT100 and F200 reader with an accuracy of 0.02 K . The pressure is measured with a Paroscientific 9000 series pressure transmitter with a 1 kPa accuracy.

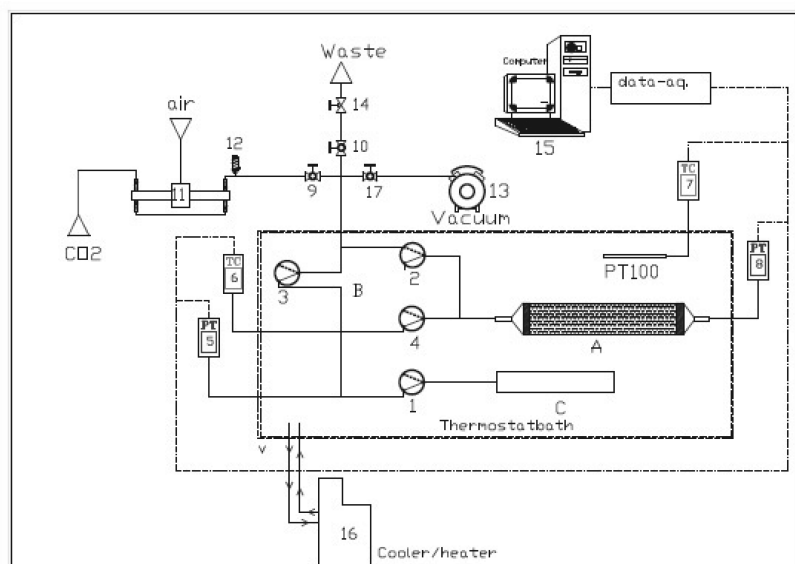


Figure 4.2: Technical drawing of the manometric apparatus. The sample cell is denoted by A. The reference cell consists of parts B and C with the connecting tubing.

4.2.2 Samples

The helium used is 99.996 volume-% pure. The critical properties of He are 5.1953 K, 227.46 kPa and 17399 mole/m³. The carbon dioxide used is at least 99.990 volume-% pure. The critical properties of CO₂ are 304.1282 K, 7.3773 MPa and 10624.9 mole/m³. He and CO₂ are supplied by Linde Gas. Impurities in the CO₂ are reported by the manufacturer as < 60 ppmv N₂, < 5 ppmv O₂ and < 25 ppmv H₂O. The tubing and apparatus are rinsed prior to the experiments to avoid (air) contamination. Air contamination of the CO₂ changes its density behavior significantly in particular near its critical point as discussed by (van Hemert et al., 2007).

4.2.3 Experimental procedure

The entire set-up is immersed into a thermostatically controlled bath kept at a constant temperature of 318.11±0.02 K. Sufficient delays (> 1 h) are taken into account for every pressure measurement to ensure that the gas in the set-up is at thermal equilibrium. The cells and tubing are evacuated and rinsed with He or CO₂. The sample cell is filled via the reference cell up to pressure P_s and then isolated by closing the valve connecting the two cells. The reference cell is filled up to pressure P_r (≈ 20 MPa). The connecting valve is opened and the pressure in both cells equilibrates at $P_{r,s}$. This procedure is repeated for various values of P_s . The densities are calculated from the measured pressures and temperatures. Based on these densities, the sample cell volume is determined.

4.2.4 Data processing and error analysis

The data processing is based on the mass balance

$$n_r + n_s = n_{r,s} , \quad (4.1)$$

where n_r [kg] is the mass of the gas in the isolated reference cell, n_s [kg] is the mass of the gas in the isolated sample cell and $n_{r,s}$ [kg] is the mass of the gas in the two connected cells. The amount of mass of gas in a cell is defined as $n \equiv \rho V$. Inserting this definition in Eq. 4.1 and solving for V_s gives

$$V_s = V_r \frac{\rho_r - \rho_{r,s}}{\rho_{r,s} - \rho_s} , \quad (4.2)$$

where ρ_r , ρ_s and $\rho_{r,s}$ are the densities of the gas in the isolated reference cell, isolated sample cell and the two connected cells, respectively. The volumes

4.2 Material and methods

of the reference cell and sample cell are V_r and V_s . The densities are calculated using an EoS based on the measured pressures and temperatures, $\rho_\gamma = \rho(P_\gamma, T; \text{EoS})$. It is interesting to note that Eq. 4.2 is not very sensitive for systematic errors. In other words, if ρ_r , ρ_s and $\rho_{r,s}$ are multiplied by the same factor no difference in the V_s is observed. This limits the usefulness of this method to determine deviations of the EoS.

The *a priori* error is defined here as the error caused by the limited accuracy of the pressure and temperature measurements. The change in the cell volumes due to pressure and temperature is negligible as the bulk modulus of steel is 160 GPa and the thermal expansion coefficient is $1.2 \times 10^{-5} \text{ K}^{-1}$. The *a priori* error in V_s from errors in pressure and temperature, $\delta V_s^{P,T}$, is calculated using the standard error analysis Taylor (1996).

$$\delta V_s^{P,T} = \sqrt{\frac{(\delta \rho_r)^2}{[\rho_{r,s} - \rho_s]^2} + \frac{[\rho_r - \rho_{r,s}]^2}{[\rho_{r,s} - \rho_s]^4} (\delta \rho_s)^2 + \frac{[\rho_r - \rho_s]^2}{[\rho_{r,s} - \rho_s]^4} (\delta \rho_{r,s})^2}. \quad (4.3)$$

The uncertainty of the calculated density, $\delta \rho$, due to the limited pressure and temperature accuracy is calculated by $\delta \rho_\gamma = \partial_P \rho_\gamma \delta P + \partial_T \rho_\gamma \delta T$. These partial derivatives are numerically calculated.

An estimate of the error caused by the EoS is calculated using the above mentioned standard error analysis. It is assumed that deviations in the EoS are random and that the relative uncertainty in the three densities is equal. These assumptions simplify the calculation of the resulting error and provide an estimate of the accuracy. However, the resulting error underestimates the actual error, because systematic deviations cancel out. The uncertainty in V_s due to the limited accuracy of the EoS, δV_s^{EoS} , is

$$\delta V_s^{\text{EoS}} = \alpha \sqrt{\frac{(\rho_r)^2}{[\rho_{r,s} - \rho_s]^2} + \frac{[\rho_r - \rho_{r,s}]^2}{[\rho_{r,s} - \rho_s]^4} (\rho_s)^2 + \frac{[\rho_r - \rho_s]^2}{[\rho_{r,s} - \rho_s]^4} (\rho_{r,s})^2}, \quad (4.4)$$

where α is the relative random error in ρ_s , ρ_r and $\rho_{r,s}$. The α factor is introduced in this study to give an estimate of the accuracy of EoS for the calculated gas densities. A more comprehensive approach for the determination of the accuracy of the EoS is left for future work.

4.2.5 Equations of State

The density of He is calculated using (a) the (MA) modified Benedict-Webb-Rubin EoS of McCarty and Arp (1990); (b) the (PRT) Peng-Robinson with the 1995 alpha function of Twu Poling et al. (2001). The MA is the EoS that describes He density with the highest accuracy at the experimental conditions. It is considered to be accurate within 0.1%. Densities calculated with the PRT are smaller than MA calculated densities. The density deviation is given as a scaled density difference

$$\Delta\rho_{\text{rel}} = \frac{\rho(P, 318.11; \text{EoS}) - \rho(P, 318.11; \text{ref. EoS})}{\rho(P, 318.11; \text{ref. EoS})} . \quad (4.5)$$

and for He is approximated by

$$\Delta\rho_{\text{rel}}^{\text{He}} \approx -\frac{P}{8.7} - \frac{1}{19.16} , \quad (4.6)$$

which results in a maximum deviation of 2.3% at 20 MPa.

The density of CO₂ is calculated using the (SW) Span and Wagner (1996) EoS, the (SKE) Sun et al. (2005) EoS and the (PRSV) Stryjek-Vera modification of the Peng-Robinson (Angus et al., 1976; Poling et al., 2001; Stryjek and Vera, 1986). The SW EoS is the most accurate EoS for CO₂ and reproduces experimental densities in the pressure and temperature range of interest with an accuracy of 0.02% Klimeck et al. (2001); Nowak et al. (1997). Fig. 4.3 presents the relative density deviations of SKE and the PRSV with respect to the SW.

4.3 Results and discussion

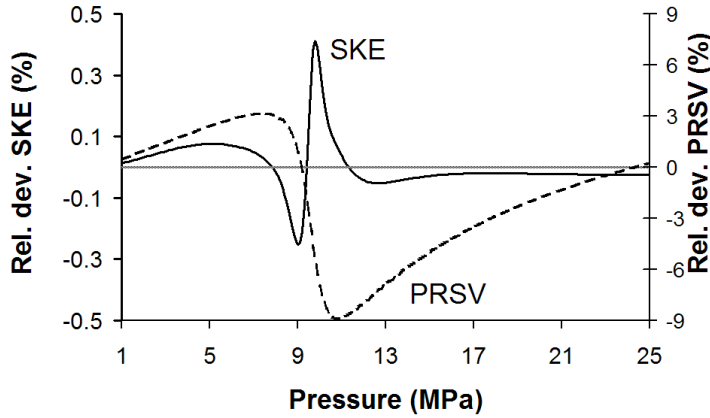


Figure 4.3: Relative deviations, Eq. 4.5 for CO₂ densities calculated with the SKE and PRSV at 318.11 K. Deviations vary between -0.3% and 0.4% for SKE and -9% and 3% for the PRSV.

4.3 Results and discussion

Fig. 4.4 shows that the determination of the volume using He and applying the MA deviates less than 0.15% while applying the PRT results in errors up to 2.25%. The volume deviations are interpreted using constant relative random errors in the densities (Eq. 4.4 in subsection data processing and error analysis). Fig. 4.5 shows that deviations from applying the PRT can be explained with a random error (α) of 0.1%. This deviation is a factor of 20 smaller than the maximum actual deviation of the PRT calculated densities. The explanation for this is that uncertainties in the densities cancel out due to the ratio in Eq. 4.2. Fig. 4.5 shows that the deviations from applying the MA can be explained by a random error (α) of 0.005%, This is a factor of two smaller than the stated accuracy of the MA with respect to the density calculations (0.1%; McCarty and Arp (1990)).

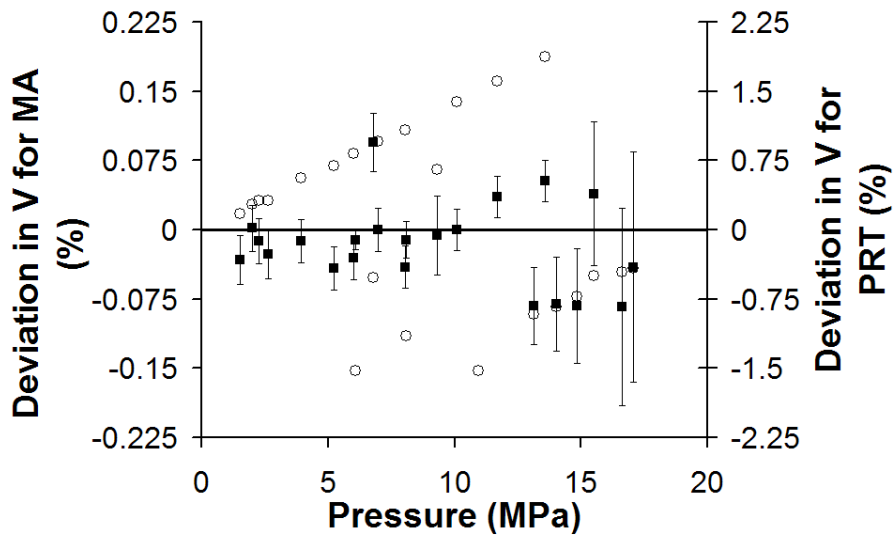


Figure 4.4: He experiment at 318.11 K. Deviations of the sample cell volumes using MA (■, left y-axis), and PRT (○, right y-axis). Determinations with MA are an order of magnitude more accurate than with PRT. Plotted errorbars are *a priori* estimates due to pressure and temperature uncertainties.

4.3 Results and discussion

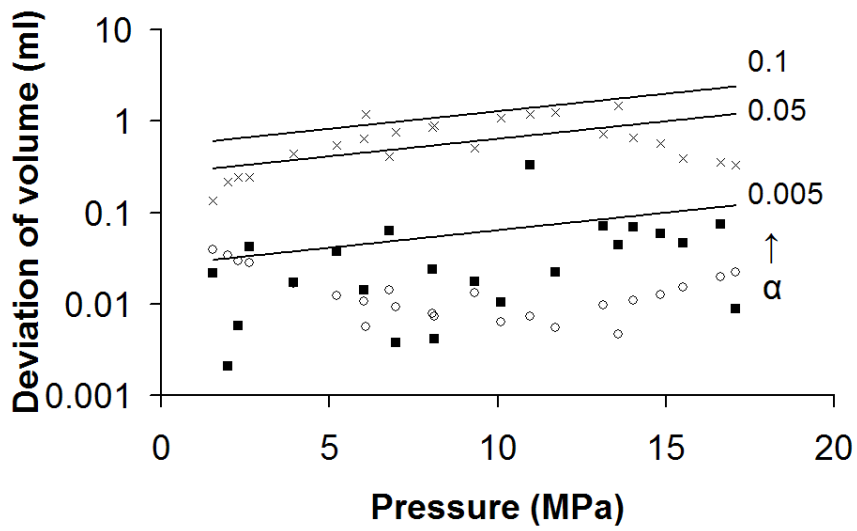


Figure 4.5: He experiment, 318.11 K: Deviations resulting from applying the MA (■) and the PRT (×). Calculated *a priori* errors (○). The lines represent mean error estimates of the EoS for different random uncertainties ($\alpha=0.005; 0.05; 0.1$). These lines give the maximum lower limit estimate of the uncertainty introduced by the EoS.

Fig. 4.6 shows that volume measurements with CO₂ are less accurate than with He. This is expected as the pressure-density behavior of a gas is more complex near its critical temperature. Volume deviations applying the SW, SKE and PRSV have a maximum of 5, 6 and 50%, respectively. The deviations for all three EoS's are considerably larger than the *a priori* errors of approximately 1%. Fig. 4.6 demonstrates that the data set is best described by applying the SW, as expected.

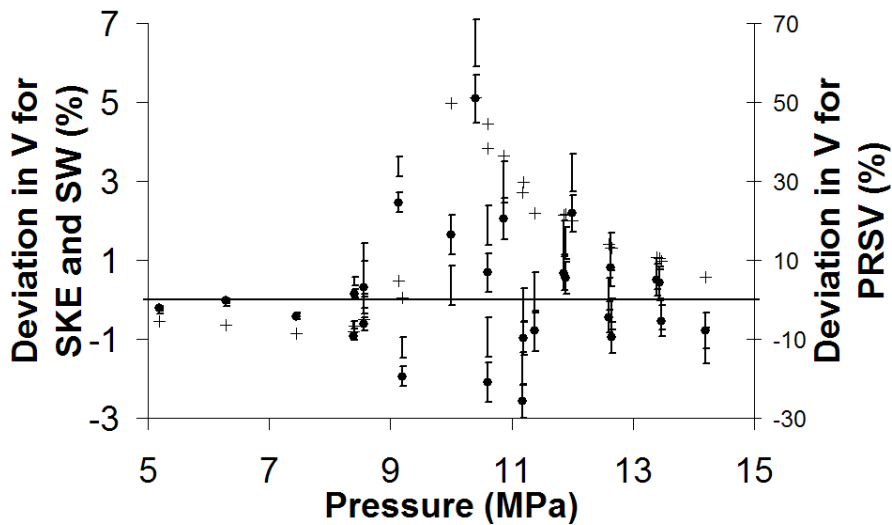


Figure 4.6: CO₂ experiment at 318.11 K. Deviations of the sample cell volumes using SW (•, left y-axis), SKE (only error bars, left y-axis) and the PRSV (+, right y-axis). Deviations are at a maximum near 10 MPa, where $\partial_P \rho$ is at a maximum. PRSV determinations are an order of magnitude less accurate than SW or SKE determinations. Differences between SW and SKE are minimal. Plotted errorbars are *a priori* estimates due to pressure and temperature uncertainties.

Fig. 4.7 shows that the deviations from applying PRSV can be explained by a random uncertainty (α) of 4.0% or less. This is a factor of 2 smaller than the actual deviation of the PRSV calculated densities (Fig. 4.3). As previously explained, the assumption of the error being random instead of systematic (Fig. 4.3) overestimates the influence of the EoS density uncertainty. The He discrepancy is concealed due its linear behavior. The non-ideal behavior of CO₂

4.3 Results and discussion

(Fig. 4.1) makes it easier to detect systematic discrepancies than for He.

Fig. 4.7 shows that deviations from applying the SW are explained by a random error of $\alpha \approx 0.2\%$. This is a factor of 10 higher than the SW accuracy, reported by Klimeck et al. (2001). In addition, the errors when applying the SKE require a random error (α) of 1.0% or less. This is a factor of 2 larger than the actual discrepancy of 0.4% (Fig. 4.3). The atypical overestimation of the SKE error reflects the complicated behaviour of CO₂ at the conditions of interest. The error in the SW EoS is specific for CO₂ and exceeds the *a priori* error estimate. The most likely cause of the deviating behaviour is contamination of the CO₂. Post-experimental analysis of the gas did not show contaminants within the detection limit of 0.01%. Additional investigation, beyond the scope of this study, is required to confirm whether contaminants below 0.01% can realistically explain the deviations. The *a priori* error estimate for manometric sorption experiments (see 3) may have to be updated to incorporate the observed discrepancies. In particular, an additional error of 0.2% in the densities for pressures between 8 to 12 MPa at 318 K seems prudent. The initial estimate of this influence increases the *a priori* uncertainty in the manometric sorption from 0.06 mole/kg (3) to 0.1 mole/kg.

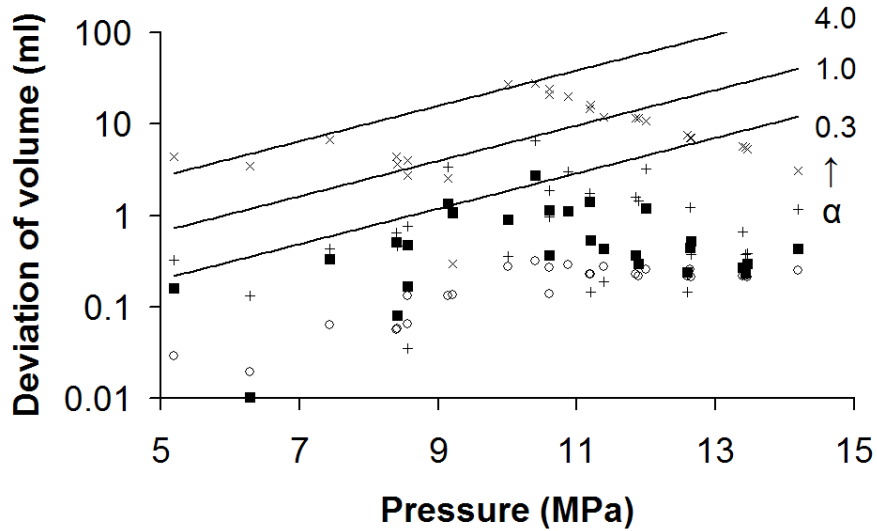


Figure 4.7: CO₂ experiment at 318.11 K. Deviations resulting from applying the SW (■), SKE (+) and the PRSV (×). Calculated *a priori* errors (○). The lines represent maximum error estimates of the EoS for different random uncertainties ($\alpha=0.3; 1.0; 3.0$). These lines give the worst case estimate of the lower limit uncertainty introduced by the EoS. The *a priori* errors are larger for CO₂ than for He, because its partial derivatives $\partial_{F\rho}$ and $\partial_{T\rho}$ are larger. Observed deviations of the Sun, Kiselev and Ely EoS are slightly higher than with the Span and Wagner EoS.

4.4 Conclusions

A straightforward and cost-effective approach for the verification of an equation of state (EoS) for use in manometric sorption experiments has been suggested and demonstrated. Furthermore, this approach can be used to determine densities at elevated pressures and temperatures based on densities at low pressure and temperature. The pressure and temperature sensors limit the accuracy of volume measurements at 318.11 K to 0.15% for He and 1% for CO₂, respectively.

The suggested method generally underestimates the error of the EoS. This is especially true for an EoS that calculates consistently too low or too high density values.

The following relative random uncertainties associated with an EoS have been estimated:

- 2% for the 9% accurate Peng-Robinson with Stryjek-Vera modification for CO₂.
- 0.2% for the 2% accurate Peng-Robinson Twu EoS for He.
- 1.0% for the 0.4% accurate Sun, Kiselev and Ely multi-parameter crossover EoS for CO₂.
- 0.2% for the 0.02% accurate Span and Wagner reference EoS. The higher uncertainty is likely caused by contaminations below the detection limit (0.01%).
- The error in the McCarty and Arp (1990) equation of state for helium does not introduce an experimental error that is significant in comparison to the experimental error of the pressure and temperature measurements.

It is concluded that the presented method can provide valuable insight into the accuracy of an EoS using only a manometric sorption apparatus. This is of particular interest for sorption experiments with gas mixtures, because such experiments require an equation of state that describes the density of the gas mixtures properly. At this time, equations of state that are sufficiently accurate for manometric determinations near the critical point are generally only available for a limited number of pure gases.

Chapter 5

Inter-laboratory comparison of supercritical CO₂ sorption in activated carbon

Abstract

To assess and improve the quality of experimentally determined high-pressure sorption isotherms of carbon dioxide on coals, an inter-laboratory study was conducted among four European research laboratories: Delft University of Technology (DUT) in the Netherlands, RWT Aachen University (RWT) in Germany, Faculté Polytechnique Mons (FPM) in Belgium and Institut National de l'Environnement Industriel et des Risques (INERIS) in France. Sorption is measured on activated carbon Filtrasorb 400 (F400) at 318 K up to 16 MPa using the manometric (DUT and RWT) and gravimetric (FPM and INERIS) method. Previous inter-laboratory comparisons for CO₂ sorption data on coal at high pressures showed significant deviations, which were attributed to variations in the moisture content of the sample. Using F400 allows evacuation at 473 K ensuring that the sample is completely dry. Furthermore, CO₂ sorption on F400 is well-represented in literature. These experiments on F400 provide a reference and serve to validate the different apparatus.

Sorption data show the same qualitative behavior as reported in literature. Sorption increases with gas density up to a maximum around 5 MPa

and then decreases. The data sets are fitted by a Langmuir-type and Dubinin-Radushkevich-type equation to facilitate comparison. The fitted parameters agree with their weighted average within three times the *a posteriori* error for the Langmuir and within five times for the Dubinin-Radushkevich. The good agreement of the inter-laboratory sorption data in the fitted parameters validates the accuracy of the different apparatus for the sorption determination of supercritical CO₂.

5.1 Introduction

Among the various options considered for the geological storage of carbon dioxide (CO₂), the injection of CO₂ into deep, unminable coal seams, in combination with the production of coalbed methane, is considered a niche technology. The European RECOPOL¹ project, funded by research programs CATO² and MOVECBM³, has demonstrated the technical feasibility of CO₂ injection into typical European Carboniferous coal seams. Laboratory experiments conducted by the two partner groups at the Delft University of Technology (The Netherlands) and RWT Aachen University (Germany) provided fundamental information on the interaction of CO₂ and CH₄ with natural coals under in-situ conditions. However, considerable problems in the reproducibility of supercritical CO₂ sorption were revealed. Similar problems were encountered by other groups and have been addressed by two recent inter-laboratory studies (Goodman et al., 2004, 2007) of CO₂ sorption on Argonne Premium coals, initiated by the U.S. Department of Energy-National Energy Technology Laboratory (DOE-NETL). The result of these studies was that, in spite of considerable improvements in accuracy, the quality of CO₂ sorption measurements does not yet meet the standards required for reliable modeling and predictions. The time and temperature for evacuation in this study have been increased to ensure no remnant moisture is present. Goodman et al. (2007) hypothesized that differences in sorption were caused by differences in the moisture content.

The first inter-laboratory study (Goodman et al., 2004) compared the sorption of CO₂ on dry coals at 295 and 328 K up to a pressure of 7 MPa as measured by five laboratories. Five types of coal, covering a maturity range from 0.25 to 1.68% vitrinite reflectance, were used. The preparation procedure involved drying of the samples for 36 h at 353 K under vacuum. It was

¹<http://recopol.nitg.tno.nl>

²<http://www.co2-cato.nl>

³<http://www.movecbm.eu>

5.1 Introduction

found that sorption for medium- to low-rank coals deviated by more than 100%. Sorption data on high-rank coals was considered to be sufficiently accurate. The second inter-laboratory study (Goodman et al., 2007) compared the sorption of CO₂ on moisture-equilibrated coals at 298 K and 328 K up to a pressure of 15 MPa as measured by six laboratories. Moisture equilibration was achieved by a modified ASTM D1412-99⁴ procedure. Three types of coal, covering a maturity range from lignite to high volatile bituminous, were used. Sorption data showed good agreement for pressures up to 8 MPa. However, at higher pressures sorption diverged significantly for the different laboratories.

The aim of this study is to assess and improve the quality of sorption data at high pressures for supercritical carbon dioxide. In contrast to earlier inter-laboratory tests (Goodman et al., 2004, 2007), this study is set up as an open project with information exchange and regular seminars. The exchange of information facilitated the elimination of error sources, leading to increased accuracy and standards and procedures for these types of experiments. This study is the first phase of an European inter-laboratory project aimed at collecting and comparing baseline results on the performance of the experimental devices of the participating laboratories. Therefore, a well-characterized activated carbon sample, Filtrasorb 400 (F400), is used for this series of measurements. Advantages of using F400 are that F400 is homogeneous, readily available and its chemical composition and micropore structure are similar to those of coal. Furthermore, F400 is resistant to high temperatures facilitating water removal, one of the main error sources in previous inter-laboratory comparisons. The F400 has been used in CO₂ sorption studies by other researchers (Fitzgerald et al., 2005; Humayun and Tomasko, 2000; Pini et al., 2006). Their results are compared with the results of this study in chapter 3. Experiments have been performed at 318 K up to 16 MPa; conditions typical for coalbeds suited for CO₂ storage.

The CO₂ sorption is determined with the manometric (Busch et al., 2003; Krooss et al., 2002; Siemons and Busch, 2007; van Hemert et al., 2009) and the gravimetric method (Bae and Bhatia, 2006; De Weireld et al., 1999; Pini et al., 2006; Sakurovs et al., 2007). These two methods are based on different physical principles; the manometric method determines sorption from the decrease in the pressure in a cell of known volume; the gravimetric method measures the weight increase of the sorbent immersed in sorbate. Both methods provide accurate excess sorption isotherms for simple and well-characterized

⁴ASTM D1412-99: Standard Test Method for Equilibrium Moisture of Coal at 96 to 97 Percent Relative Humidity

sorption systems (e.g. methane sorption on activated carbon).

The different data sets are fitted, without using the *a priori* errors, by two simple equations to facilitate comparison. The simple equations are Eq. 5.1 and 5.2. The former is based on the Langmuir equation, while the latter is based on the Dubinin-Radushkevich equation. Both equations are modified for excess sorption experiments as suggested by Sakurovs et al. (2007). The physical validity of the equations and the fitted parameters are outside the scope of this thesis. The Langmuir type equation is

$$m_{\text{excess}}^{\text{CO}_2, \text{F400}} = \hat{\rho}_{\text{sorbed}}^{\text{CO}_2, \text{F400}} \bar{V}_{\text{micropore}}^{\infty, \text{CO}_2, \text{F400}} \frac{\rho^{\text{CO}_2}}{K_L + \rho^{\text{CO}_2}} \left(1 - \frac{\rho^{\text{CO}_2}}{\hat{\rho}_{\text{sorbed}}^{\text{CO}_2, \text{F400}}} \right), \quad (5.1)$$

where K_L describes the increasing occupation of the microporosity with increasing density, ρ^{CO_2} ; $\hat{\rho}_{\text{sorbed}}^{\text{CO}_2, \text{F400}}$ is the constant density of the CO_2 sorbed in the F400 and $\bar{V}_{\text{micropore}}^{\infty, \text{CO}_2, \text{F400}}$ is the specific maximum occupied volume of CO_2 sorbed in the F400 at infinite gas density. The Dubinin-Radushkevich (DR) equation is

$$m_{\text{excess}}^{\text{CO}_2, \text{F400}} = m_0^{\text{CO}_2, \text{F400}} \exp\left(-D^{\text{CO}_2, \text{F400}} \left[\ln \frac{\hat{\rho}_{\text{sorbed}}^{\text{CO}_2, \text{F400}}}{\rho^{\text{CO}_2}} \right]^2\right) \left(1 - \frac{\rho^{\text{CO}_2}}{\hat{\rho}_{\text{sorbed}}^{\text{CO}_2, \text{F400}}} \right), \quad (5.2)$$

where $m_0^{\text{CO}_2, \text{F400}}$ is the maximum sorption capacity of CO_2 in the F400 and $D^{\text{CO}_2, \text{F400}}$ is a constant that depends on the heat of adsorption and the affinity of the CO_2 for the F400.

5.2 Materials and methods

5.2.1 Sample and sample preparation

Activated carbon, Filtrasorb 400 (F400), is obtained from Calgon Carbon Corporation of the Chemviron Carbon GmbH (Germany). Proximate⁵ and ultimate⁶ analysis of the Filtrasorb 400 are shown in Table 5.1 and 5.2. Aliquots of the same batch are distributed among the laboratories to exclude heterogeneity effects. The BET surface and the Dubinin-Radushkevich micropore volume of the F400 in this study is determined with 77 K nitrogen adsorption as 1063

⁵ASTM D3172 - 07a Standard Practice for Proximate Analysis of Coal and Coke.

⁶ASTM D3176 - 89(2002) Standard Practice for Ultimate Analysis of Coal and Coke.

5.2 Materials and methods

m²/g and 510 cm³/kg (Gensterblum et al.), respectively. The properties of similar carbons have been reported by Fitzgerald et al. (2005); Humayun and Tomasko (2000); Jagiello and Thommes (2003).

Table 5.1: Proximate analysis of the dried Filtrasorb 400. Standard deviation reflects the variability of the coal sample used in the experiments. The natural variation in Filtrasorb 400 is expected to be larger.

Moisture mass-%	Vol. matter mass-% (w.f.)	Fix. Carbon mass-% (d.a.f.)	Ash mass-% (w.f.)
1.52±0.17	1.32±0.03	91.06±0.28	6.1±0.1

Table 5.2: Ultimate analysis of dried Filtrasorb 400. Ultimate analysis sums to less than 100%, because only major constituents are reported. Standard deviation reflects the variability of the coal sample used in the experiments.

Carbon mass-%	Hydrogen mass-%	Nitrogen mass-%	Sulfur mass-%	Oxygen mass-%
89.55±0.22	0.21±0.02	0.25±0.04	0.77±0.01	5.77±0.01

Table 5.3 shows the specifics, such as sample weight, for the different experiments. All measurements are performed on sample material dried at 473 K for at least 24 h. The drying procedures differed slightly among the three laboratories, but contact of the sample with air is avoided after drying. DUT degases the detached sample cell in an electric oven at an evacuation pressure of less than 100 Pa absolute. Contact with air is avoided by filling the sample cell with He when transferring to the apparatus. RWT degases the sample at 10⁻² Pa inside the sorption apparatus. FPM and INERIS degas the sample inside the gravimetric apparatus for 24 h at 10⁻¹ Pa absolute with a temperature ramp of 1 K/min⁻¹ from room temperature to 473.1 K. Gas phase densities are calculated from pressure and temperature measurements using an appropriate equation of state (EoS); Helium density is calculated using a modified Benedict-Webb-Rubin EoS (McCarty and Arp, 1990); carbon dioxide densities are calculated using the Span and Wagner EoS (Span and Wagner, 1996).

5.2.2 Apparatus

The manometric and gravimetric method for determination of sorption are based on different physical principles. The methods are discussed in detail by

Inter-laboratory comparison

Table 5.3: Details of the experiments.

	T [K]	M_0 [mg]	purity CO ₂ [vol-%]	t_{equil} [h]
DUT	318.11	34950±30	99.990	30
	318.12	35570±10		3
FPM	318.5	1685.65±0.02	99.996	1-3
	318.6	1939.77±0.02		
RWT	318.6	5000±0.1	99.995	1-2
	318.8	7000±0.1		
INERIS	318.2	2015.1±0.1	99.998	24

Goodman et al. (2004, 2007). The manometric method determines sorption from the decrease in the mass of the gas using the principle of mass conservation. The gravimetric method determines the sorption from the weight increase of the sample corrected for the buoyancy effect. Both methods determine excess sorption data (Sircar, 2001), which disregards the volume occupied by the sorbed phase. Furthermore, both methods assume that volume changes in the sorbent are negligible. Note that when the density of the sorbate changes, it has an opposite effect in manometric and gravimetric sorption experiments. In principle, this can be used to determine swelling effects of the sorbent. Table 5.4 shows important properties specific for each apparatus.

Table 5.4: Specifics of the apparatus of the different laboratories.

	$\max(P)$ [MPa]	σ_P [kPa]	σ_T [K]	V^{cell} [mm ³]	V^{ref} [mm ³]	$\sigma_s^{\text{a priori}}$ [mole/kg]
DUT	20.7	±1	±0.02	12152±9, 3524±4	78330±60, 75900±100	±0.1
FPM	10.0	±10	±0.15	-	-	±0.4
RWT	25.0	±13	±0.25	1778.5±0.3	13085±1	±0.001
INERIS	5.0	±0.01	±0.1	-	-	±0.4

Manometric apparatus

Manometric measurement of sorption is based on the principle of mass conservation. The excess sorption is defined as the difference between the total and the apparent amount of gas in the set-up. The apparent amount of gas is determined by multiplication of the gas density with the volume accessible to gas.

5.2 Materials and methods

Gas is cumulatively added from a reference cell to the sample cell. The excess sorption is determined from

$$m_N^{\text{excess,CO}_2,\text{F400}} = \sum_{i=1}^N \frac{V^{\text{ref}}}{M_{\text{CO}_2} M_0} \left(\rho_i^{\text{f,CO}_2} - \rho_i^{\text{e,CO}_2} \right) - \frac{\rho_N^{\text{e,CO}_2} V^{\text{s,He}}}{M_{\text{CO}_2} M_0}, \quad (5.3)$$

where subscript i to N denote the different sorption steps; V^{ref} is the volume of the reference cell; $V^{\text{s,He}}$ is the volume accessible to gas in the sample cell; M_0 is the initial mass of F400; $\rho_i^{\text{f,CO}_2}$ is the calculated density of CO_2 in the isolated reference cell before it is added to the sample cell and $\rho_i^{\text{e,CO}_2}$ is the calculated density of CO_2 at equilibrium. The volume accessible to gas in the sample cell, $V^{\text{s,He}}$, is determined by means of He expansion at the start of each experiment. The He apparent density of F400, $\rho^{\text{F400,He}}$, is related to $V^{\text{s,He}}$ by

$$\rho^{\text{F400,He}} = M_0 / (V^{\text{cell}} - V^{\text{s,He}}), \quad (5.4)$$

where V^{cell} is the volume of the empty sample cell.

The DUT apparatus is discussed in detail in 3. The DUT set-up uses a 9000 series Paroscientific pressure sensor and a Pt100 RTD temperature sensor. The entire set-up is immersed in a thermostatically controlled bath that keeps temperature constant within 0.03 K. The cells are connected by pneumatically actuated 2-position Valco valves. The *a priori* error is estimated at 0.1 mole/kg for each data point based on the discrepancy in the duplicates in chapter 3. The extended error analysis of chapter 3 is not used here.

The RWT apparatus is discussed in detail in Busch et al. (2003). The main difference with the DUT apparatus is that the sample size of the RWT apparatus is six times smaller. The RWT apparatus uses 0.05% full-scale accurate Tecsis Series P3382 pressure sensors with internal diaphragm. Temperatures are monitored using a Roessel Messtechnik GmbH (type K, NiCr-Ni) thermocouples and a Keithley Model 2000 Multimeter equipped with a 2001-TCSCAN Thermocouple Scanner Card with cold junction compensation. Temperature measurements are calibrated using a high-precision (class A) Pt100 Resistive Temperature Detector. Two pneumatically actuated Valco 3-port switching valves with 1/16" connectors are used to control the gas flow into the reference volume and the sample cell. The temperature is kept constant in the entire set-up (valves, pressure sensor, measuring cell) by a thermostatically controlled air bath (Heraeus, Binder, Varian) with a temperature stability of ± 0.1 K. The *a priori* uncertainty is determined at approximately 0.005 mmol by the RWT authors using a blank isotherm. This corresponds to an error of 0.001 mole/kg in

the excess sorption isotherm. s is six times smaller. The RWT apparatus uses 0.05% full-scale accurate Tecsis Series P3382 pressure sensors with internal diaphragm. Temperatures are monitored using a Roessel Messtechnik GmbH (type K, NiCr-Ni) thermocouples and a Keithley Model 2000 Multimeter equipped with a 2001-TCSCAN Thermocouple Scanner Card with cold junction compensation. Temperature measurements are calibrated using a high-precision (class A) Pt100 Resistive Temperature Detector. Two pneumatically actuated Valco 3-port switching valves with 1/16" connectors are used to control the gas flow into the reference volume and the sample cell. The temperature is kept constant in the entire set-up (valves, pressure sensor, measuring cell) by a thermostatically controlled air bath (Heraeus, Binder, Varian) with a temperature stability of ± 0.1 K. The a priori uncertainty is determined at approximately 0.005 mmol by the RWT authors using a blank isotherm. This corresponds to an error of 0.001 mole/kg in the excess sorption isotherm.

The sorbent is exposed to the sorbate, CO_2 , at constant temperature and pressure. The sorbate mass, m , is measured directly. Sorption is determined by

$$m^{\text{excess,CO}_2,\text{F400}} = \frac{1}{M_{\text{CO}_2}} \left(\frac{\Delta M}{M_0} + \frac{\rho^{\text{CO}_2}}{\rho^{\text{F400,He}}} \right) \quad (5.5)$$

where M_{CO_2} is the molecular mass of CO_2 , m_0 is the initial weight of the sample, Δm is the measured weight increase and $\rho^{\text{CO}_2}/\rho^{\text{F400,He}}$ accounts for the buoyancy. $\rho^{\text{F400,He}}$ is determined at the start of the experiment using helium, which is assumed to be non-adsorbing (Rouquerol et al., 1999).

Gravimetric apparatus

The FPM set-up is discussed in detail by De Weireld et al. (De Weireld et al., 1999). The INERIS apparatus is nearly identical. The most important aspects of the FPM apparatus are discussed here for the sake of completeness. The weight increase is measured with a 10 μg accurate Rubotherm magnetic suspension balance. The magnetic system couples an electromagnet linked to the balance with a permanent magnet at the top of the suspension system for the crucible containing the sorbent. The micro balance and the adsorption chamber are separated allowing experiments at high temperature (243 K to 393 K), high pressure (vacuum - to 10.0 MPa) and corrosive conditions. Pressure is measured with three different pressure sensors, viz. a MKS Baratron 621B with a resolution of 1.3 Pa for secondary vacuum to 133.3 kPa, a MKS Baratron 621B with a resolution of 32.5 Pa for secondary vacuum up to 3.333

5.3 Results and discussion

MPa and a Endress-Hauser Cerabar PMP 635 with a resolution of 100 kPa and an accuracy of 0.1% for its selected range. Temperature measurements of the gas phase for the determination of the density are performed with a Pt100 probe with an accuracy of 0.15 K. The installation is located in a thermostatically controlled oven ensuring constant temperature during experiments. This homogeneous temperature field avoids condensation of sub-critical gases (Belmakhout et al., 2004; Dreisbach et al., 2002). The *a priori* errors of the FPM and INERIS data is estimated at 5% of the maximum sorption (0.4 mole/kg).

5.3 Results and discussion

Table 5.5 shows the temperature, maximum measured excess sorption, extrapolated density of the sorbed CO₂, regressed micropore volume of the F400 and its helium apparent density of the different data sets. Chapter 3 discusses the method for determination of extrapolated density, regressed micropore volume and helium apparent density. Intra-laboratory deviations in the maximum measured excess sorption is 0.05 mole/kg or less. Deviations between DUT and FPM in the maximum measured excess sorption are as large as the intra-laboratory deviations; The data of RWT is 0.2 mole/kg higher and the data of INERIS is 0.2 mole/kg lower. Intra-laboratory deviations in the regressed micropore volume are 43 cm³/kg for FPM, 10 cm³/kg for RWT and 2 cm³/kg for DUT. Inter-laboratory deviations of the micropore volume are large with a maximum value of 131 cm³/kg. The micropore volumes, except for one FPM value, are less than the 510 cm³/kg for N₂ sorption at 77 K. The same behavior is observed by Humayun and Tomasko (2000). Inter-laboratory deviations in the extrapolated sorbed phase density are 0.51 kmole/m³ for FPM, 0.1 kmole/m³ for DUT and 0.02 kmole/m³ for RWT. Inter-laboratory deviations of the density are large with a maximum of 2.14 kmole/m³. These deviations are as large as the discrepancies of previous work (Chapter 3). The helium apparent densities of F400, $\rho^{F400,He}$, agree within 8%. The 0.04 kg/m³ discrepancy in this density between DUT and RWT results from different assumptions on the behavior of He on F400 at 318 K for 0.1 to 15 MPa. DUT assumes Langmuir-like behavior (van Hemert et al., 2009), while RWT assumes He is non-adsorbing (Rouquerol et al., 1999). Reprocessing the DUT He experiment with the assumption of negligible He sorption results in a similar He apparent density of F400 of 2.11 kg/m³. The higher He apparent density by INERIS is most likely caused by an undetermined experimental error. The low maximum measured excess sorption is a direct result of the high apparent density.

Inter-laboratory comparison

Table 5.5: Experimental parameters.

	T [K]	$\max(m^{CO_2 F400})$ [mole/kg]	$\bar{V}_{\text{micropore}}^{F400, CO_2}$ [cm ³ /kg]	$\hat{\rho}_{\text{sorbed}}^{CO_2, F400}$ [kmole/m ³]	$\rho^{F400, He}$ [kg/m ³]
DUT A	318.12	7.86	408	23.17	2.08
DUT B	318.11	7.91	410	23.27	2.06
FPM A	318.5	7.88	496	21.24	2.14
FPM B	318.6	7.85	539	20.73	2.20
RWT A	318.6	8.14	451	22.23	2.11
RWT B	318.8	8.12	461	22.25	2.11
INERIS	318.2	7.67	-	-	2.28

Fig. 5.1 shows that the intra-laboratory duplicate experiments of CO₂ sorption on F400 at 318 K by DUT, RWT and FPM are in excellent agreement (deviations less than 0.3 mole/kg). Deviations between the data sets of different laboratories is small (less than 0.6 mole/kg). However, the discrepancies do not always agree with the *a priori* error estimation. The DUT data is taken as base data. The most prominent discrepancies between DUT and the other three laboratories are

- FPM data is lower at 12 MPa with increasing discrepancy up to the end of the data set at 14 MPa.
- RWT data is higher between 4 and 8 MPa.
- INERIS data is lower from 4 MPa to the end of the data set at 5 MPa.

These deviations, with a maximum of 0.6 mole/kg, between the different laboratories is considered to be an acceptable level of accuracy. In addition, the discrepancies in this study are smaller than those reported by Goodman et al. (2007).

The fitted parameters of Eq. 5.1 in Table 5.6 agree within three times the *a posteriori* error. INERIS data is excluded, because its limited range does not support a single fitting solution. It is interesting to note that the Langmuir micropore volumes and Langmuir sorbed phase densities are in fair agreement with the regressed micropore volumes and extrapolated sorbed phase densities of Table 5.5. The *a posteriori* errors, based on the discrepancy between the fitted equation and the data, are approximately equal for all data sets. The smaller *a posteriori* errors of DUT data may possibly be caused by the higher accuracy

5.3 Results and discussion

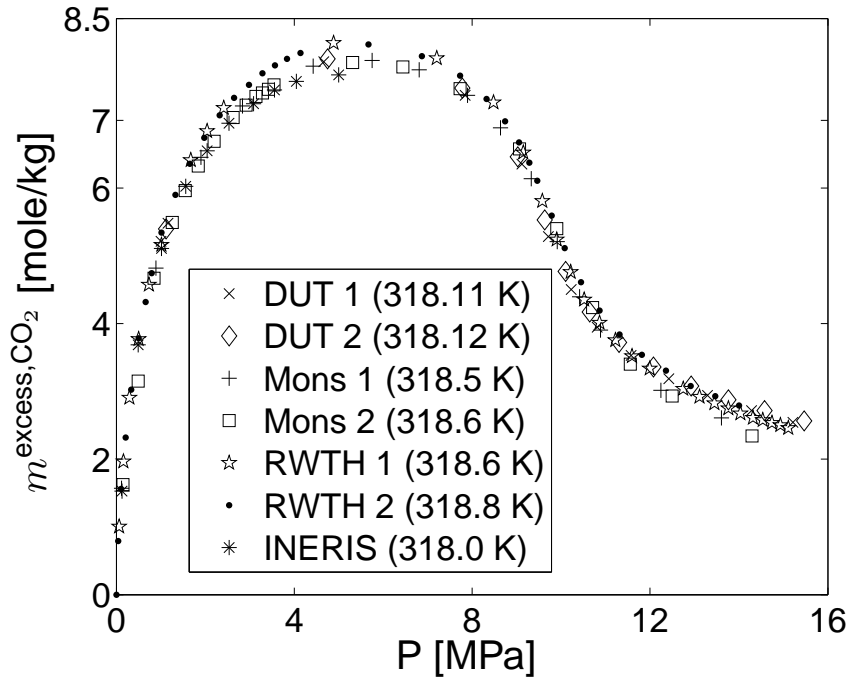


Figure 5.1: Excess CO₂ sorption data on activated carbon Filtrasorb F400 vs. pressure as measured by the different laboratories.

sensors of the DUT apparatus. It is interesting to note the good agreement between the original *a priori* error of chapter 3 and this *a posteriori* error.

The fitted parameters of Eq. 5.2 in Table 5.7 agree within five times the *a posteriori* error, except for the INERIS data. The large discrepancy in the INERIS parameters is caused by the deviating helium apparent density and the limited range of the data set. The increased variation of the DubininRadushkevich parameters compared to variation of the Langmuir parameters may be caused by the more complex mathematical form of the first equation, which is more sensitive for experimental errors. The *a posteriori* errors are equal for all FPM, RWT and DUT data sets. The fitted sorbed densities using the DubininRadushkevich equation are in fair agreement with the extrapolated sorbed

Inter-laboratory comparison

Table 5.6: Parameters of Eq. 5.1 fitted to the different data sets. Accuracy of the parameters is determined by bootstrapping the residuals. σ_{χ^2} is determined from the residuals by assuming it is normally distributed. Q_{fit} is determined using the *a priori* estimates. The averages are weighted averages.

	$\overline{V}_{\text{micropore}}^{\infty, \text{CO}_2, \text{F400}}$ [$10^{-6} \times \text{m}^3/\text{kg}$]	K_L [mole/m ³]	$\hat{\rho}_{\text{sorbed}}^{\text{CO}_2, \text{F400}}$ [kmole/m ³]	σ_{χ^2} [$\frac{\text{mole}}{\text{kg}}$]	Q_{fit} [-]
DUT A	451.5±3.1	371±9	22.57±0.11	0.067	0.943
DUT B	452.7±2.2	383±9	22.71±0.08	0.049	0.989
FPM A	472.6±7.8	396±29	21.90±0.36	0.19	0.995
FPM B	474.0±6.4	428±20	21.90±0.29	0.16	1.000
RWT A	469.4±6.8	348±17	22.09±0.19	0.17	0.000
RWT B	455.0±4.9	350±14	22.66±0.27	0.18	0.000
<i>average</i>	455.5±1.60	375±5	22.56±0.06		

phase densities of Table 5.5.

The parameter Q is a computed probability quantifying the quality of the fit using a certain model equation (Press et al., 2002). Generally, a model is accepted for a Q value of ≥ 0.001 . However, a value of ≈ 1.00 is typical when the *a priori* error is overestimated. The Q values for DUT, FPM and INERIS of both equations suggest that their respective *a priori* errors are overestimated. The Q value of both equations for the RWT data shows that the equations can be statistically rejected. An alternative possibility is that the RWT *a priori* error of 0.001 mole/kg is too small. The σ_{χ^2} , *a posteriori* errors based on a normal distribution of the discrepancy between the equations and the data, provide an estimate of the actual *a priori* errors between 0.05-0.2 mole/kg for every data set.

Fig. 5.2 shows the experimental data and their description with Eq. 5.1 and 5.2 with their weighted averaged parameters. The differences between the inter-laboratory data sets are as large as the differences between the two fitted equations. In order to determine which equation describes the data set more accurately, *a priori* errors equal or smaller than the σ_{χ^2} are required.

The discrepancies between the fitted parameters are a better indicator of the experimental errors than the *a priori* estimates or the observed deviations in the Fig. 5.1. The maximum of these discrepancies are 0.19 mole/kg in $\hat{\rho}_{\text{sorbed}}^{\text{CO}_2, \text{F400}}$ and $\overline{V}_{\text{micropore}}^{\infty, \text{CO}_2, \text{F400}}$ and 0.86 mole/kg in $m_0^{\text{CO}_2, \text{F400}}$ between DUT A and FPM

⁷value excluded from the weighted average.

5.3 Results and discussion

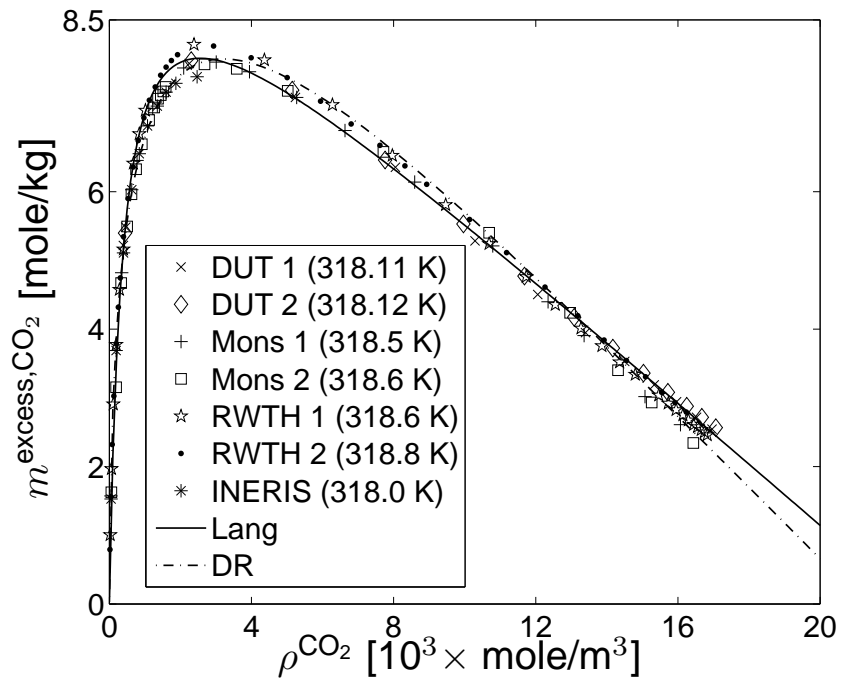


Figure 5.2: Excess CO₂ sorption isotherms on activated carbon Filtrasorb F400 vs. CO₂ density. Eq. 5.1 and 5.2 with weighted averages of the fitted parameters (Table 5.6 and 5.7) are plotted to show that the deviation of the fitted equations is approximately as large as the deviations of the data.

Inter-laboratory comparison

Table 5.7: Parameters of Eq. 5.2 fitted to the different data sets. Accuracy of the parameters is determined by bootstrapping the residuals. σ_{χ^2} is determined from the residuals by assuming it is normally distributed. Q_{fit} is determined using the *a priori* estimates. The averages are weighted, excluding the INERIS data.

	$m_0^{\text{CO}_2, \text{F400}}$ [mole/kg]	$D^{\text{CO}_2, \text{F400}}$ [$\times 10^{-3}$]	$\rho_{\text{sorbed}}^{\text{CO}_2, \text{F400}}$ [kmole/m ³]	σ_{χ^2} [mole/kg]	1.00-Q [-]
DUT A	10.49±0.14	41.4±1.6	22.02±0.22	0.14	0.045
DUT B	10.53±0.13	40.9±1.8	22.21±0.19	0.13	0.087
FPM A	10.98±0.09	47.6±1.1	20.81±0.17	0.12	0.999
FPM B	11.35±0.12	51.8±1.4	20.56±0.22	0.17	1.000
RWT A	11.21±0.11	47.4±1.0	21.22±0.13	0.16	0.000
RWT B	11.33±0.09	47.6±0.9	21.05±0.17	0.17	0.000
INERIS ⁷	11.17±0.03	61.3±10	13.33±0.39	0.04	1.000
<i>average</i>	11.05±0.04	47.0±0.5	21.27±0.07		

B. These discrepancies are smaller than the 1.0 mole/kg discrepancy observed by Goodman et al. (2007). In addition, the discrepancies in this study do not increase rapidly at higher pressures. Moreover, this study is closer to the critical temperature of CO₂ 10 K, which complicates determination of sorption. Therefore, it is concluded that the coordinated effort of the four laboratories to determine the sorption of near-critical CO₂ is successful. Workshops and exchange of technical information among the member groups substantially contributed to an improvement of sample preparation, measuring procedures and the identification of potential errors and pitfalls in the determination of high-pressure CO₂ sorption isotherms. This study provides a starting point for future supercritical CO₂ sorption determinations. The logical next step is to compare, and if necessary optimize, sorption experiments of supercritical CO₂ at high pressures on natural coals.

5.4 Conclusions

The sorption data of CO₂ on Filtrasorb 400 of the participating laboratories are in good agreement at the temperature of interest (around 318 K). The maximum observed deviation is ≤ 0.5 mole/kg (6.3% of the maximum excess sorption). Intra-laboratory repeatability is even better with discrepancies ≤ 0.3 mole/kg (3.8% of the maximum excess sorption). The higher discrepancies in the inter-laboratory comparison is caused by as of yet unidentified systematic uncertainties. However, the discrepancies are smaller than in previous inter-laboratory comparisons of CO₂ sorption: the coordinated effort to determine the sorption of near-critical CO₂ is considered successful. This study validates the accuracy of the manometric and gravimetric apparatus for sorption determination of supercritical CO₂.

The sorption data is fitted to a Langmuir-type and DubininRadushkevich type equation to facilitate comparison. The Langmuir-type parameters for every data set agree with the weighted averaged parameters within three times the *a posteriori* error, while the DubininRadushkevich parameters for every data set agree with the weighted averaged parameters within five times the *a posteriori* error. The higher variation of the DubininRadushkevich parameters is likely caused by the greater mathematical flexibility of this equation. In order to determine which equation describes the data set more accurately, improved *a priori* errors will be required.

Inter-laboratory comparison

Table 5.8: Nomenclature of chapter 5

<i>Symbol</i>	<i>Unit</i>	<i>Physical quantity</i>
$m^{\text{excess,CO}_2,\text{F400}}$	mole/kg	Excess sorption of CO ₂ on F400
$m_0^{\text{CO}_2,\text{F400}}$	mole/kg	Dubinin-Radushkevich maximum sorption capacity
K_L	kmole/m ³	Langmuir parameter
$D^{\text{CO}_2,\text{F400}}$	-	Dubinin-Radushkevich parameter
M_0	kg	Weight of the degassed F400 sample
ΔM	kg	Weight increase in gravimetric experiment
V^{ref}	m ³	Reference cell volume of a manometric apparatus
$V^{\text{s,He}}$	m ³	Volume accessible to He in the manometric sample cell
V^{cell}	m ³	Volume of the empty manometric sample cell
$\bar{V}_{\text{micropore}}^{\text{F400,CO}_2}$	cm ³ /kg	Specific micropore volume of F400 for CO ₂
$\bar{V}_{\text{micropore}}^{\infty,\text{CO}_2,\text{F400}}$	cm ³ /kg	Langmuir specific micropore volume of F400 for CO ₂
P	MPa	Pressure
T	K	Temperature
Q	-	Computed probability quantifying the quality of the fit
M_{CO_2}	kg/mole	Molecular weight of CO ₂
t_{equil}	h	Time taken for equilibration CO ₂ with F400
$\rho_{\text{sorbed}}^{\text{CO}_2,\text{F400}}$	kmole/m ³	Assumed constant density of CO ₂ sorbed in F400
ρ^{CO_2}	kg/m ³	Density of supercritical CO ₂
$\rho^{\text{F400,He}}$	kg/m ³	Apparent helium density of F400
Superscripts		
e		manometric equilibrium phase parameter
f		manometric filling phase parameter
Subscripts		
i		parameter for manometric step i
N		parameter for manometric step N

Chapter 6

Sorption of N₂, CH₄ and CO₂ in coal

Abstract

The production of coalbed methane by injection of gas, known as Enhanced Coalbed Methane, is considered a economical viable secondary production method. An additional advantage is that the injection gas can be carbon dioxide, making ECBM eligible for Carbon Credits. The effectiveness of enhancing methane production and CO₂ storage depends on the sorption behavior of the gas constituents. Therefore, (de)sorption of N₂, CH₄ and CO₂ on dry Selar Cornish coal has been determined with the manometric method for temperatures of 318 K and 338 K and pressures up to 160 bar.

The following new observations are made based on these experiments: 1) The excess sorption isotherms of N₂ and CH₄ on Selar Cornish coal show no hysteresis, 2) the change of the excess sorption with temperature for CH₄ and CO₂ are different for Selar Cornish coal than reported in literature for other coals, 3) times for attaining equilibrium are longer than expected and increase in the order He, N₂, CH₄, CO₂, 4) while the time required for equilibration and its temperature dependency varies with the type of gas, it does not vary with pressure or pressure history.

6.1 Introduction

Concerns about global warming has generated interest in reducing the emissions of the greenhouse gas, carbon dioxide (CO₂). Large quantities of CO₂ are produced by the utilization of fossil fuels. Instead of emitting this CO₂, it can be sequestered in geological formations, e.g., saline aquifers, (depleted) gas reservoirs and coalbeds (Bachu, 2008). The advantage of sequestering CO₂ in coalbeds is that it simultaneously enhances the production of the initially present methane (CH₄) (White et al., 2005), alleviating some of the costs associated with the sequestration.

The physical and chemical processes in the coalbed when sequestering CO₂ and producing CH₄ are not fully understood. It is expected that the sorption behavior of the different gas components has a large influence on the effectiveness of CO₂ storage and enhancement of methane production in the field. Multiple experimental studies of gas sorption on coal have been published (see e.g. Busch et al., 2007; Chaback et al., 1995; Clarkson and Bustin, 1999; Day et al., 2008a; Degance et al., 1992; Dutta et al., 2008; Fitzgerald et al., 2005, 2006; Goodman et al., 2007; Majewska et al., 2009; Mazumder et al., 2006; Mohammad et al., 2009; Ottiger et al., 2006; Saghafi et al., 2007; Siemons and Busch, 2007). However, the current data set is insufficient to identify the correct hypothesis on sorption behavior (see e.g. Chapter 1). Therefore, additional accurate data on the sorption of gas in coal with changing pressure, temperature, gas composition and coal is required.

This chapter presents the excess equilibrium (de)sorption isotherms of CO₂, CH₄ and N₂ on a Selar Cornish (United Kingdom) coal at temperatures of 318 K and 338 K up to a pressure of 160 bar. The pressure and temperature range investigated is set by the limit of the apparatus, but encompasses the range of *in situ* conditions of deep coalbeds. The data has been determined with two newly developed manometric apparatus. It has been suggested that the time necessary for reaching sorption equilibrium is quite long (Day et al., 2008a; Dutta et al., 2008; Majewska et al., 2009; Mohammad et al., 2009; Pone et al., 2009). Therefore, the time necessary for reaching equilibrium has been explicitly considered. The *a priori*¹ and *a posteriori*² errors of the determinations are included.

¹ *A priori* errors are estimated from the experimental error of the measurements, physical validity of the assumptions and accuracy of the equations used in the determination.

² *A posteriori* errors are the observed discrepancies between duplicate measurements.

6.2 Materials and methods

6.2 Materials and methods

6.2.1 Materials

Experiments are performed with a semi-anthracite from the Selar Cornish, South Wales Coalfield. The vitrinite reflectance of the coal is $R_{\max}=2.41$ and compositional analysis is reported in Table 6.1. The stored coal block is broken with a sledgehammer, crushed, sieved with a standard sieve and finally evenly split in experimental batches. The fraction between 1.5 and 2.0 mm has been used in this study. Sieving was brief in order to avoid dust production. Batches of 50 to 70 cm³ were sealed and stored at ~276 K until ready for use in the experiments. The helium apparent density, explained in section 3.2.4, is determined once at 318 K ($\rho_{318\text{ K}}^{*,\text{SelarCornish,He}}$ is 1410 ± 20 kg/m³).

The optimal procedure for the initial evacuation of the sample is evacuation of the sample cell in a thermostatically controlled oven at 378 K for at least 24 hours. To avoid contamination of the sample with air during transport from the oven to the set-up, the sample cell is filled with helium and sealed. The first experiment (N₂) at 318 K used a sub-optimal evacuation procedure. The suboptimal procedure is evacuation of the sample cell built in the set-up at 318 K for 48 h. Between N₂ and CH₄ experiments that use the same coal sample the built-in sample cell is evacuated at 338 K. The change in the volumes was minimal for these experiments.

Table 6.1: Properties of the used U.K. Selar Cornish coal.

Proximate analysis ³				
Moisture mass-%	Vol. matter mass-% (w.f.)	Ash mass-% (w.f.)	Fix. Carbon mass-% (d.a.f.)	
0.64±0.04	9.61±0.02	4.38±0.06	85.37±0.01	
Ultimate analysis ³				
Carbon mass-%	Hydrogen mass-%	Nitrogen mass-%	Sulfur mass-%	Oxygen mass-%
85.2±1.3	3.28±0.03	0.77±0.05	0.92±0.01	5.60±0.01
Microscope analysis (Siemons, 2007)				
R _{max} %	Vitrinite vol-%	Liptinite vol-%	Inertinite vol-%	Minerals vol-%
2.41	73.6	24.6	0.0	1.8

³Standard deviations reflect the variability of the coal in the one block used for the experiments.

The two 318 K CO₂ isotherms are obtained from a single sample; the sample is re-evacuated in an oven at 378 K before the determination of the second isotherm. The mass change and volume ratio change suggest a change in the sample, possibly caused by the extraction of coal-constituents by supercritical CO₂ extraction (see e.g. Kolak and Burruss, 2006). Table 6.2 shows the purity and critical constant of the gases used in this study. All gases are purchased with the specified purity from Linde Gas.

Table 6.2: Critical properties and purity of the gases used in this chapter.

Gas	T _c [K]	P _c [MPa]	ρ _c [mole/m ³]	Purity [%]
He	5.1953	0.22746	17399	99.996
N ₂	126.192	3.3958	11183.9	99.9995
CH ₄	190.564	4.5992	10139.	99.9995
CO ₂	304.1282	7.3773	10624.9	99.9995

6.2.2 Manometric apparatus

Experiments with CO₂ used a high accuracy apparatus, described in detail in chapter 3. The experiments with N₂ and CH₄ used a new standard accuracy apparatus described here. This apparatus (Fig. 6.1) has been developed for simultaneously determining duplicate sorption isotherms and thus consists of 5 stainless-steel cells: two sample-containing cells, two reference cells and one common reservoir. Pressures are measured using Drück PTX611 pressure transducers with an accuracy of 0.05 bar.

The entire set-up is immersed in a water-filled thermostatically controlled bath, which keeps the temperature constant within 0.05 K. Temperature is determined with Automated System Laboratories PT100 sensor at the start and end of an experiment. K-type thermocouples in the reference cells monitor the temperature during the experiment to ensure thermal equilibrium is attained. The pressure transducers and thermocouples are connected to a Keithley KPCI-3108 data-acquisition and control card connected to a PC with a 16 channel, 16 bits single ended analog input. The valves are controlled with a personal computer via the data-acquisition and control card. Control of the valves is on a time interval basis. The acquisition software is written in Testpoint V3.4. The

The variability for the entire coal is larger as can be seen by comparing the values here with the values in Siemons (2007).

6.2 Materials and methods

acquisition software scans the measurements every one or two seconds and records them every 10 seconds.

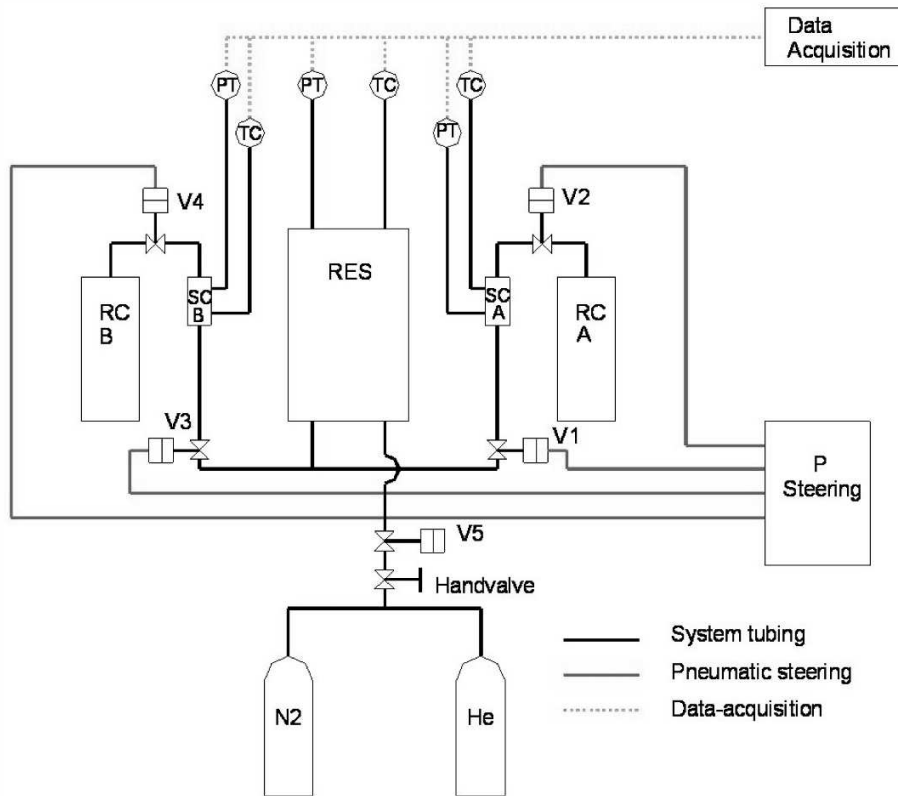


Figure 6.1: Technical drawing of the manometric apparatus. RES is the reservoir, RC A is the reference cell A and RC B is the reference cell B, duplicate of A, SC A is the sample cell A and SC B is the sample cell B, duplicate of A, PT indicates the pressure transducers and TC are the thermocouples.

6.2.3 Experimental procedure

The experimental procedure consists of four consecutive steps: (1) Helium leak rate determination; (2) Determination of the volume accessible to gas with

He, (3) Actual sorption and desorption experiment with CO₂, N₂, or CH₄ (4) Optional check of the volume accessible to gas with He.

The He leak rate is determined at approximately 200 bar and at the temperature of the following experiment for at least 24 hours. The effect of leakage has not been explicitly examined in this chapter. The procedure for determining the volume accessible to gas with He is identical to the procedure of the actual (de)sorption experiment. Before the (de)sorption experiment, the built-in sample cell is evacuated at the temperature of the experiment for at least 24 hours to minimize contamination with He. A sorption experiment consists of two parts: (1) determination of the sorption isotherm and (2) determination of the desorption isotherm⁴. For the sorption isotherm, gas is added step-wise to the evacuated sample cell until a pressure of 140 to 180 bar is reached. For the desorption isotherm, gas is extracted sequentially from the sample cell until a pressure of around 5.0 MPa is reached. Table 6.3 shows the sample weights, time intervals and χ 's of the different experiments. Experimental procedure is discussed in more detail in chapter 3.

Exp.	T [K]	τ_{eq} [h]	M [g]	χ [-]
N ₂	318.20	~30	38.44	6.458±0.005
			38.59	7.027±0.004
	338.06	~48	31.51	7.034±0.008
			35.05	7.015±0.008
CH ₄	318.11	~252	35.05	6.995±0.004
			31.51	6.979±0.003
	338.06	~30	35.05	6.995±0.004
			31.51	6.979±0.003
CO ₂	318.05	~72	38.17	3.969±0.028
			37.78	4.102±0.012
	337.55	~72	37.20	4.084±0.002

Table 6.3: Experimental conditions and parameters of this chapter. T is the temperature of the experiment, τ_{eq} is the time taken for attaining equilibrium after gas adding gas to or removing gas from the sample cell, χ is the parameter related to the volume accessible to gas in the sample cell and M is the mass of the evacuated coal sample.

⁴Sorption and desorption signify that gas is added to or removed from the sample cell, respectively.

6.2 Materials and methods

6.2.4 Data analysis

Measured properties are pressure and temperature; these are converted to density values, ρ in mole/m³, using a highly accurate reference EoS. The equations of state used for helium is published by McCarty and Arp (1990), for or nitrogen and methane by Wagner and Span (1993), for carbon dioxide by Span and Wagner (1996). The excess amount of CO₂ sorbed is computed with Eq. 3.1 modified to disregard leakage

$$m_N^{\text{excess,CO}_2,\text{SelarCornish}} = \frac{1}{M} \sum_{i=1}^N V_i^r (\rho_i^{\text{f,gas}} - \rho_i^{\text{e,gas}}) - \frac{\rho_N^{\text{e,gas}} V^{\text{s,He}}}{M}, \quad (6.1)$$

where m_N^{excess} in [mole/kg] is the N^{th} determined excess sorption point. $\rho_i^{\text{e,gas}}$ [mole/m³] is the gas density after stabilization of the reference and sample cell in step i . $\rho_i^{\text{f,gas}}$ is the stable gas density after gas addition to the reference cell for step i . V_i^{ref} is the volume of the reference cell used in step i . The superscript gas denotes N₂, CO₂ or CH₄. M is the sample mass. the ratio of the volumes accessible to gas in the sample cell and the reference cell is denoted by χ .

$V^{\text{s,He}}$ is the volume accessible to gas in the sample cell determined using helium. The sorption of helium is assumed to be negligible, which is substantiated by the data. $V^{\text{s,He}}$ is related to the χ parameter by $\chi = \frac{V^{\text{sc}}}{V^{\text{ref}}}$. χ is determined by using equation

$$\chi = \frac{\rho_i^{\text{e,gas}} - \rho_i^{\text{f,gas}}}{\rho_{i-1}^{\text{e,gas}} - \rho_i^{\text{e,gas}}}, \quad (6.2)$$

where the ρ 's are defined similarly as in Eq. 6.1. The nomenclature is the same as in chapter 3.

6.2.5 *A priori* error analysis

An *a priori* error is an estimate of the accuracy of a determination based on the experimental error of the used measurements, physical validity of the used assumptions and accuracy of the used equations. Appendix F is an example of a comprehensive *a priori* error analysis of a manometric determination. The *a priori* error in this chapter is estimated using the experimental error in the pressure and temperature measurements, *a posteriori* experimental error in the determination of χ , error associated with the incomplete evacuation of the sample cell (see Appendix C) and the limited accuracy of the equation of state. The error caused by the occurrence of leakage is not explicitly estimated, but is

sure to be less than 0.05 mole/kg. The *a priori* errors for nitrogen and methane range between 0.005 and 0.015 mole/kg, while the errors for carbon dioxide range between 0.02 and 0.08 mole/kg.

6.3 Results and discussion

The following experiments have been performed (Details in Table 6.3): Sorption and desorption of N₂ at 318 K and 338 K (both in duplicate); Sorption and desorption of CH₄ at 338 K (in duplicate); A few sorption points of CH₄ at 318 K (in duplicate); Sorption and desorption of CO₂ at 318 K (in duplicate); A single sorption and desorption of CO₂ at 338 K. Details of the different experiments are given in Table 6.3.

A limited number of data points are determined for CH₄ at 318 K because determination of a full sorption isotherm would take in excess of six months. The single high pressure data point for CH₄ at 318 K is determined after determination of the CH₄ at 338 K sorption isotherm, but before the associated desorption isotherm.

Equilibrium has not been attained for experiment with CO₂. The times allowed for equilibration in the CO₂ experiments are chosen in such a way that the completed experiment could be included in the thesis. Additional experiments with CO₂ using different coals at a later date show that the time necessary to attain equilibrium is around two weeks at 338 K (Figs. I.1 in Appendix I).

Figs. I.2 in Appendix I shows the observed decrease in pressure due to sorption of N₂, CH₄, CO₂ in coal at 318 and 338 K. The time necessary for helium was within one hour at 318 K and 338 K. It is clear that the time necessary to attain equilibrium depends on the gas component and varies with temperature. However, the time necessary did not vary much with pressure or whether gas was being sorbed or desorbed. These observations provide insight in the time-dependent behavior of gases in coal.

6.3 Results and discussion

Fig. 6.2 shows the N₂ sorption isotherms in Selar Cornish coal. The data is in good qualitative and quantitative agreement with literature (see e.g. Ottiger et al., 2008). The *a posteriori* error is two times the *a priori* error at 318 K and four times the *a priori* error at 338 K. This discrepancy may have been caused by sample heterogeneity. The 12±5% decrease in N₂ sorption when increasing the temperature from 318 K to 338 K is approximately the same as the 13% decrease when increasing the temperature from 318 K to 343 K observed for the Italian Sulcis coal (Ottiger et al., 2008).

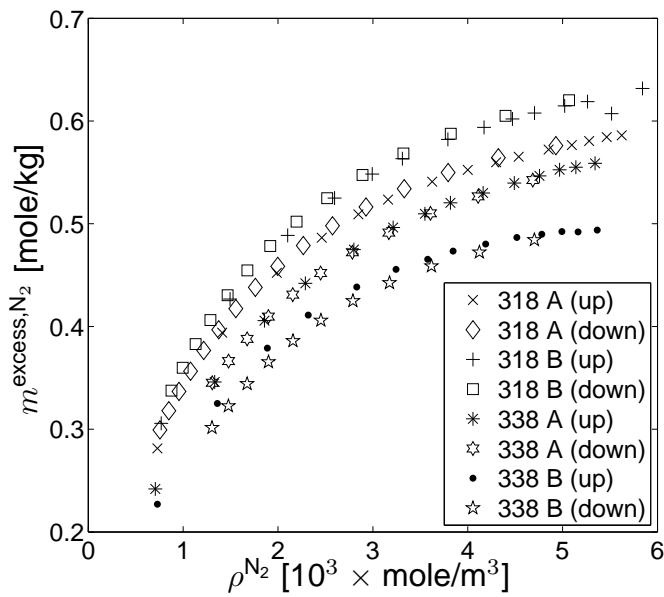


Figure 6.2: N₂ excess sorption on Selar Cornish coal at 318 K and 338 K. The *a posteriori* errors for the duplicate measurements are 0.04 mole/kg at 318 K and 0.07 mole/kg at 338 K. The sorption at $\approx 5.5 \times 10^3$ mole/m³ decreases from 0.60 ± 0.02 mole/kg at 318 K to 0.53 ± 0.05 mole/kg at 338 K.

Fig. 6.3 shows the CH₄ sorption isotherm in Selar Cornish coal. The data is in fair qualitative and quantitative agreement with literature (see e.g. Ottiger et al., 2008). The *a posteriori* and *a priori* errors are approximately equal: differences between the duplicates are not significant. The N₂ sorption isotherms at 338 K are determined using the same samples as the CH₄ isotherms and only the N₂ data has large *a posteriori* errors. A possible cause is that the sorption of N₂ is more sensitive to sample heterogeneity. The 2% decrease in CH₄ sorption when increasing the temperature from 318 to 338 K is not a significant difference. Ottiger et al. (2006) reports a 14% in CH₄ sorption on Italian Sulcis coal when increasing the temperature from 318 K to 333 K. This difference in the behavior of sorption for changes in temperature is of great interest as it suggests that the change in sorption with temperature is very dependent on the type of coal.

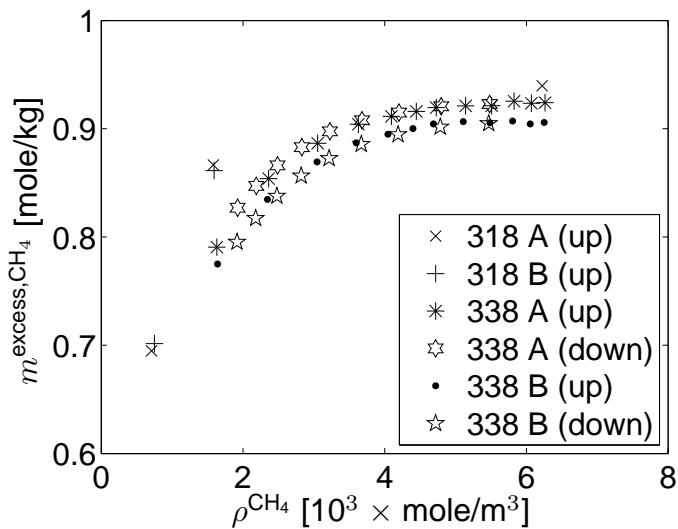


Figure 6.3: CH₄ excess sorption in Selar Cornish coal at 318 K and 338 K. The *a posteriori* errors of the duplicate measurements are 0.01 mole/kg at 318 K and 0.02 mole/kg at 338 K. The sorption at approximately $6.2 \times 10^3 \text{ mole/m}^3$ decreases from 0.94 mole/kg at 318 K to 0.92 ± 0.01 mole/kg at 338 K.

6.3 Results and discussion

Fig. 6.4 shows the CO₂ sorption isotherms in Selar Cornish coal. The data is in fair quantitative and qualitative agreement with literature data (see e.g. Ottiger et al., 2008; Sakurovs et al., 2008). The *a posteriori* error of the sorption data is equal to the *a priori* error: differences in the duplicate data are not significant. The *a posteriori* error of the desorption data is three times larger than the *a priori* error. Possible causes for this discrepancy are discussed later. It is interesting to note that the change in the mass and volume of the coal sample used for both determinations at 318 K did not incur a significant change in the sorption isotherm. This suggests that the sorption properties of the coal do not vary with supercritical extraction. The 9±1% decrease in CO₂ sorption maximum when increasing the temperature from 318 K to 338 K is a significant difference, except when considering the *a posteriori* error of the desorption duplicate at 318 K. Sakurovs et al. (2008) report a 10% decrease for U.S.A. Pocahontas # 3 coal when increasing the temperature from 308 K to 328 K and Ottiger et al. (2008) reports a 2% decrease for Italian Sulcis Coal when increasing the temperature from 318 K to 333 K. It is most likely that the sensitivity of the sorption for changes in the temperature is related to a property of the coal. Additional research is required to determine what property (e.g. compositional or the structural) of the coal dictates the change in sorption with temperature.

Figs. 6.2, 6.3 and 6.4 show that the ratio of maximum excess sorption N₂:CH₂:CO₂ is 1:1.5:2.6 at 318 K and 1:1.5:2.0 at 338 K. This order and ratio are consistent with literature (see e.g. Busch et al., 2003; Mastalerz et al., 2004; Ottiger et al., 2008). A more comprehensive discussion of the observed relationship of sorption with gas type, coal type and temperature is outside the scope of this thesis.

Single experiments (de)sorption isotherms of N₂ and CH₄ agree within the *a priori* error estimate. However, the sorption isotherms of CO₂ do show some hysteresis. The desorption isotherm is higher than the sorption isotherm for determinations at 318 K, while the desorption isotherm is lower for the determination at 338 K. Possible causes for a higher desorption isotherm are leakage, insufficient equilibration or contamination of the carbon dioxide with gaseous components of the coal. The most likely cause for a lower desorption isotherm is contamination of the carbon dioxide with gaseous components of the coal. Alternatively, it may be possible that the hysteresis is a manifestation of a physical process, e.g., swelling.

The lack of hysteresis in the (de)sorption isotherms of N₂ and CH₄ is remarkable as hysteresis in such isotherms is often encountered (see e.g. Bell and Rakop, 1986; Busch et al., 2003; Jessen et al., 2008). A likely explanation

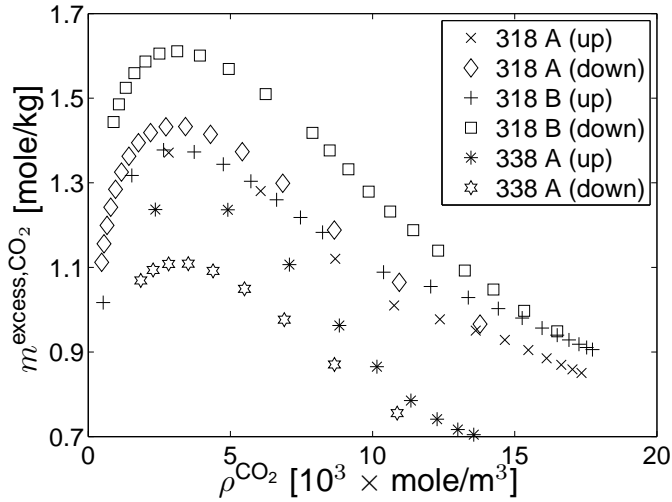


Figure 6.4: CO₂ excess sorption in Selar Cornish coal at 318 K and 338 K. The desorption isotherm is lower than the sorption isotherm at 338 K. The desorption isotherms are higher than the sorption isotherms at 318 K. The *a posteriori* at 318 K is 0.07 mole/kg or less for sorption data and 0.2 mole/kg or less for desorption data. The estimated sorption maximum at approximately 5×10^3 mole/m³ decreases from 1.36 ± 0.03 mole/kg to 1.24 mole/kg when increasing the temperature from 318 K to 338 K.

for the observed hysteresis in literature is that it is an experimental artifact caused by insufficient equilibration due to short time allowed for equilibration. The explicit consideration of time necessary to attain equilibrium in the N₂ and CH₄ experiments has prevented the occurrence of this experimental artifact. The lack of hysteresis is an important observation on the physical and chemical principles of supercritical gas sorption in coal.

6.4 Summary

Sorption data of carbon dioxide, methane and nitrogen on Selar Cornish coal at a temperature of 318 K and 338 K in the pressure range of 1.0 to 16.0 MPa has been determined using a state-of-the-art manometric apparatus and a normal

6.4 Summary

manometric apparatus. The following observations have been made regarding the accuracy of the determinations

- *A priori* errors of determinations of sorption of methane and nitrogen with the new normal accuracy apparatus are equal to or less than 0.02 mole/kg.
- *A posteriori* errors of the sorption of methane with the new normal accuracy apparatus is 0.02 mole/kg or better, which is in agreement with the *a priori* error.
- *A posteriori* errors of the sorption of nitrogen with the new normal accuracy apparatus is 0.07 mole/kg, which is four times the *a priori* error. Sample heterogeneity is a likely explanation for this discrepancy.
- *A priori* errors of determination of sorption of carbon dioxide with the state-of-the-art manometric apparatus are equal to or less than 0.08 mole/kg.
- *A posteriori* errors of the sorption of carbon dioxide with the improved apparatus is 0.07 mole/kg or better at 318 K, which is in agreement with the *a priori* error.
- *A posteriori* errors of the desorption data of carbon dioxide with the improved manometric apparatus is 0.2 mole/kg or better at 318 K, which is more than three times the *a priori* error.

Accurate sorption data is required to develop a theory that can predict the sorption of gas in coal. The development of such a theory will stimulate the production of methane from underground coals to meet local or global demand for fossil fuels and may also allow the sequestration of carbon dioxide in underground coals to reduce emission of carbon dioxide. The following observations have been made that are relevant for the development of a sorption theory.

- The excess sorption isotherm of nitrogen on Selar Cornish monotonically increases to a maximum of 0.60 ± 0.02 mole/kg at 318 K and 0.53 ± 0.05 mole/kg at 338 K. The excess isotherm of N_2 shows no hysteresis.
- The excess sorption of methane on Selar Cornish monotonically increases to a plateau of 0.94 ± 0.01 mole/kg at 318 K and 0.94 ± 0.01 mole/kg at 338 K. The excess isotherm of CH_4 shows no hysteresis.

Sorption of N₂, CH₄ and CO₂ in coal

- The excess sorption of carbon dioxide on Selar Cornish coal increases with increasing gas density up to a density of approximately 4×10^{-6} mole/m³ with a maximum of 1.36 ± 0.03 mole/kg at 318 K and a maximum of 1.24 mole/kg at 338 K. After the peak the excess sorption decreases strongly with increasing density of the carbon dioxide. This behavior is in agreement with recent gravimetric measurements in literature for CO₂ sorption in coal. The excess isotherm of CO₂ shows some hysteresis. The cause of this hysteresis is not known, but it is likely an experimental artifact.
- The excess sorption isotherms demonstrate that excess sorption vary with the type of gas and temperature. Comparison with literature shows that the coal sample influences the relationship between sorption and temperature.
- The lack of hysteresis in the N₂ and CH₄ isotherms shows that N₂ and CH₄ sorption is independent of the pressure history. This observation is of direct relevance for the modeling of coalbed methane production by injection of gas. In addition, the lack of hysteresis demonstrates the importance of using adequate time to achieve equilibrium during the experiment.
- The time required for attaining sorption equilibrium depends on the properties of the gas and the temperature. The time required for attaining equilibrium is the same whether gas is sorbing or desorbing. The influence of pressure on the time required for attaining equilibrium is minimal at most.

Chapter 7

Conclusions

This study presents a state-of-the-art apparatus for the manometric determination of excess sorption. The reproducibility and the accuracy of the equipment are verified by reference experiments and an inter-laboratory comparison. Initial experiments with this apparatus have provided new observations on the process of sorption of supercritical gas on coal, such as the absence of hysteresis and the change of sorption with temperature.

The production of CH₄ from coalbeds, with or without concurrent sequestration of the greenhouse gas CO₂, can be beneficial for society as it assists in meeting the global demand for energy. However, the physical and chemical processes are only partly understood, which can easily lead to sub-optimal production strategies for coalbed methane production. As gas in a coalbed is mainly in a sorbed state, the process by which gases (de)sorb on coal is crucial. The progress in determining the type of process is hampered by a lack of consistent data. Therefore, this thesis provides the means for the accurate determination of supercritical gas sorption on coal. In addition, some data of supercritical gas sorption on coal has been determined. The effectiveness of methane production from a coal sample by injection of single gases and gas mixtures has been investigated. The most important conclusions of each chapter are discussed below.

Chapter 2 investigates the production of coalbed methane using gas injection. At least 88% of the CH₄ initially in place could be produced by injection of pure CO₂, pure N₂, a mixture of CO₂ and N₂ or a mixture of CO₂ and H₂. By injecting gas more coalbed methane is produced than primary production. The

experiments show similar behavior as previously published data, suggesting that the physical and chemical processes do not radically change with the specifics of the coal, higher pressure, higher temperature or the use of an intact coal sample. An additional conclusion is that the production of the strong sorbing component when injecting a binary gas mixture does not change when the weak sorbing component is replaced by an even weaker sorbing component.

Chapter 3 gives a detailed description of the improved manometric apparatus for measuring the sorption of supercritical gas on coal. The main conclusions are that the *a posteriori* error¹ has a maximum of 0.15 mole/kg and that the *a priori* error² has a maximum of 0.06 mole/kg. Relevant sources of error are contamination of the CO₂, experimental error of the determined volume accessible to gas in the sample cell, experimental error of the pressure and temperature measurements, the occurrence of leakage or the error in the model to estimate the amount of leakage and the inaccuracy in the equation of state to calculate the density of the gas.

Chapter 4 examines the accuracy of the reference equation of state for helium and carbon dioxide. Both equations are used in manometric sorption experiments to calculate gas densities from pressure and temperature measurements. The error in the equation of state for helium does not introduce an experimental error that is significant in comparison to the experimental error of the pressure and temperature measurements. For carbon dioxide there is a discrepancy of about 0.2% between the calculated and the determined density. The cause for this discrepancy is likely a minor impurity (less than 0.01 vol.-%). Incorporation of this discrepancy in the *a priori* error estimate of the manometric sorption determination of carbon dioxide at a temperature of 318 K and for pressures up to 17.0 MPa increases the estimate minimally.

Chapter 5 is an independent assessment of the experimental error of the manometric apparatus of Chapter 3 using an inter-laboratory comparison. The maximum deviation in fitted parameters is observed for the modified Dubinin-Radushkevich equation Eq. 5.2. This deviation is at most 13% and at most five times the error estimated by bootstrapping the residuals. These deviations are quite small and the determinations with the new apparatus are considered to be in excellent agreement with the determinations of the other three laboratories.

Chapter 6 presents the first set of sorption data of carbon dioxide in coal, from Selar Cornish (United Kingdom), determined using the new apparatus of

¹A *posteriori* error is the observed discrepancy between duplicate experiments

²A *a priori* errors are estimated from the experimental error of the measurements, physical validity of the assumptions and accuracy of the equations used in the determination.

Chapter 3. In addition, sorption data of methane and nitrogen in the same coal have been determined using a different, normal accuracy, apparatus. These determinations have resulted in three new experimental observations that are of importance for the development of a sorption theory: The sorption and subsequent desorption of nitrogen and methane in Selar Cornish coal agree within the *a priori* error of 0.02 mole/kg, i.e., hysteresis is not present in the isotherms; The relationship between sorption and temperature is different for carbon dioxide, methane and nitrogen; Comparison with literature shows that the relationship between sorption and temperature also depends on the coal sample.

In conclusion, this thesis presents a state-of-the-art apparatus that can be used to study the characteristics of the sorption in coal, e.g., its relationship with temperature, pressure, properties of the coal and properties of the gas. Interesting observations on the behavior of sorption in coal have been made. Accurate data is required for better understanding of the sorption and is required for the development of a theory that describes sorption. This theory will improve the predictive ability of field scale simulation. These improved simulations will facilitate identification of locations and optimal development strategies for the production of methane from and the sequestration of carbon dioxide in underground coals. The production of methane can help to meet the local or global demand for energy and the sequestration of carbon dioxide can help to reduce emission of carbon dioxide.

Appendix A

Publications

This thesis has resulted in the following publications

P. van Hemert, J. Bruining, E.S.J. Rudolph, K-H.A.A. Wolf and J.G. Maas. Improved manometric setup for the accurate determination of supercritical carbon dioxide sorption. *Review of Scientific Instruments*, 80, 3:035103, 2009.

P. van Hemert, K-H.A.A. Wolf and J. Bruining. The intrinsic reliability of manometric sorption apparatus using supercritical carbon dioxide. *SPE Annual Technical Conference and Exhibition*. page SPE 110497, Anaheim, California, USA, 11-14 November, 2007.

P. van Hemert, E.S.J. Rudolph, J. Bruining, and K-H.A.A. Wolf. Estimate of Equation of State Uncertainty for Manometric Sorption Experiments: Case Study With Helium and Carbon Dioxide. *SPE Journal*, SPE 110497, In Press, accepted manuscript.

Y. Gensterblum, P. van Hemert, P. Billefont, A. Busch, D. Charri ree, D. Li, B.M. Krooss, G. de Weireld, D. Prinz and K.-H.A.A. Wolf. European inter-laboratory comparison of high pressure carbon dioxide sorption isotherms. *Carbon*, In Press, accepted manuscript.

E. Battistutta, P. van Hemert, J. Bruining and K-H.A.A. Wolf. Sorption of methane, nitrogen and carbon dioxide in Selar Cornish coal. *International Journal of Coal Geology*, submitted for publication.

Publications

P. van Hemert, E.S.J. Rudolph, K-H.A.A. Wolf and J.G. Maas. Alternative equation for sorption data interpretation. *International Coalbed Methane Symposium; Proceedings*, paper 0614, Tuscaloosa, Alabama, USA, 2006.

P. van Hemert, K-H.A.A. Wolf, J.G. Maas. Adsorption of carbon dioxide and a hydrogen-carbon dioxide mixture. *International Coalbed Methane Symposium; Proceedings*, paper 0615, Tuscaloosa, Alabama, USA, 2006.

S. Mazumder, P. van Hemert, A. Busch, K-H.A.A. Wolf and P. Tejera-Cuesta. Flue gas and pure carbon dioxide sorption properties of coal: A comparative study. *International Journal of Coal Geology*, 67(4):267-279, 2006.

S. Mazumder, A. Busch, K-H.A.A. Wolf, P. van Hemert and A. Busch. Laboratory experiments on environmental friendly means to improve coalbed methane production by carbon dioxide/flue gas injection. *Transport in Porous Media*, 75(1):63-92, 2008.

Appendix B

Derivation of data interpretation equation

This appendix derives Eq.5.3. It is a cumulative version (see also van Hemert et al., 2006) of the equation presented by e.g. Siemons and Busch (2007), that uses a stepwise approach. Additional terms have been included to calculate leakage effects. The amount of excess sorbed gas is the difference between the amount of total and free gas in the sample cell, i.e.,

$$Mm_N^{\text{excess}} = n_N^{\text{total}} - V^s \rho_N^e . \quad (\text{B.1})$$

n_N^{total} is the total amount of gas in the sample cell. The amount of free gas in the sample cell is given by the volume accessible to gas and the density of the gas ($V^s \rho_N^e$).

The total amount of gas in the sample cell is given by

$$n_N^{\text{total}} = n^{\text{start}} + n_N^{\text{added}} - n_N^{\text{l}} , \quad (\text{B.2})$$

where n^{start} is the amount of gas at the start of the experiment, n_N^{added} is the summed amount of gas added via the reference cell and n_N^{l} is the amount of gas leaked. The amount of leaked gas is given by Eq. 3.2 and derived in Appendix D. The amount of gas added (and extracted) via the reference cell is expressed by

$$n_N^{\text{added}} = \sum_{i=1}^N V_i^r (\rho_i^f - \rho_i^e) . \quad (\text{B.3})$$

Derivation of data interpretation equation

Using the initial condition of negligible gas at the start of the experiment, i.e., $n^{\text{start}} = 0$ and substituting Eqs. B.3 and B.2 in B.1 results in

$$m_N^{\text{excess}} = \sum_{i=1}^N \frac{V_i^r}{M} (\rho_i^f - \rho_i^e) - \frac{V^s}{M} \rho_N^e - \frac{n_N^l}{M} . \quad (\text{B.4})$$

Appendix C

Influence of contamination on the determination of CO₂ sorption

Impurities in the CO₂ influence the accuracy of the excess sorption experiment. This is clear since the derivation of Eq. 5.3 only considers the presence of a single pure gas. The presence of impurities invalidates the equation of state (EoS) and the single component molar balance. Some He may remain in the sample cell because He is used during transport, for leak rate determination and for determination of the volume accessible to gas in the sample cell before the actual sorption experiment. Indeed, 15 to 25 kPa of He pressure remains in the sample cell after evacuation. This remnant He is the main impurity in the sorption experiments, i.e., impurities in the bottled CO₂ and contamination by air are negligible. Consideration of the He contamination and ignoring the effect of leakage modifies Eq. 5.3 to

$$m_N^{\text{excess,CO}_2,\text{F400}} = \sum_{i=1}^N \frac{V_i^I}{M} \left(\rho_i^{\text{f,CO}_2} - x_i^{\text{e,CO}_2} \rho_i^{\text{e,He-CO}_2} \right) - \frac{V^{\text{s,He}}}{M} x_N^{\text{e,CO}_2} \rho_N^{\text{e,He-CO}_2}, \quad (\text{C.1})$$

where $\rho_i^{\text{e,He-CO}_2}$ is the density of the He-CO₂ mixture in step i. The CO₂ in the reference cells during the filling phase is considered to be pure. The mole

Influence of contamination on the determination of CO₂ sorption

fraction of carbon dioxide in the equilibrium phase, x^{e,CO_2} , can be obtained from

$$1 - x^{e,\text{CO}_2} = x^{e,\text{He}} = \frac{n^{\text{He}}/V^{\text{s,He}}}{(n^{\text{He}} + n^{\text{CO}_2})/V^{\text{s,He}}} = \frac{\rho^{\text{He,vacuum}}}{\rho^{e,\text{He-CO}_2}} \quad (\text{C.2})$$

The density of the remnant He after evacuation, $\rho^{\text{He,vacuum}}$, is constant throughout an experiment, because V^{s} and n^{He} are constant and He sorption is small. It is assumed that the molar density of the mixture, $\rho^{e,\text{He-CO}_2}$, can be approximated as an ideal mixture

$$\rho^{\text{He-CO}_2} = x^{\text{CO}_2} \rho^{\text{CO}_2} + (1 - x^{\text{CO}_2}) \rho^{\text{He}} \quad (\text{C.3})$$

Using Eq. C.3 for the equilibrium phase into Eq. C.2 leads to a quadratic equation in x^{e,CO_2} . The solution of this equation is

$$x^{e,\text{CO}_2} = \frac{\rho^{e,\text{He}} - \frac{1}{2} (\rho^{e,\text{CO}_2} + E)}{\rho^{e,\text{He}} - \rho^{e,\text{CO}_2}} \quad (\text{C.4})$$

with $E = \left[4\rho^{\text{vacuum,He}} (\rho^{e,\text{He}} - \rho^{e,\text{CO}_2}) + (\rho^{e,\text{CO}_2})^2 \right]^{1/2}$.

Now, the errors associated with the He contamination can be calculated. The remnant He pressure were 13 and 10 kPa for the two experiments. The following calculations are based on a remnant He pressure of 15 kPa and a constant temperature of 318.11 K. This corresponds to a He density after evacuation, $\rho^{\text{He,vacuum}}$, of 5.7 mole/m³. This number of moles of He is less than the total amount of CO₂ for any step i . The amount of He is 0.16% in the first step and decreases for additional steps. The remnant helium is thus negligible in comparison to the overall molar balance. i.e., assumption of $n^{\text{start}} = 0$ is justified. The value of 5.7 mole/m³ for $\rho^{\text{He,vacuum}}$ corresponds to a CO₂ molefraction values of 0.987 in the first measurement step and decreases in additional steps. The corresponding densities of He-CO₂ mixture are at most 0.13% less dense than pure CO₂.

Calculating mole fractions with Eq. C.4 and the corresponding mixture densities with Eq. C.3 and substitution in Eq. C.1 results in excess sorption values 0.01 to 0.05 mole/kg higher than the values calculated without consideration of He contamination with Eq. 5.3 values. This systematic error is approximately as large as the other *a priori* errors (see Appendix F). Thus the experimental accuracy of this set-up is limited at 0.01 to 0.05 mole/kg. Further improvements in accuracy require a decrease in the remnant pressure after evacuation. This constitutes the use of other valves in the set-up.

Appendix D

Leak-rate model

Leakage always occurs during manometric measurements and can be the main cause of inaccuracy. The ideal situation is that the leakage is negligible in comparison to the sorption. However, it was found that in sorption experiments at pressures above 10 MPa and lasting several days leakage is often significant. Therefore, a leak-rate model is incorporated to correct for the leakage or to ensure that the effect of leakage is negligible. This model is only applicable for experiments with relatively small leakage. Appendix E discusses the conditions in which the model is applicable.

Combination of the mass balance equation ($V\partial_t\rho + R = 0$) with density driven mass transfer ($R = k\rho$), leads to

$$\rho^{\text{leak}}(t) = \rho^{\text{exam}} e^{-k(t-t^{\text{exam}})/V} \quad \text{for } t \geq 0 \quad , \quad (\text{D.1})$$

where $\rho^{\text{leak}}(t)$ is the density of gas decreasing due to diffusion out of the cell of volume V . The used boundary condition is $\rho(t = t^{\text{exam}}) = \rho^{\text{exam}}$. k is the leak-rate constant. Atmospheric CO_2 concentration and air diffusion into the cell are disregarded. The amount of leaked gas for $0 \leq t \leq t^{\text{exam}}$ is then given by

$$n^{\text{leak,l}}(t) = V\rho^{\text{exam}} \left[e^{kt^{\text{exam}}/V} - e^{-k(t-t^{\text{exam}})/V} \right] \quad , \quad (\text{D.2})$$

and for $t \geq t^{\text{exam}}$ by

$$n^{\text{leak,ll}}(t) = V\rho^{\text{exam}} \left[1 - e^{-k(t-t^{\text{exam}})/V} \right] + n^{\text{leak,l}}(t^{\text{exam}}) \quad . \quad (\text{D.3})$$

Eq. 3.2 is Eq. D.3 with Eq. D.2 with parameters relevant for the apparatus. Leakage from the reference cell to the outside during the filling phase has no

Leak-rate model

influence on the sorption measurements. The experiment specific leak rate constants are determined with a He leak test before the sorption experiment. The CO₂ leak rate constant is calculated with $k^{\text{He}}/k^{\text{CO}_2} \approx 3$. This dependency was observed in reference experiments with an empty set-up. The CO₂ leak rate constant is considered to be accurate within 20%.

Appendix E

Negligibility of the influence of sorption on the leakage correction

The purpose of this appendix is to show that the leakage correction in appendix D is useful as long as the characteristic times for sorption and leakage are sufficiently separated. For this reason, the influence of sorption on the leakage is investigated. We compare the case without the effect of sorption to the case with the effect of sorption to demonstrate that the effect is small.

Consider a vessel with a sorbent of mass M , a volume accessible to gas V , gas density ρ^{forward} and sorption m^{forward} . The total number of moles in the vessel is $n^{\text{total,forward}} = V\rho^{\text{forward}} + Mm^{\text{forward}}$. Volume of the sorbed phase is considered negligible. Gas density and sorption are in equilibrium when $m^{\text{forward}} = \gamma\rho^{\text{forward}}$. Time dependent behavior of the density due to leakage is described with the same model as in Appendix D: $V\frac{d\rho}{dt} = -k\rho$. Time dependent behavior of density and sorption is described by $M\frac{dm^{\text{forward}}}{dt} = \omega(\gamma\rho^{\text{forward}} - m^{\text{forward}})$. This is in line with the suggestion by Prigogine for the description of reaction rates near equilibrium Prigogine et al. (1948). Combination results in

$$V\frac{d\rho^{\text{forward}}}{dt} + M\frac{dm^{\text{forward}}}{dt} = -k\rho^{\text{forward}} \quad (\text{E.1})$$

Using boundary conditions $\rho^{\text{forward}}(t=0) = \rho^0$ and $m^{\text{forward}}(t=0) = \omega\rho^0$, Eq. E.1 is solved by Laplace transforms. The time dependent density and

Negligibility of the influence of sorption on the leakage correction

amount of leaked gas of the forward model are given by

$$\rho^{\text{forward}}(t) = A \left(s^1 e^{s^1 t} - s^2 e^{s^2 t} \right) + B \left(\frac{e^{s^1 t}}{s^1} - \frac{e^{s^2 t}}{s^2} \right) , \quad (\text{E.2})$$

$$n^{\text{forward}}(t) = k \left(A e^{s^1 t} - A e^{s^2 t} + BC(t) \right) , \quad (\text{E.3})$$

with

$$A = \frac{\rho^0}{s^1 - s^2} , \quad B = \frac{\omega [M\gamma\rho^0 + \rho^0 V]}{MV (s^1 - s^2)} ,$$

$$C(t) = \frac{e^{s^1 t} - 1}{s^1} - \frac{e^{s^2 t} - 1}{s^2} ,$$

$$s^{1,2} = \frac{-\frac{1}{2}kM - \frac{1}{2}M\gamma\omega - \frac{1}{2}V\omega \pm D}{MV} \quad \text{and}$$

$$D = \frac{1}{2} \sqrt{(kM + M\gamma\omega + V\omega)^2 - 4MVk\omega} .$$

Now the amount of leaked gas from the forward model, with sorption, can be compared to the amount of leaked gas from Appendix D, without sorption. The ratio of these two leaked amounts, $\frac{n^{\text{leak}, l}(\tau)}{n^{\text{forward}}(\tau)}$, is examined as a function of the characteristic sorption time, $\tau = \omega t/M$. Four values of γ , spanning realistic sorption magnitudes, were used. Fig. E.1 shows that ignoring sorption leads to large errors when the characteristic time of sorption and leakage are similar ($\frac{\omega V}{Mk} = 1$). Fig. E.2 shows that ignoring sorption leads to errors less than 10% for $\omega V/Mk = 25$. This agrees with the simple notion that the amount of leakage is not influenced by sorption if sorption is much faster than leakage.

In our experiments $\frac{\omega V^s}{Mk^{\text{CO}_2}} \gg 25$, so the simple leak rate model can be used to correct for the leakage. In experiments with $k_a V_f / M k_l \leq 25$, the simple leak rate model may still be useful, depending on the actual parameter values, especially γ . In such circumstances, a better approximation of the sorption isotherm will be required in order to prove the negligibility of sorption on the leakage correction. In this appendix a linear sorption isotherm is used, because it allows an analytical expression for the relevant characteristic times.

Table E.1: Input parameters for the comparison of the forward and leak-rate models.

V [m ³]	M [kg]	ρ^0 [mole/m ³]	ρ^p [mole/m ³]
70×10^{-6}	35×10^{-3}	17×10^3	16×10^3

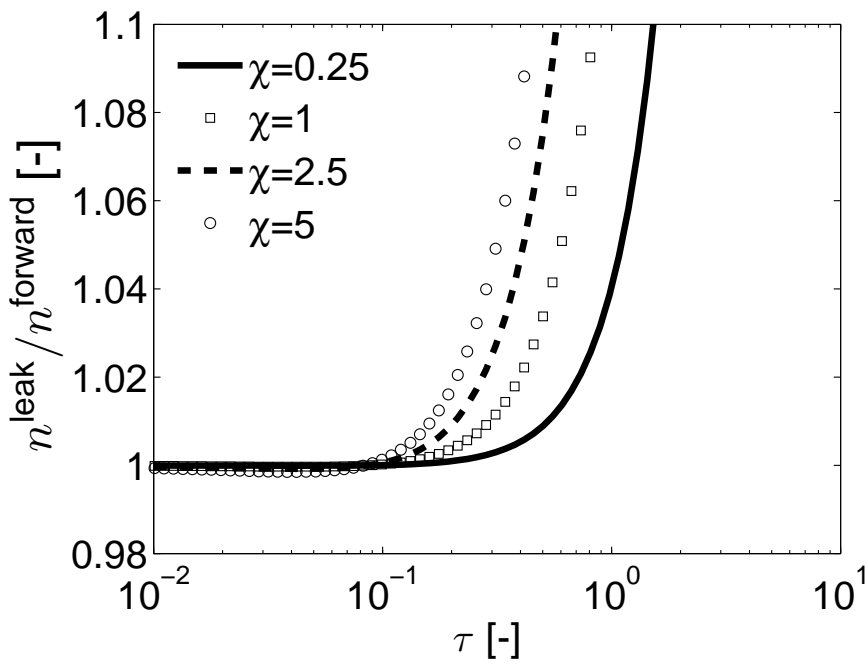


Figure E.1: Ratios of the leaked gas as calculated by the simple leak model and E.3 for $k_a V_f / M k_i = 1$ versus the characteristic sorption time. It is clear that the two models differ significantly for all values of χ and that the leak-rate model (Appendix D) is unusable.

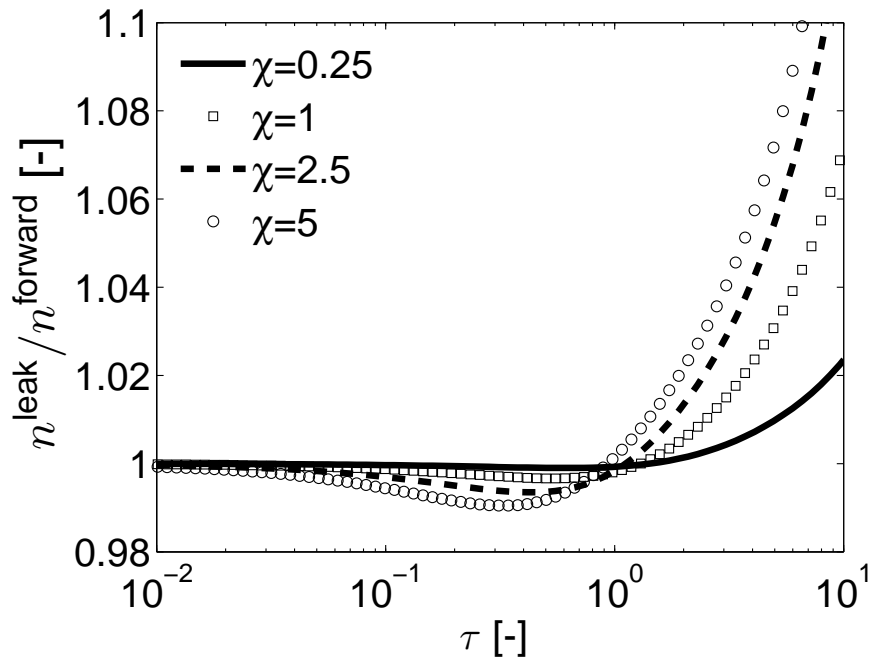


Figure E.2: Ratios of the leaked gas as calculated by the simple leak model and Eq. E.3 for $k_a V_f / M k_l = 25$ versus the characteristic sorption time. Deviation between the two models is 10% or less at $\tau \rightarrow 10$ for all values of χ . The leak-rate model (Appendix D) is applicable under these conditions.

Appendix F

A priori uncertainty analysis

A useful tool to determine the accuracy of experimental data is an *a priori* analysis of the uncertainties associated with the experiment. An *a priori* uncertainty analysis supposes that the main uncertainty in the determination are the uncertainties in parameters used for the determination and calculates the error in the determined parameter as propagated by the parameter errors. In this article, the existence of other uncertainties has been safeguarded by rigorous specification of procedures and empty cell calibration experiments.

The *a priori* error, calculated in this appendix, is estimated at 0.02 to 0.06 mole/kg. The error due to the presence of He is estimated at similar values. The observed discrepancy between the duplicate experiments has a maximum of 0.12 mole/kg. The discrepancy between the *a priori* uncertainty estimate and the maximum observed uncertainty is a factor of two. This is acceptable, but possible causes for the discrepancy are (1) underestimation of the *a priori* error, (2) unaccounted leakage and (3) an additional slower sorption process.

It is important to emphasize the cumulative nature of manometric measurements. We use the term cumulative to stress that measurement O depends on all previous ($O - 1$) measurements. This means that (a) measured points are not independent within a data set, (b) an error in a data point propagates to all subsequent data points and (c) the effect of leakage is cumulative throughout the experiment.

The uncertainties in the two reference cell volumes are 4 mm³ (0.1%) and 9 mm³ (0.07%). The uncertainty in the sample mass, M , is 0.02 g (0.06%) at most. The uncertainties in the reference cells and sample mass are negligible effect in the sorption data. The uncertainties in the volume accessible to gas,

A priori uncertainty analysis

V^s , the leak rate constant k and the calculated densities ρ are significant and specifically considered in the following paragraphs.

The uncertainty in the gas accessible sample cell volume, V^s , is $0.1 \times 10^{-6} \text{ m}^3$ (0.2%) (see Appendix G). The uncertainty in excess sorption due to the uncertainty in V^s is given by

$$\delta_{V^s} m_N^{\text{excess}} = \frac{1}{2} |m_N^{\text{excess}}(V^s + \delta V^s; \dots) - m_N^{\text{excess}}(V^s - \delta V^s; \dots)| \quad . \quad (\text{F.1})$$

The uncertainty in the calculated leaked amounts is determined by the 20% uncertainty in the leak rate constant, k . The leak rate model and its uncertainty is discussed in Appendix D. The uncertainty in the excess sorption due to the uncertainty in k is given by

$$\delta_k m_N^{\text{excess}} = \frac{1}{2} |m_N^{\text{excess}}(k - \delta k; \dots) - m_N^{\text{excess}}(k + \delta k; \dots)| \quad . \quad (\text{F.2})$$

Uncertainties in the computed density values are caused by uncertainties in pressure, temperature and the uncertainty of the used equation of state. Fig. F.1 shows the uncertainty in ρ as calculated for these three uncertainties. The uncertainty in the excess sorption due to the uncertainties in the densities is calculated with

$$\delta_\rho m_N^{\text{excess}} = \frac{1}{M} \sqrt{\sum_{i=1}^N \left[(V_i^f \delta \rho_i^f)^2 + ((V_i^f + \delta_{iN} V^s) \delta \rho_i^e)^2 \right]} \quad . \quad (\text{F.3})$$

The *a priori* errors estimated with Eq. F.1, F.2 and F.3 for the first sorption data set is shown in Fig. F.2. The order of magnitude is similar for all three types of uncertainty. Total *a priori* uncertainty is thus between 0.02 and 0.06 mole/kg. The leaked amount and its error are negligible in the second, shorter, experiment. However, the *a priori* uncertainty estimate is not appreciably changed.

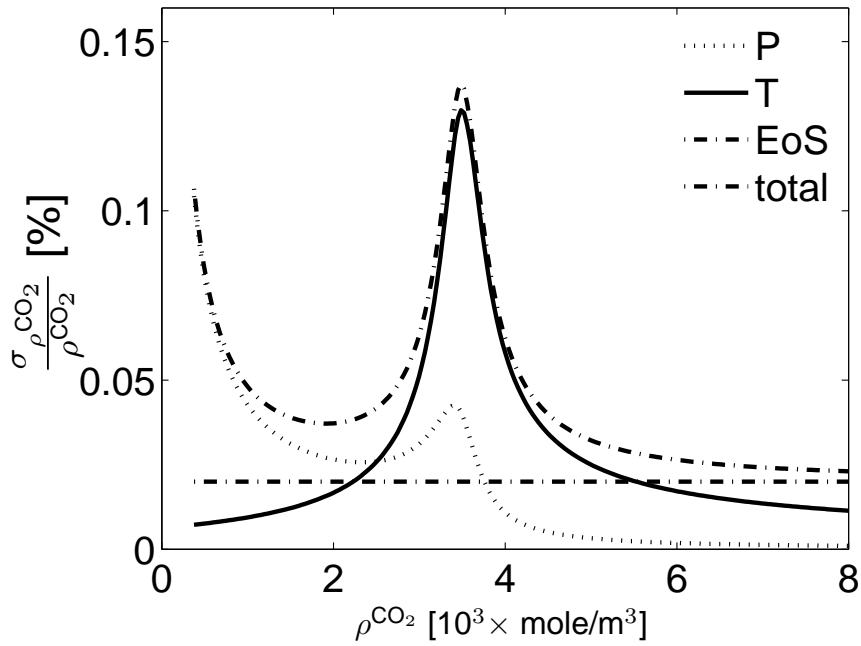


Figure F.1: Relative error in the density of CO₂ at 318.1 K for 1 kPa, 20 mK and 0.02% in the EoS uncertainty Klimeck et al. (2001). Pressure uncertainty dominates at low densities, since $\lim_{P \rightarrow 0} \frac{\delta P}{P} = \infty$. Temperature error dominates near $3.0 \cdot 10^3 \times \text{mole/m}^3$, where the density is very sensitive to temperature. The EoS error dominates at densities above $6.0 \cdot 10^3 \times \text{mole/m}^3$, where uncertainty in pressure and temperature is negligible.

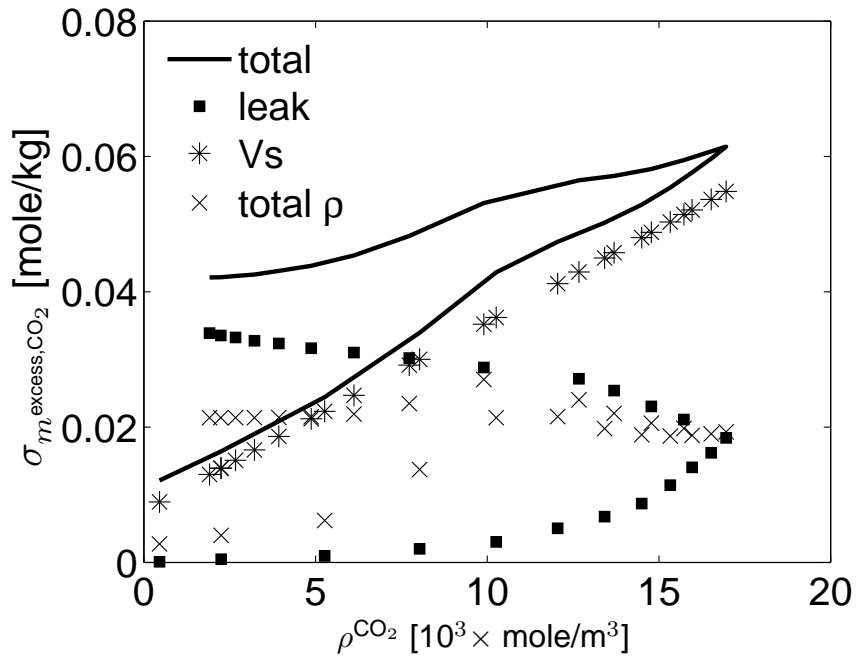


Figure F.2: Uncertainty in the first sorption data set for the uncertainties in V^s , leakage and ρ 's. The uncertainty in V^s is linear with density and dominates above $10.0 \cdot 10^3 \times \text{mole/m}^3$. The uncertainties in leakage and the ρ 's is cumulative throughout the experiment and are high in the data. Uncertainty in the leakage is the main uncertainty in the desorption data below $7.0 \cdot 10^3 \times \text{mole/m}^3$.

Appendix G

Interpretation of helium sorption experiment

The volume accessible to gas in the sample cell, V^s , is an important parameter in the interpretation of sorption experiments. Previous work generally assumes that He sorption is negligible. However, both Sircar (2001) and Gumma and Talu (2003) demonstrated that this assumption is not always valid and suggested alternative experimental procedures to determine V^s . These procedures determine He sorption from its temperature dependency over a wide range of temperatures. These procedures were not adopted, because of the limited operating temperature of the equipment. To incorporate the effect of He sorption on the Filtrasorb 400, an alternative approach is used based on the ansatz that He sorption in Filtrasorb 400 can be described with the Langmuir equation using Langmuir parameters b^{He} and s_{∞}^{He} . The Langmuir equation adequately describes the sorption of He on silicilates as demonstrated by the data of Gumma and Talu (2003).

Using the Langmuir equation for m^{excess} in Eq. B.4 with remnant He (n^{start}) and neglecting leakage results in

$$\frac{M s_{\infty}^{\text{He}} b^{\text{He}} \rho_N^{\text{e,He}}}{1 + b^{\text{He}} \rho_N^{\text{e,He}}} = n^{\text{start,He}} + \sum_{i=1}^N V_i^r \left[\rho_i^{\text{f,He}} - \rho_i^{\text{e,He}} \right] - V^s \rho_N^{\text{e,He}} \quad (\text{G.1})$$

Interpretation of helium sorption experiment

with the remnant He (free and sorbed) given by

$$n^{\text{start,He}} = \rho^{\text{He,vacuum}} V^s + \frac{M s_{\infty}^{\text{He}} b^{\text{He}} \rho^{\text{He,vacuum}}}{1 + b^{\text{He}} \rho^{\text{He,vacuum}}} \quad (\text{G.2})$$

Nomenclature is given in Table 5.8. The parameters V^s , b^{He} and s_{∞}^{He} are determined by fitting Eq. G.1 to the He density values calculated from the measured pressures and temperatures McCarty and Arp (1990). The “lsqnonlin” function from the Optimization Toolbox™ in Matlab®¹ is used for fitting.

Fig. G.1 confirms the ansatz that a Langmuir equation can describe He sorption in Filtrasorb 400. Consideration of the He sorption decreases the V^s value by 2% and the uncertainty in its determination by a factor of four.

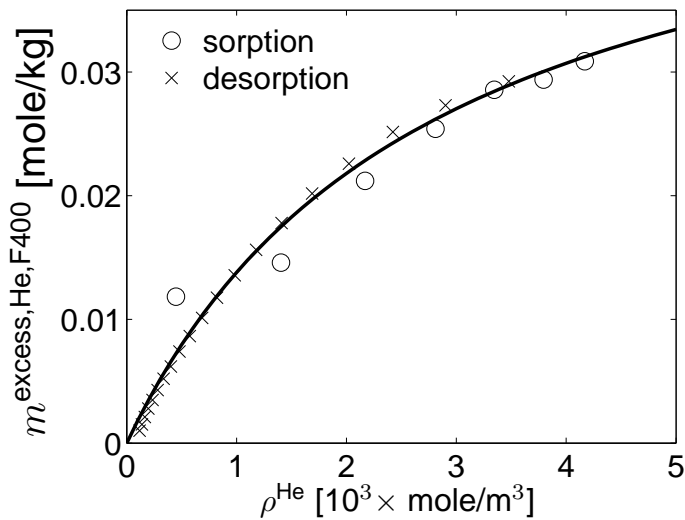


Figure G.1: Helium sorption in Filtrasorb 400 at 318.11 K. The fitted He Langmuir isotherm (line) is consistent with the sorption (o) and desorption (x) measurements. The fitted values of the Langmuir equation are $s_{\infty}^{\text{He}}=0.05\pm0.03$ mole/kg and $b^{\text{He}}=0.4\pm0.2 \times 10^{-3}$ m³/mole.

¹<http://www.mathworks.com/>

Appendix H

Determination of micropore volume and sorbed phase density

The absolute sorbed amount is by definition

$$m^{\text{absolute}} \equiv \rho_{\text{sorbed}} \bar{V}_{\text{micropore}} ,$$

where $\bar{V}_{\text{micropore}}$ is the specific micropore volume filled with sorbed gas and ρ_{sorbed} is the density of the sorbed gas. The relationship between the excess sorption, m^{excess} , and the absolute sorption is

$$m^{\text{excess}} = m^{\text{absolute}} - \rho \bar{V}_{\text{micropore}} = (\rho_{\text{sorbed}} - \rho) \bar{V}_{\text{micropore}} \quad (\text{H.1})$$

with ρ as the gas density. Eq. H.1 shows that excess sorption is zero when the sorbed phase density equals the gas phase density ($\rho_{\text{sorbed}} = \rho$ at $m^{\text{excess}} = 0$). It is assumed that both the filled specific micropore volume and density of the sorbed phase are approximately constant at high gas densities, i.e. in the linear part of the excess sorption isotherm in Fig. 3.2. It follows that m^{excess} is a linear function of ρ with $-\bar{V}$ as the slope. Thus both the density of the sorbed phase and the specific micropore volume can be determined from a linear regression through the high density excess sorption data.

Table H.1 shows the quality of the linear regressions. The standard deviation from linear regression, $\sigma_{m^{\text{excess}}}$, is in good agreement with the repeatability

Determination of micropore volume and sorbed phase density

Table H.1: Accuracy of the linear regressions to estimate specific micropore volume and sorbed phase density.

	T [K]	R ² [-]	$\sigma_{m^{\text{excess}}}$ [mole/kg]
Pini et al. (2006) ¹	318.4	0.9992	0.04
here ²	318.11	0.997	0.1

and *a priori* error (see section 3.3 and Appendix F). Calculations show that the error of our measurements is not normally distributed, which is expected from the *a priori* analysis.

Appendix I

Pressure development due to sorption in coal

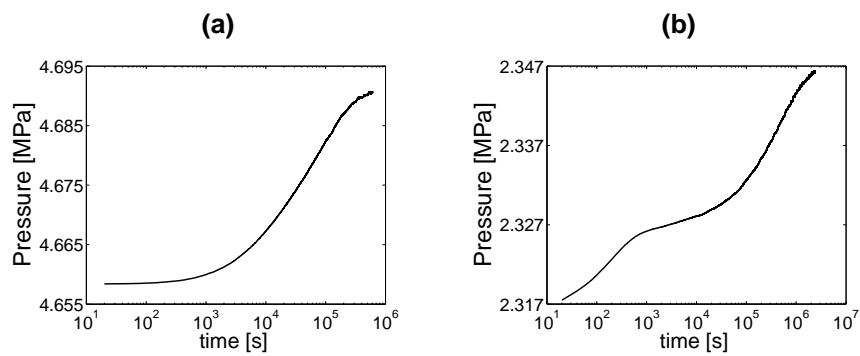


Figure I.1: Pressure increase in the improved manometric apparatus 3 for desorption of CO₂ from (a) Brzeszcze coal particulates at 337.81 K and (b) Velenje coal dust at 318.22. The pressure is almost stable for Brzeszcze after 10 days and for Velenje after 28 days. These long times for equilibration show that reaching equilibrium between coal and CO₂ can take considerable time.

Pressure development due to sorption in coal

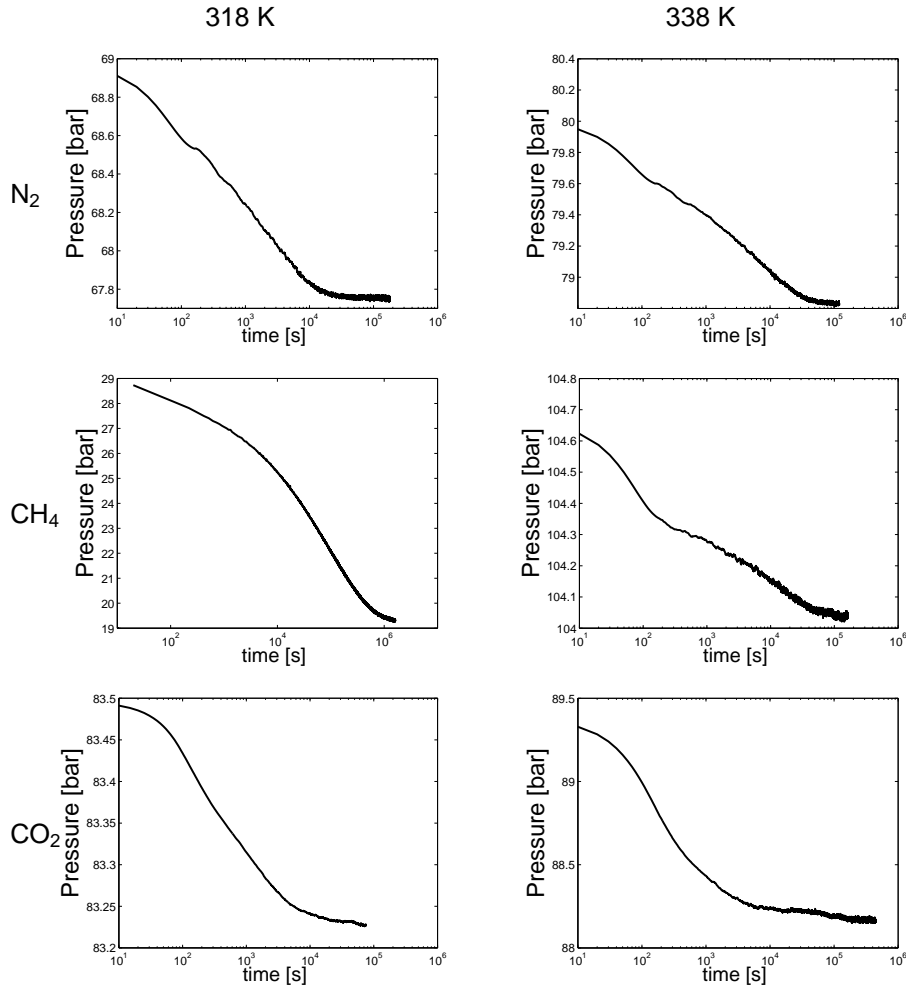


Figure I.2: Some examples of pressure decreases during sorption of N₂, CH₄ and CO₂ at 318 and 338 K in Selar Cornish coal particulates. It is clear that the sorption is different for the different gases and varies with the temperature. Some initial irregularities are observed, mainly in Fig. (b), caused by temperature effects due to the expansion and compression of gas. These temperature effects last approximately 10² seconds.

Appendix J

Excess sorption data of CO₂ on Chemviron Filtrasorb 400

Excess sorption data of CO₂ on Chemviron Filtrasorb 400

Table J.1: Excess sorption data of CO₂ on Chemviron Filtrasorb 400 at 318.11 K determined for this article. The number of data points in general is kept limited to keep cumulative errors in the desorption data at a minimum. The number of data point of the first data set is small to minimize the time required for the experiment.

ρ^{CO_2}	m^{ex}	ρ^{CO_2}	m^{ex}	ρ^{CO_2}	m^{ex}
mole/m ³	mole/kg	mole/m ³	mole/kg	mole/m ³	mole/kg
sorption 1		desorp 1			
457	5.39	15729	2.90		
2253	7.79	14781	3.29		
5270	7.32	13697	3.75		
8032	6.23	12675	4.19		
10261	5.18	9900	5.44		
12054	4.41	7728	6.42		
13419	3.86	6120	7.08		
14500	3.42	4873	7.51		
15329	3.09	3934	7.76		
15967	2.83	3222	7.88		
16525	2.61	2670	7.90		
16956	2.43	2245	7.85		
		1916	7.76		
sorption 2		desorp 2a		desorp 2b	
446	5.41	13513	4.02	1215	7.43
2303	7.92	10636	5.33	1093	7.27
5154	7.48	8368	6.37	991	7.10
7791	6.46	6630	7.09	904	6.95
9975	5.51	5293	7.58	830	6.79
11721	4.74	4269	7.88	766	6.64
13073	4.16	3483	8.04	710	6.50
14175	3.70	2879	8.10	661	6.36
15039	3.34	2413	8.07	617	6.22
15721	3.06	2051	8.00	579	6.09
16249	2.85	1767	7.88	544	5.97
16676	2.68	1543	7.74	513	5.85
17069	2.53	1362	7.59	485	5.73

Bibliography

- S. Angus, B. Armstrong, and K. de Reuck, editors. *International Thermodynamic Tables of the Fluid State- 3, Carbon Dioxide*. Pergamon Press, Oxford, United Kingdom, 1976.
- S. Bachu. carbon dioxide storage in geological media: Role, means, status and barriers to deployment. *Progress in Energy and Combustion Science*, 34(2): 254–273, 2008.
- J. S. Bae and S. K. Bhatia. High-pressure adsorption of methane and carbon dioxide on coal. *Energy and Fuels*, 20(6):2599–2607, 2006.
- G. Bell and K. Rakop. Hysteresis of methane/coal sorption isotherms. In *SPE 61st Annual Technical Conference*, volume 15454, page 10, New Orleans, U.S.A., 1986.
- Y. Belmabkhout, M. Frere, and G. De Weireld. High-pressure adsorption measurements. a comparative study of the volumetric and gravimetric methods. *Measurement Science & Technology*, 15(5):848–858, 2004.
- J. M. Blackman, J. W. Patrick, and C. E. Snape. An accurate volumetric differential pressure method for the determination of hydrogen storage capacity at high pressures in carbon materials. *Carbon*, 44(5):918–927, 2006.
- W. S. Borghard, E. W. Sheppard, and H. J. Schoennagel. An automated, high-precision unit for low-pressure physisorption. *Review of Scientific Instruments*, 62(11):2801–2809, 1991.

- D. P. Broom. The accuracy of hydrogen sorption measurements on potential storage materials. *International Journal of Hydrogen Energy*, 32(18):4871–4888, 2007.
- A. Busch, Y. Gensterblum, and B. M. Krooss. Methane and CO₂ sorption and desorption measurements on dry argonne premium coals: pure components and mixtures. *International Journal of Coal Geology*, 55(2-4):205–224, 2003.
- A. Busch, Y. Gensterblum, B. M. Krooss, and N. Siemons. Investigation behaviour of high-pressure selective adsorption/desorption carbon dioxide and methane on coals: An experimental study. *International Journal of Coal Geology*, 66(1-2):53–68, 2006.
- A. Busch, Y. Gensterblum, and B. M. Krooss. High-pressure sorption of nitrogen, carbon dioxide, and their mixtures on argonne premium coals. *Energy and Fuels*, 21(3):1640–1645, 2007.
- J. J. Chaback, W. D. Morgan, and D. Yee. Sorption of nitrogen, methane, carbon dioxide and their mixtures on bituminous coals at in-situ conditions. In *7th International Conference on Fluid Properties and Phase Equilibria for Chemical Process Design*, pages 289–296, Snowmass Village, Co, 1995.
- J. H. Chen, D. S. H. Wong, C. S. Tan, R. Subramanian, C. T. Lira, and M. Orth. Adsorption and desorption of carbon dioxide onto and from activated carbon at high pressures. *Industrial & Engineering Chemistry Research*, 36(7): 2808–2815, 1997.
- C. R. Clarkson and R. M. Bustin. The effect of pore structure and gas pressure upon the transport properties of coal: a laboratory and modeling study. 1. isotherms and pore volume distributions. *Fuel*, 78(11):1333–1344, 1999.
- S. Day, G. Duffy, R. Sakurovs, and S. Weir. Effect of coal properties on carbon dioxide sorption capacity under supercritical conditions. *International Journal of Greenhouse Gas Control*, 2(3):342–352, 2008a.
- S. Day, R. Sakurovs, and S. Weir. Supercritical gas sorption on moist coals. *International Journal of Coal Geology*, 74(3-4):203–214, 2008b.
- J. de Swaan Arons, H. J. van der Kooij, and K. Sankaranarayanan. *Efficiency and Sustainability in the Energy and Chemical Industries*. Marcel Dekker, New York, 2004.

- G. De Weireld, M. Frere, and R. Jadot. Automated determination of high-temperature and high-pressure gas adsorption isotherms using a magnetic suspension balance. *Measurement Science & Technology*, 10(2):117–126, 1999.
- A. E. Degance, W. D. Morgan, and D. Yee. High-pressure adsorption of methane, nitrogen and carbon dioxide on coal substrates. In *6th International Conf on Fluid Properties and Phase Equilibria for Chemical Process Design*, pages 215–224, Cortina Ampezzo, Italy, 1992.
- F. Dreisbach, R. Seif, and H. W. Losch. Gravimetric measurement of adsorption equilibria of gas mixture CO/H₂ with a magnetic suspension balance. *Chemical Engineering & Technology*, 25(11):1060–1065, 2002.
- P. Dutta, S. Harpalani, and B. Prusty. Modeling of CO₂ sorption on coal. *Fuel*, 87(10-11):2023–2036, 2008.
- J. E. Fitzgerald, M. Sudibandriyo, Z. Pan, R. L. Robinson, and K. A. M. Gasem. Modeling the adsorption of pure gases on coals with the sld model. *Carbon*, 41(12):2203–2216, 2003.
- J. E. Fitzgerald, Z. Pan, M. Sudibandriyo, R. L. Robinson, K. A. M. Gasem, and S. Reeves. Adsorption of methane, nitrogen, carbon dioxide and their mixtures on wet tiffany coal. *Fuel*, 84(18):2351–2363, 2005.
- J. E. Fitzgerald, R. L. Robinson, and K. A. M. Gasem. Modeling high-pressure adsorption of gas mixtures on activated carbon and coal using a simplified local-density model. *Langmuir*, 22(23):9610–9618, 2006.
- W. H. Gao, D. Butler, and D. L. Tomasko. High-pressure adsorption of carbon dioxide on nay zeolite and model prediction of adsorption isotherms. *Langmuir*, 20(19):8083–8089, 2004.
- Y. Gensterblum, P. v. Hemert, P. Billemont, A. Busch, D. Charrière, D. Li, B. M. Krooss, G. d. Weireld, D. Prinz, and K.-H. Wolf. European inter-laboratory comparison of high pressure carbon dioxide sorption isotherms. i: activated carbon. *Carbon*, In Press, Accepted Manuscript.
- T. Gentzis. Subsurface sequestration of carbon dioxide - an overview from an alberta (canada) perspective. In *15th Annual Meeting of the Society-for-Organic-Petrology*, pages 287–305, Halifax, Canada, 1998.

- A. L. Goodman, A. Busch, G. J. Duffy, J. E. Fitzgerald, K. A. M. Gasem, Y. Gensterblum, B. M. Krooss, J. Levy, E. Ozdemir, Z. Pan, R. L. Robinson, K. Schroeder, M. Sudibandriyo, and C. M. White. An inter-laboratory comparison of carbon dioxide isotherms measured on argonne premium coal samples. *Energy & Fuels*, 18(4):1175–1182, 2004.
- A. L. Goodman, A. Busch, R. M. Bustin, L. Chikatamarla, S. Day, G. J. Duffy, J. E. Fitzgerald, K. A. M. Gasem, Y. Gensterblum, C. Hartman, C. Jing, B. M. Krooss, S. Mohammed, T. Pratt, R. L. Robinson, V. Romanov, R. Sakurovs, K. Schroeder, and C. M. White. Inter-laboratory comparison II: carbon dioxide isotherms measured on moisture-equilibrated argonne premium coals at 55 degrees C and up to 15 MPa. *International Journal of Coal Geology*, 72:153–164, 2007.
- A. Graveland and E. Gisolf. Exergy analysis: An efficient tool for process optimization and understanding. demonstrated on the vinyl-chloride plant of akzo nobel. In *European Symposium on Computer Aided Process Engineering (ESCAPE 8)*, pages S545–S552, Brugge, Belgium, 1998.
- S. Gumma and O. Talu. Gibbs dividing surface and helium adsorption. *Adsorption-Journal of the International Adsorption Society*, 9(1):17–28, 2003.
- P. C. Hackley, P. D. Warwick, and F. C. Breland. Organic petrology and coalbed gas content, wilcox group (paleocene-eocene), northern louisiana. In *22nd Annual Meeting of the Society-for-Organic-Petrology*, pages 54–71, Louisville, KY, 2005.
- S. D. Hersee and J. M. Ballingall. The operation of metalorganic bubblers at reduced pressure. *Journal of Vacuum Science & Technology a-Vacuum Surfaces and Films*, 8(2):800–804, 1990.
- A. P. Hinderink, F. Kerckhof, A. B. K. Lie, J. D. Arons, and H. J. vanderKooi. Exergy analysis with a flowsheeting simulator .1. theory; calculating exergies of material streams. *Chemical Engineering Science*, 51(20):4693–4700, 1996.
- T. Hocker, A. Rajendran, and M. Mazzotti. Measuring and modeling supercritical adsorption in porous solids. carbon dioxide on 13x zeolite and on silica gel. *Langmuir*, 19(4):1254–1267, 2003.

- T. Hoshino, K. Nakamura, and Y. Suzuki. Adsorption of carbon-dioxide to polysaccharides in the supercritical region. *Bioscience Biotechnology and Biochemistry*, 57(10):1670–1673, 1993.
- R. Humayun and D. L. Tomasko. High-resolution adsorption isotherms of supercritical carbon dioxide on activated carbon. *AIChE Journal*, 46(10):2065–2075, 2000.
- J. Jagiello and M. Thommes. Comparison of DFT characterization methods based on N₂, Ar, CO₂, and H₂ adsorption applied to carbons with various pore size distributions. In *Carbon 2003 Conference*, pages 1227–1232, Oviedo, Spain, 2003.
- K. Jessen, G. Q. Tang, and A. R. Kovscek. Laboratory and simulation investigation of enhanced coalbed methane recovery by gas injection. *Transport in Porous Media*, 73(2):141–159, 2008.
- G. S. Jodlowski, P. Baran, M. Wojcik, A. Nodzenski, S. Porada, and J. Milewska-Duda. Sorption of methane and carbon dioxide mixtures in polish hard coals considered in terms of adsorption-absorption model. *Applied Surface Science*, 253(13):5732–5735, 2007.
- W. M. Jones, P. J. Isaac, and D. Phillips. The adsorption of carbon dioxide and nitrogen at high pressures by porous plugs of lampblack. *Transactions of the Faraday Society*, 55(11):1953–1958, 1959.
- S. Katyal, M. Valix, and K. Thambimuthu. Study of parameters affecting enhanced coal bed methane. *Energy Sources Part A-Recovery Utilization and Environmental Effects*, 29(3):193–205, 2007.
- M. H. Kim, C. J. Glinka, and R. N. Carter. In situ vapor sorption apparatus for small-angle neutron scattering and its application. *Review of Scientific Instruments*, 76(11):10, 2005.
- J. Klimeck, R. Kleinrahm, and W. Wagner. Measurements of the (p, rho, t) relation of methane and carbon dioxide in the temperature range 240 k to 520 k at pressures up to 30 mpa using a new accurate single-sinker densimeter. *Journal of Chemical Thermodynamics*, 33(3):251–267, 2001.
- J. J. Kolak and R. C. Burruss. Geochemical investigation of the potential for mobilizing non-methane hydrocarbons during carbon dioxide storage in deep coal beds. *Energy & Fuels*, 20(2):566–574, 2006.

- B. M. Krooss, F. van Bergen, Y. Gensterblum, N. Siemons, H. J. M. Pagnier, and P. David. High-pressure methane and carbon dioxide adsorption on dry and moisture-equilibrated pennsylvanian coals. *International Journal of Coal Geology*, 51(2):69–92, 2002.
- Z. Majewska, G. Ceglarska-Stefanska, S. Majewski, and J. Zietek. Binary gas sorption/desorption experiments on a bituminous coal: Simultaneous measurements on sorption kinetics, volumetric strain and acoustic emission. *International Journal of Coal Geology*, 77(1-2):90–102, 2009.
- M. Mastalerz, H. Gluskoter, and J. Rupp. Carbon dioxide and methane sorption in high volatile bituminous coals from indiana, usa. *International Journal of Coal Geology*, 60(1):43–55, 2004.
- M. Mavor, C. Hartman, and T. Pratt. Uncertainty in sorption isotherm measurements. *International Coalbed Methane Symposium, University of Alabama, Tuscaloosa; Proceedings*, 2004.
- S. Mazumder. *Dynamics of CO₂ in coal as a reservoir*. PhD in geotechnology, Delft University of Technology, 2007. ISBN 9789090217550.
- S. Mazumder, P. van Hemert, A. Busch, K.-H. Wolf, and P. Tejera-Cuesta. Flue gas and pure co2 sorption properties of coal: A comparative study. *International Journal of Coal Geology*, 67(4):267–279, 2006.
- S. Mazumder, K.-H. Wolf, P. van Hemert, and A. Busch. Laboratory experiments on environmental friendly means to improve coalbed methane production by carbon dioxide/flue gas injection. *Transport in Porous Media*, 75(1):63–92, 2008.
- R. D. McCarty and V. D. Arp. A new wide range equation of state for helium. 35:1465–1475, 1990.
- B. Metz, O. Davidson, H. de Conick, M. Loos, and M. L.A., editors. *Special Report on Carbon Dioxide Capture and Storage*. Cambridge Univ. Press, Cambridge, U. K., 2005.
- J. Milewska-Duda and J. Duda. Mathematical-modeling of the sorption process in porous elastic-materials. *Langmuir*, 9(12):3558–3566, 1993.
- J. Milewska-Duda, J. T. Duda, G. Jodlowski, and M. Kwiatkowski. A model for multilayer adsorption of small molecules in microporous materials. *Langmuir*, 16(18):7294–7303, 2000.

- S. A. Mohammad, J. S. Chen, J. E. Fitzgerald, R. L. Robinson, and K. A. M. Gasem. Adsorption of pure carbon dioxide on wet argonne coals at 328.2 k and pressures up to 13.8 mpa. *Energy & Fuels*, 23(1):1107–1117, 2009.
- P. Nowak, T. Tielkes, R. Kleinrahm, and W. Wagner. Supplementary measurements of the (p,p,t) relation of carbon dioxide in the homogeneous region at t=313 k and on the coexistence curve at t=304 k. *Journal Of Chemical Thermodynamics*, 29(8):885–889, 1997.
- S. Ottiger, R. Pini, G. Storti, M. Mazzotti, R. Bencini, F. Quattrocchi, G. Sardu, and G. Derui. Adsorption of pure carbon dioxide and methane on dry coal from the Sulcis Coal Province (sw Sardinia, Italy). *Environmental Progress*, 25(4):355–364, 2006.
- S. Ottiger, R. Pini, G. Storti, and M. Mazzotti. Measuring and modeling the competitive adsorption of carbon dioxide, methane, and nitrogen on a dry coal. *Langmuir*, 24(17):9531–9540, 2008.
- P. Pendleton and A. Badalyan. Gas adsorption data uncertainty and propagation analyses. *Adsorption-Journal of the International Adsorption Society*, 11:61–66, 2005.
- R. Pini, S. Ottiger, A. Rajendran, G. Storti, and M. Mazzotti. Reliable measurement of near-critical adsorption by gravimetric method. *Adsorption-Journal of the International Adsorption Society*, 12(5-6):393–403, 2006.
- R. Pini, S. Ottiger, A. Rajendran, G. Storti, and M. Mazzotti. Near-critical adsorption of carbon dioxide on 13x zeolite and n2o on silica gel: lack of evidence of critical phenomena. *Adsorption-Journal of the International Adsorption Society*, 14:133–141, 2008.
- E. Poirier, R. Chahine, A. Tessier, and T. K. Bose. Gravimetric and volumetric approaches adapted for hydrogen sorption measurements with in situ conditioning on small sorbent samples. *Review of Scientific Instruments*, 76(5), 2005.
- B. Poling, J. Prausnitz, and J. O’Connell. *The properties of gases and liquids*. McGraw-Hill Professional, New York, fifth edition, 2001.
- J. D. N. Pone, P. M. Halleck, and J. P. Mathews. Methane and carbon dioxide sorption and transport rates in coal at in-situ conditions. *Energy Procedia*, 1(1):3121–3128, 2009. doi: DOI: 10.1016/j.egypro.2009.02.093.

- W. H. Press, S. Teukolsky, W. T. Vetterling, and B. P. Flannery. *Numerical Recipes in C*. Cambridge Univ. Press, Cambridge, U. K., 2002.
- I. Prigogine, P. Outer, and C. L. Herbo. Affinity and reaction rate close to equilibrium. *J. Phys. Colloid Chem*, 52(2):321–333, 1948.
- S. R. Reeves. Enhanced CBM recovery, coalbed carbon dioxide sequestration assessed. *Oil & Gas Journal*, 101(27):49–53, 2003.
- R. C. Reid, J. M. Prausnitz, and B. E. Poling. *The properties of gases and liquids*. McGraw Hill Book Co., New York, NY, United States, 1987.
- E. Robens, J. U. Keller, C. H. Massen, and R. Staudt. Sources of error in sorption and density measurements. *Journal of Thermal Analysis and Calorimetry*, 55(2):383–387, 1999.
- F. Rouquerol, J. Rouquerol, and K. Sing. *Adsorption by Powders and Porous Solids*. Academic Press, San Diego, U.S.A., 1 edition, 1999.
- A. Saghafi, M. Faiz, and D. Roberts. Carbon dioxide storage and gas diffusivity properties of coals from sydney basin, australia. *International Journal of Coal Geology*, 70(1-3):240–254, 2007.
- R. Sakurovs, S. Day, S. Weir, and G. Duffy. Application of a modified Dubinin-Radushkevich equation to adsorption of gases by coals under supercritical conditions. *Energy and Fuels*, 21(2):992–997, 2007.
- R. Sakurovs, S. Day, S. Weir, and G. Duffy. Temperature dependence of sorption of gases by coals and charcoals. *International Journal of Coal Geology*, 73(3-4):250–258, 2008.
- A. R. Scott, W. R. Kaiser, and W. B. Ayers. Thermogenic and secondary biogenic gases, san-juan basin, colorado and new-mexico - implications for coalbed gas producibility. *Aapg Bulletin-American Association of Petroleum Geologists*, 78(8):1186–1209, 1994.
- N. Siemons. *Carbon Dioxide Transport and Retention in Coal*. PhD in geotechnology, Delft University of Technology, 2007.
- N. Siemons and A. Busch. Measurement and interpretation of supercritical carbon dioxide sorption on various coals. *International Journal of Coal Geology*, 69(4):229–242, 2007.

- S. Sircar. Measurement of gibbsian surface excess. *AIChE Journal*, 47(5): 1169–1176, 2001.
- S. Solomon, D. Qin, M. Manning, Z. Chen, M. Marquis, K. B. Averyt, M. Tignor, and H. L. Miller, editors. *Climate Change 2007: The Physical Science Basis. Contribution of Working Group I to the Fourth Assessment Report of the Intergovernmental Panel on Climate Change*. Cambridge University Press, Cambridge, United Kingdom and New York, NY, USA, 2007.
- R. Span and W. Wagner. A new equation of state for carbon dioxide covering the fluid region from the triple-point temperature to 1100 K at pressures up to 800 MPa. *Journal of Physical and Chemical Reference Data*, 25(6):1509–1596, 1996.
- R. Staudt, A. Herbst, S. Beutekamp, and P. Harting. Adsorption of pure gases and mixtures on porous solids up to high pressures. *Adsorption-Journal of the International Adsorption Society*, 11(3-4):379–384, 2005.
- S. H. Stevens, V. A. Kuuskraa, D. Spector, and P. Riemer. carbon dioxide sequestration in deep coal seams: Pilot results and worldwide potential. In B. R. P. W. A. Eliasson, editor, *4th International Conference on Greenhouse Gas Control Technologies (GHGT-4)*, pages 175–180, Interlaken, Switzerland, 1998a.
- S. H. Stevens, D. Spector, R. and P. Riemer. Enhanced coalbed methane recover using carbon dioxide injection: worldwide resource and carbon dioxide sequestration potential. *SPE*, 48881, 1998b.
- R. Stryjek and J. H. Vera. Prsv - an improved peng-robinson equation of state for pure compounds and mixtures. *Canadian Journal Of Chemical Engineering*, 64(2):323–333, 1986.
- M. Sudibandriyo, Z. J. Pan, J. E. Fitzgerald, R. L. Robinson, and E. A. M. Gasem. Adsorption of methane, nitrogen, carbon dioxide, and their binary mixtures on dry activated carbon at 318.2 k and pressures up to 13.6 mpa. *Langmuir*, 19(13):5323–5331, 2003.
- L. Sun, S. B. Kiselev, and J. F. Ely. Multiparameter crossover equation of state: Generalized algorithm and application to carbon dioxide. 233(2):204, 2005.
- I. Suzuki. Apparatus for volume measurement by helium expansion measured with a temperature-compensated, differential tensimeter having symmetrical design. *Review Of Scientific Instruments*, 54(7):868–870, 1983.

- J. Taylor. *An Introduction to Error Analysis: The Study of Uncertainties in Physical Measurements*. University Science Books, second edition, 1996.
- F. van Bergen, H. J. M. Pagnier, and P. van Tongeren. Peat, coal and coalbed methane. In T. E. Wong, D. A. Batjes, and J. de Jager, editors, *Geology of the Netherlands*, pages 265–282. 2007.
- P. van Hemert, K.-H. Wolf, and J. G. Maas. Alternative equation for sorption data interpretation. In *International Coalbed Methane Symposium; Proceedings*, Tuscaloosa, Alabama, USA, 2006.
- P. van Hemert, K.-H. Wolf, and J. Bruining. The intrinsic reliability of manometric sorption apparatus using supercritical carbon dioxide. In *SPE Annual Technical Conference and Exhibition*, page SPE 110497, Anaheim, California, USA, 11-14 November, 2007.
- P. van Hemert, J. Bruining, E. Rudolph, K.-H. Wolf, and J. G. Maas. Improved manometric set-up for the accurate determination of supercritical carbon-dioxide sorption. *Review of Scientific Instruments*, 80(3):035103, 2009.
- W. F. C. van Wageningen, H. M. Wentinck, and C. Otto. Report and modeling of the movecbm field tests in poland and slovenia. *Energy Procedia*, 1(1): 2071–2078, 2009.
- W. Wagner and R. Span. Special equations of state for methane, argon, and nitrogen for the temperature-range from 270-k to 350-k at pressures up to 30-mpa. *International Journal Of Thermophysics*, 14(4):699–725, 1993.
- C. M. White, D. H. Smith, K. L. Jones, A. L. Goodman, S. A. Jikich, R. B. La-Count, S. B. DuBose, E. Ozdemir, B. I. Morsi, and K. T. Schroeder. Sequestration of carbon dioxide in coal with enhanced coalbed methane recovery - a review. *Energy and Fuels*, 19(3):659–724, 2005.
- T. Whorf and C. D. Keeling. Rising carbon. *New Scientist*, 157(2124):54–54, 1998.
- H. G. Yu, G. Z. Zhou, W. T. Fan, and H. P. Ye. Predicted carbon dioxide enhanced coalbed methane recovery and carbon dioxide sequestration in china. *International Journal of Coal Geology*, 71(2-3):345–357, 2007.
- L. Zhou, S. P. Bai, W. Su, J. Yang, and Y. P. Zhou. Comparative study of the excess versus absolute adsorption of carbon dioxide on superactivated carbon for the near-critical region. *Langmuir*, 19(7):2683–2690, 2003.

N. Zupanc, A. W. Clarke, and J. A. Trinnaman, editors. *2007 Survey of Energy Resources*. World Energy Council, London, United Kingdom, 2007. ISBN 0 946121 26 5.

Acknowledgments

This thesis would not have been possible without the academic, technical and social support of so many. For this support I am truly grateful. The contributions of some deserves special mention and these contributions are discussed below.

Hans Bruining, my highly valued promotor, was an inspiration to work with. He, with great patience, taught me on a wide variety of subjects including scientific writing, scientific models and the obligation of the fortunate to assist the less-fortunate.

Karl-Heinz Wolf, my indispensable copromoter, did not only procure the funds required for this thesis, but also provided the scientific freedom and helpful advice whenever necessary.

Susanne Rudolph's diligent assistance as a supervisor improved the academic level of this entire thesis. In addition, without her efforts chapter 2 could not have been included.

Jos Maas, using his invaluable experience with experimental work, advised me many times on the difficulties I encountered with the manometric apparatus. His support was instrumental to obtain scientific rigor in the experiments, without this rigor the value of this thesis would not be as high.

Pierre Billemont, Andreas Büsch, Delphine Charriéree, Yves Gensterblum, Bernd Krooss, Dong Lia, Dirk Prinz and Guy de Weireld contributed as co-authors of the draft of chapter 5. Without their help, an independent assessment of the accuracy of the apparatus would not have been possible; this addition truly upgrades the entire thesis. In addition, it was the support of Niels van Wageningen in the initial phase that made this international project possible. Moreover, Yves Gensterblum helped me tremendously in gaining insight in the characteristics of the manometric method.

Elisa Battistutta's efforts as a co-author and experimental researcher made

the addition of chapter 6 to the thesis possible.

The technical expertise and assistance of Henk van Asten, Jan Etienne, Karel Heller, Andre Hoving, Henny van der Meulen and Leo Vogt was essential in the development, construction and maintenance of the manometric apparatus, the heart of the thesis, as well as of great help in the execution of the experiments.

Joost van Meel, Harry Veld, Jos Pureveen and Fons Marcelis contributed to thesis by providing CT scans, image analyses, material analyses or gas analyses.

I thank my two Msc. students, Jorge and Olivia, who were of tremendous help in the data processing necessary for chapter 2.

The support of my entire family is greatly appreciated. It is especially good to know that my mother and sister are proud of me and that they support me in all my endeavors.

I am impressed by the ability of my life partner, Meike Schrover, to tolerate my esoteric ramblings. For this I am eternally grateful. I cannot thank her enough for her support, understanding and confidence in me. Moreover, her entire family was marvelously supportive of me.

I am thankful for the social support I received from all of my friends. This support was crucial for the perseverance necessary for writing this thesis. The advice and support offered by Jojanneke, Karin, Peter and Robbert deserves special mention. In addition, I am grateful for the support of my paranymphs, Johan and Paul, to weather the storm of my defense.

I spent five pleasant years at the department of Geotechnology. The frequent discussions on a legion of subjects with all of my colleagues played an important role in my life. I am grateful to all of my coworkers for this pleasant atmosphere. I am especially grateful for the many discussions with Bouko, Christiaan, Hamidreza, Hein, Jelke, Koen, Marcin, Menne, Nikolai, Rouhollah, Rudi, Saikat, Willem-Jan and Yufei.

Jodo is a martial art that complements my chosen vocation well and that strengthens the merits and revises the flaws of my character/personality. I am fortunate that I can practice this martial art with my comrades from dojo Ken Sei Kan: Christian, Ferry, Johan, Kimberley, Richard, Wijnand and, in particular, Sensei Jef Heuvelmans.

About the author

Patrick van Hemert was born on July 2, 1979 in 's-Hertogenbosch, the Netherlands. After having obtained his 'Gymnasium' certificate in 1997 at the 'Stedelijk Gymnasium te 's-Hertogenbosch', he started studying Geochemistry at the 'Universiteit Utrecht'. In 2003, Patrick obtained his MSc degree in Geochemistry. The research was conducted at the department of Geotechnology of the 'Technische Universiteit Delft', and the title of his thesis was 'A comparative study of the sorption properties of coal for pure carbon dioxide and flue gas & Inductive investigation of the carbon monoxide producing properties of coal sequestered carbon dioxide'. In 2004, he continued his career at the department of Geotechnology of the 'Technische Universiteit Delft' and started his PhD research under the supervision of Prof. dr. J. Bruining and Dr. K-H.A.A. Wolf, which resulted in this dissertation.